Szent István University

Postgraduate School of Veterinary Science

Biological evaluation of new beta-emitting radiopharmaceuticals for therapy of malignant and chronic diseases

PhD Dissertation

Dr Domokos Máthé

2009

Szent István Egyetem Állatorvostudományi Doktori Iskola

Témavezető és témabizottsági tagok:

.....
Dr. Jánoki Győző A. PhD PharmD
korábbi Igazgatóhelyettes, főosztályvezető
Országos „Frédéric Joliot-Curie" Sugárbiológiai és Sugáregészségügyi Kutatóintézet Budapest
jelenleg ügyvezető igazgató, Medi-Radiopharma Kft.
témavezető

Prof. Dr. Halasy Katalin PhD DSc
egyetemi tanár
Anatómiai és Szövettani Tanszék
Állatorvostudományi Kar
Szent István Egyetem, Budapest

néhai †Prof. Dr. Rudas Péter PhD DSc
tanszékvezető egyetemi tanár
Élettani és Biokémiai Tanszék
Állatorvostudományi Kar
Szent István Egyetem, Budapest

Az értekezés a Dr. Sáfrány Géza PhD DSc, főigazgató-helyettes vezetésével az Országos „Frédéric Joliot-Curie" Sugárbiológiai és Sugáregészségügyi Kutatóintézetben 2009. november 2-án tartott műhelyvita eredményeként nyerte el végleges formáját.

Az értekezés angol nyelven készült, 8 példányban. Ez a .... példány.

……
Dr. Máthé Domokos

Contents

List of Abbreviations

%IA:	Percent of injected (radio)activity
%IA/g:	Percent of injected activity per gram of tissue or organ
%ID/g:	Percent of injected dose per gram of tissue or organ
AIA:	Antigen-induced arthritis
ALKP:	Alkalic phosphatase
ALT:	Alanine aminotransferase
AR:	Analytical reagent
AUC:	Area under the curve
AUD:	Area under the data
CT:	X-ray Computed Tomography
DOTA:	1,4,7,10-tetra-azacyclododecane N, N', N'', N'''-J-tetraacetic acid
DOTA-TOC:	1,4,7,10-tetra-azacyclododecane N, N', N'', N'''-J-tetraacetic acid-D-Phe^{1}-Tyr^{3}-octreotide
DOTA-TATE:	1,4,7,10-tetra-azacyclododecane N, N', N'', N'''-J-tetraacetic acid-D-Phe^{1}-Tyr^{3}-octreotate
DOTMP	1, 4, 7, 10 tetraazacyclododecane tetramethylene phosphonic acid
DTPA:	Diethylene-triamine pentaacetic acid
DV:	Dorsoventral view
EDDA:	Ethylene-diamine N,N diacetic acid
EDTMP:	Ethylene diamine-N,N,N',N'- tetrakis(methylene phosphonic acid)
EOB:	End of bombardment
$E_{\beta(max)}$:	Maximal energy of the emitted beta-negative particle
E_{γ}:	Gamma photon energy
FCS:	Fetal calf serum
FT-IR:	Fourier-transform infrared
GGT:	Gamma-glutamyl-transferase
HRGP:	High resolution general purpose collimator
HYNIC:	Hydrazino-nicotinic acid
IT:	Isotope therapy
ITLC:	Instant thin layer chromatography
LEHR:	Low energy high resolution collimator
HRGP:	High resolution general purpose collimator
MIP:	Maximum intensity projection
MRT:	Mean Residence Time
MTD:	Maximal tolerated dose
NMR:	Nuclear magnetic resonance
PRRS:	Peptide receptor scintigraphy
PRRT:	Peptide receptor radionuclide therapy
RIT:	Receptor isotope therapy
RNT:	Radionuclide Therapy
RT:	Room temperature

SCID:	Severely compromised immunodeficient
SD:	Standard deviation
SPECT:	Single Photon Emission Computed Tomography
SS:	Somatostatin
SSR2A:	Somatostatin 2A receptor
SSTR(2A):	Somatostatin 2A receptor
$T_{1/2}$:	Half-life, terminal elimination half-life
TATE:	Tyr^3-Octreotate
TC:	Total clearance
TOC:	Tyr^3-Octreotide
V_D:	Volume of distribution
VD:	Ventrodorsal view
V_{ss}:	Volume of distribution in steady state
WBC:	White blood cell

Summary

The dissertation presents an overview of the research conducted by the author examining the possibilities and roles of animal models in the development of novel, dual-use radiopharmaceutical systems for imaging and radionuclide therapy. The aims are embedded in the analysis of application of these radiopharmaceuticals in different animal model types.

The first part presents the use of healthy animal models and artificial models of disease in the development diagnostic and therapeutic radiopharmaceuticals for the bone and joint system. The first study presents the preparation of ^{177}Lu, an isotope emitting gamma and beta rays and suitable for both therapy and imaging. Preparation of the bone-seeking carrier EDTMP molecule and the circumstances of the labelling reaction is also given. Studies present the role of healthy animal models in the molecule development: pharmacokinetics, imaging, and biodistribution analysis were obtained in mouse, rabbit, rat and dog species. An escalating radioactivity dose toxicity study is also presented in the dog. Results indicate exclusive bone binding of the labelled molecule that can not be detected in other organs one day after intravenous injection neither by imaging nor by biodistribution measurements. The author has also shown using the animal models that the molecule is taken up by the cortical area of remodeling bones, and it is very weakly present in the spongiosa, thus marrow toxicity is low. No toxic side-effects could be shown in dogs even at an injected dose of 37 MBq/kg bodyweight. Application of healthy animal models has had an important role because it revealed interspecies pharmacokinetic differences that in turn carry important consequences for human application. Application of an artificial disease model was investigated in the second study, in the development of a tin colloid radiopharmaceutical, labelled also with a beta and gamma emitting isotope ^{188}Re. The study describes the room temperature preparation reaction of the radiocolloid and it presents its effects on synovium in a rabbit rheumatoid arthritis model of antigen-induced arthritis. In the second part, the author presents the use of naturally, spontaneously occurring dog cancers as animal models for the development of somatostatin analogue peptides (DOTA-TOC, HYNIC-TOC) that can be labelled with both therapeutic and diagnostic (^{90}Y, ^{99m}Tc, ^{111}In, ^{177}Lu) radioisotopes. The study presented is the first application to the author's knowledge of DOTA-TOC peptide for diagnostics and therapy of dog insulinoma. The results have shown that application of RIT gives effective therapeutic results in the dog, and naturally occurring animal cancers offer a very important role in pharmaceutical research and development.

Összefoglalás

A dolgozat a szerző új, kettős használatú, képalkotási és terápiás radiofarmakon-rendszerek területén állatmodelleken folytatott kutatásainak összefoglalását adja. A dolgozat célja ezen radiofarmakonok állatmodelleken való alkalmazásának elemzése.

Az első rész egészséges állatmodellek és mesterségesen létrehozott betegség-modellek használatát mutatja be a csont-ízületi terápiában és egyúttal képalkotásban is alkalmazható új radiofamakonok fejlesztése keretében. Az első kísérletsorozat a béta és gamma-sugárzó, képalkotásra és terápiára egyaránt alkalmazható ^{177}Lu izotóp előállítását, a csonthoz kötődő EDTMP molekula előállításának és a jelölési reakción körülményeinek bemutatását adja. A vizsgálatok bemutatják a ^{177}Lu- jelzett, csonthoz kötődő EDTMP molekula előállítását, valamint az egészséges állatmodell szerepét a molekula fejlesztésében: farmakokinetikai, képalkotó, és eloszlási elemzést adnak egér és nyúl illetve patkány és kutya állatfajokon. A szerző a kutya fajon elvégzett emelkedő dózisú toxicitási vizsgálatot is ismerteti. Az eredmények szerint a molekula specifikusan az átépülő csonthoz való kötődése minden fajban egyértelmű, más szervben az intravénás beadás után 1 nappal a molekula képalkotással és biodisztibúciós vizsgálattal nem mutatható ki. A szerző azt is kimutatta, hogy a molekula az átépülő csontok kortikálisához kötődik, a spongiosa állományában csak minimálisan van jelen. Kutyán a legmagasabb 37 MBq/kg injektált dózissal sem tudott kimutatni toxikus mellékhatást. Az egészséges állatmodellek alkalmazása a fajok közötti farmakokinetikai különbségek leírása miatt a humán alkalmazhatóság számára jelentős szerepet töltött be. A betegség-modell alkalmazását a szerző a második kísérletsorozatban egy szintén béta és gamma-sugárzó izotóp, a ^{188}Re által jelzett ón kolloid esetében vizsgálja. Leírja a radiofarmakon szobahőmérsékleten való előállításának reakcióját, méreteloszlását valamint ismerteti szövettani hatásait a synoviumra antigén-indukált arthritis nyúl állatmodellen. A második részben a szerző bemutatja a természetes úton megbetegedett kutyák állatmodellként való alkalmazását terápiás és képalkotó izotópokkal (^{90}Y, ^{99m}Tc, ^{111}In, ^{177}Lu) egyaránt jelezhető, daganatdiagnosztikára alkalmas szomatosztatin-analóg peptidekkel (DOTA-TOC, HYNIC-TOC). A közölt vizsgálatsorozatban a világon elsőként alkalmaztak DOTA-TOC peptidet terápiás és diagnosztikai célra kutya insulinomában. Az eredmények alapján a RIT kutyában mellékhatások nélkül, jó eredménnyel végezhető és a természetes állati daganatok modellként fontos szerepet tölthetnek be a gyógyszerfejlesztésben.

1. Introduction

Mainly based on the work by Hungarian Nobel laureate George de Hevesy, Nuclear Medicine refers to the application of radioactive isotope atoms as tracing probes in living subjects to discover their fate and their possible roles to diagnose and treat abnormalities.

Nuclear medicine provides an outstanding possibility to study details of biochemical and physiologic reactions in the organism to understand, diagnose and cure disease. It also allows quantitative characterization of different, 'invisible' and rapidly changing processes within the organism and among its cellular constituents (Wester 2007).

The classical methods of nuclear medicine, mainly based on tracing biochemical processes and reactions is being currently transformed (Weissleder 2008). New methods of in vivo nuclear imaging apply radioisotopes to trace precisely identified and tagged molecules and to detect specific, characteristic molecular signatures of cells (Weissleder 2008, Haberkorn 2002). This approach has been adding a very valuable and long-awaited complementary feature to in vivo imaging in general (Weissleder 2008). The detection and quantification of characteristic individual molecules expressed by the cells using in vivo imaging methods i.e. Molecular Imaging (D'Asseler 2009, Mishani 2009) and the well established, validated imaging methodologies of Nuclear Medicine form together such a strong basis for individual and tailored therapies that these latter have already became in fact a reality that is coming to stay (Kato 2009, Bodei 2009). The advantages offered in therapy by isotopic targeting methods do not stop at the individual dose planning and dose delivery calculation achieved by pre-therapeutical imaging (Kato 2009). It comes naturally that new advantages are present in the concept of molecule and process-based isotope applications to selectively deliver a „magical bullet" to the diseased site (Bodei 2009, Leitha 2009), and to spare collateral damage to other, healthy organs. It is widely accepted that application of molecular imaging concepts will lead to an outstanding perspective for research on cancer with a good opportunity to break out and offer cure for previously untreatable subgroups of patients (Bodei 2009).

On the other hand, pharmaceutical discovery, development and clinical tracking of drugs has been relying on classical absorption, disposition, metabolism, excretion studies that involve a considerable amount of time and carry the inherent risk of loss due to late attrition of candidate molecules. Molecular imaging using isotopes has been found to enable researchers with a total time reduction of over 20% in the life cycle of a new compound (DiMasi 2002). In vivo investigation of animal models and their appropriate choice is the basis of any feasible improvement in either understanding disease or

developing a new molecule to fight it (Hicks 2005). The recently accelerated development of highly sensitive and quantitative nuclear imaging instrumentation is greatly contributing to more and more types of animal models entering into longitudinal studies (Hicks 2005). There the course of disease is characterized many times by quantitative imaging during every single individual animal's lifespan. Thus, the already very potent mixture of a novel concept, molecular imaging and novel instrumentation combined with longitudinal imaging has been only lacking new imaging radiopharmaceuticals that embody the new concepts. These new radiopharmaceuticals are best described (Wester 2007) as molecular imaging selector agents because they are readily able to discriminate between healthy and diseased tissue possibly at the molecular level within one clinical syndrome or illness. And if an imaging radiopharmaceutical can distinguish between diseased and unaffected cells on a molecular basis, the possibility to exploit it for therapeutic purposes should not be missed.

This is the driving force behind a concept present throughout the studies of this thesis: the 'matching pair's of radiopharmaceuticals where one targeting moiety can be used to deliver a diagnostic probe or a therapeutic isotope (sometimes both in the same time) directly to the cellular level (Bodei 2009).

Veterinary medicine, the original discipline making appropriate animal model selection for imaging and therapy studies in individualized medicine possible, is benefitting twice of the process described above. First, it is called for in appropriate selection of engineered (ie. artificially created) animal models (Maggi 2005) and second, new experimental therapies and new diagnostic imaging methods or pharmaceuticals/contrast agents would be offered for companion animals in the course of veterinary clinical trials increasing in number in the last couple of years (Paoloni 2009). Veterinary nuclear medicine will integrate some of these molecular imaging and molecular therapy methods into its armamentarium (Gordon 2009) as a midterm consequence.

Ultimately clinical trials with spontaneously diseased companion animal patients are considered a unique possibility for both human and animal patients' care improvement (Paoloni 2009). Hopefully the frontier zone between human drug development and companion animal veterinary care will be more explored based also on the results presented in this thesis. In any case, the author sincerely hopes that the applications of healthy or diseased animal models and their imaging presented here offer a basis to the improvement of veterinary companion animal care, too.

2. Aims and scope of the thesis

The wide scope of the thesis is the presentation of the concept of **entwinned molecular imaging and therapy** in animal models using radioisotopes during the development of novel dual-use (that is, human and veterinary medical applications) radiopharmaceuticals and **matching pairs** of therapeutic and diagnostic pharmacons. This scope extends to presentation of the use and place of animal models in the development of radiopharmaceuticals labelled with ^{177}Lu and ^{188}Re isotopes – both emitting gamma rays for imaging and beta-particles for localized therapy. The course of this development is presented in healthy mice, rats, rabbits and dogs and in the antigen-induced arthritis model in the rabbit.

In another study series, another facet of the initial scope is presented with the work describing evaluation of matching pairs of somatostatin-receptor 2A binding peptide radiopharmaceuticals labelled with ^{99m}Tc, ^{111}In and ^{90}Y in healthy dogs and dogs with insulinoma.

The aims of the thesis are:

a) Defining the place and showing the consequences of the application of different animal models (healthy, induced disease and spontaneous disease) in the pipeline of radiopharmaceutical development.

b) Describing effects of beta irradiation to distinct, localized parts or organ systems of the body with different energies and thus different tissue penetration for the use of human and veterinary clinical therapy within the appropriate animal species exploiting the full potential of isotopic imaging with tomographic imaging techniques such as SPECT.

c) Presenting the applicability of radionuclide therapy in veterinary medicine and observing its effects.

d) Presenting the concept of isotope therapy from „molecules to models in animals” with the use of immunohistochemistry as the reference basis of molecular imaging.

3. Literature review of the most important applications of beta-emitting radiopharmaceuticals presented

Radioisotope therapy offers a generally very effective relief for a number of diseases. Most of the time a beta-emitting radioisotope is applied in human s well as veterinary patients because of the compromise between delivery of adequate dose and chemical/biochemical characteristics of the applicable carriers and isotopes this type of radiation and the available isotopes represent. Table 1. Presents the main characteristics of some selected isotopes that are typically used in the radiopharmaceuticals presented in this dissertation.

Isotope	Half-life (days)	Energy of main beta particle peak (MeV)	Maximal tissue penetration range (mm).
^{67}Cu	2,58	0,575 gamma:185 keV	1,8
^{90}Y	2,66	2,27	12
^{177}Lu	6,7	0,497 gamma: 171 keV; 210 keV	1,5

Table 1. Main beta-emitting radioisotopes and their characteristics worldwide applied in receptor isotope therapy types presented in this dissertation

3.1 Therapy of bones and joints

Patients suffering from breast, lung, and prostate cancer may develop metastasis in bone in the advanced stage of their diseases (Goeckeler et al. 1987, McEwan et al. 1999, Maini et al. 2004). These metastatic lesions in the skeleton often lead to excruciating pain and other related symptoms, such as lack of mobility, depression, neurologic deficits, and those associated with hypercalcemia, which adversely affect the quality of life (McEwan et al. 1999, Maini et al. 2004, Lewington 1996, Twycross and Fairfield 1982, Hoskin 2003). Treatment of unresectable, often incurable multiple skeletal cancer metastases is one of the major challenges of oncological practice. Most commonly used palliative treatment modalities are external beam radiation therapy, morphine-derived analgesics and bisphosphonates (Berenson et al. 2006, Cicek and Oursler 2006, Macedo et al. 2006, Mercadante and Fulfaro 2007). However, in a significant number of patients radiotherapy is not an option due to the

location or multiplicity of tumors, and the effect of analgesia is insufficient. Radiation delivered directly and in a targeted manner to the tumor cells and their microenvironment is a possible way to overcome these obstacles. Though the conventional treatment modalities, such as ad- ministration of analgesics and external beam radiotherapy, are continuing practices, their disadvantages are manifold, owing to multiple side-effects (Hoskin 1995, Mertens et al. 1992). Radionuclide therapy (RNT), employing radiopharmaceuticals labeled with β-conversion electron-emitting radionuclides, is effectively utilized for bone pain palliation, thus providing significant improvement in the quality of life of patients suffering from pain resulting from secondary skeletal metastases. (Goeckeler et al 1987, Maini et al. 2004, Mertens et al. 1992, Deligny et al. 1990, Silberstein 1996, Knapp et al. 1998). In this context, intravenous radionuclide therapy (RNT) aimed at pain palliation of incurable multiple skeletal metastases with bone-seeking agents (Anderson et al. 2002, Bauman et al. 2005) is a well-established but yet underexploited modality (Liepe et al. 2005, Macedo et al. 2006). According to the clinical trials, RNT improves the quality of life in a higher percentage of patients than applying conventional treatment methods, also in cases where morphine derivatives or bisphosphonates give less satisfactory effect (Wang et al 2003, Sartor et al. 2004, Finlay et al. 2005, Liepe et al 2005). Several isotopes (Pandit-Taskar et al. 2004, Minutoli et al. 2005) have been applied in the above-referenced studies. Currently, the most widely used and registered preparations make use of ^{153}Sm (^{153}Sm-EDTMP) and ^{89}Sr (^{89}Sr-chloride). Other isotopes coupled to bone-seeking molecules in clinical use include ^{186}Re (Liepe et al. 2000, Oh et al 2002, Minutoli et al. 2006, Li et al. 2001) and ^{188}Re (Li et al. 2001, Oh et al 2002, Minutoli et al. 2006).

The major challenge in developing effective agents for the palliative treatment of bone pain arising from skeletal metastasis is to ensure the delivery of an adequate dose of ionizing radiation at the site of the skeletal lesion with minimum radiation-induced bone marrow suppression (Volkert and Hoffman 1999, Hosain and Spencer 1992, Srivastava and Dadachova 2001). These *in vivo* features are governed by the tissue penetration range and, hence, on the energies of the *β*- particles of the radionuclides used in the radiopharmaceutical preparations.13,15,16 $Na_3{}^{32}PO_4$ [$T_{1/2}$ = 14.26 days, $E_{B(MAX)}$ = 1.71 MeV], the first radiopharmaceutical to be used in bone pain palliation, besides having no imageable gamma photon, offers the disadvantages of causing considerable bone marrow suppression owing to the presence of higher energy *β*-, which limits their widespread use (O'Mara 1978, Robinson et al. 1987) . ^{89}Sr [$T_{1/2}$ = 50.53 days, $E\beta_{(MAX)}$ = 1.49 MeV] in the form of $^{89}SrCl_2$ (Metastron®), a commercially available product, is also an efficacious bone pain palliative, owing to its selective concentration at the skeletal lesion sites having increased the osteoblastic activity by the replacement of Ca^{2+}(Robinson et al 1987, Shini et al 1990).However, the limited capacity of the production of ^{89}Sr, owing to the very low cross-

section of ^{88}Sr (5.8 mb), contributes in making this product expensive and unaffordable for many patients. (Knapp et al. 1998, Pillai et al. 2003) The other major disadvantages toward the use of this isotope are the absence of any imageable gamma photon and the requirement of an enriched target in order to avoid the coproduction of any radionuclidic contaminant (Pillai et al. 2003).

^{153}Sm [T1/2 = 46.27 h, $E_{\beta(max)}$ = 0.81 MeV, *Ey* = 103 keV (28%)] and ^{186}Re [T1/2 = 90.64 hours, $E_{\beta(max)}$ = 1.07 MeV, *Ey* = 137 keV (9%)] are the other radionuclides used for the preparation of bone pain palliatives, owing to their ideally suited decay characteristics (Ketring 1987, Goeckeler et al 1987, Singh et al. 1989, de Klerk et al.1996, Volkert and Hoffman 1999, Serafini et al. 2001, Maini et al. 2004)

Among the two radionuclides, ^{153}Sm scored over ^{186}Re owing to the ease of production of ^{153}Sm in large quantities with adequate radionuclidic purity by the neutron activation of even natural samarium (Liepe et al. 2000). Though ^{153}Sm can be produced in adequate quantities in medium flux reactors, owing to its short half-life, a substantial quantity of the isotope produced at the end of bombardment (EOB) is lost by decay during chemical processing, preparation, and quality control of radiopharmaceuticals and subsequent transportation. It is, therefore, essential to handle large quantities of ^{153}Sm activity to compensate for decay losses during the production and delivery of the radiopharmaceutical.

^{177}Lu is presently being considered as a potential radionuclide for use in in vivo targeted radiotherapy, owing to its favorable decay characteristics (Mulligan et al. 1995, Pillai et al. 2003, Chakraborty et al. 2002, Kwekkeboom et al 2003, Das et al. 2004). ^{177}Lu decays with a half-life of 6.73 days by the emission of β- particles with maximum energies of 497 (78.6%), 384 (9.1%), and 176 keV (12.2%) to stable ^{177}Hf (Firestone 1996).The emission of suitable energy gamma photons of 113 (6.4%) and 208 keV (11%) (Firestone 1996) with relatively low abundances provides the opportunity to carry out simultaneous scintigraphic studies, which helps to monitor the proper *in vivo* localization of the injected radiopharmaceutical, as well as to perform dosimetry studies. An important aspect of consideration for the countries with limited reactor facility is the comparatively longer half-life of ^{177}Lu, which provides a logistic advantage towards facilitating supply to locations far away from the reactors. Besides this, the high thermal neutron capture cross-section *(δ* = 2100 b) of the $^{176}Lu(n,y)^{177}Lu$ reaction ensures that ^{177}Lu can be produced with sufficiently high specific activity, using the moderate flux reactors. (Pillai et al 2001, Pillai et al. 2003). Considering the lower decay loss as well as the possibility of its large-scale production using a natural target, ^{177}Lu could be a cost-effective alternative to ^{153}Sm for bone pain palliation. The low-energy, low-yield [E_Y=113 keV (6.4%), 208 keV (11%)] gamma photon emissions of ^{177}Lu allow scintigraphic detection of the tracer in vivo to estimate the dose in individual patients. The energies of *β*- particles from ^{177}Lu are adequately low, and hence, its tissue

penetration range is considerably lower than that of ^{89}Sr, ^{32}P, and even, to some extent, than the β- particles of ^{153}Sm or ^{186}Re (Brenner et al. 2001). The low range induces minimum bone marrow suppression on accumulation in skeletal lesions, which is a major advantage of this radiotherapeutic modality (Bishayee et al. 2000, Srivastava and Dadachova 2001, Chakraborty et al. 2002). The lower beta-particle energy and relatively long physical half-life allow the deposition of an adequate tumor irradiation dose with a constant dose rate (Bernhard et al 2001, Syme et al. 2004). A model calculation published suggests that ^{177}Lu is the optimal radionuclide for full beta-particle energy deposition in small tumor volumes (Bernhard et al. 2004)

Multidentate aminomethylenephosphonic acids form stable complexes with different radionuclides and have been already proven to be very effective for the palliation of bone pain (Laznicek et al. 1994, Banerjee et al. 2001). It is well documented that cyclic polyaminophosphonic acid ligands form thermodynamically more stable and kinetically more inert complexes with lanthanides, compared to their acyclic analogs (Volkert and Hoffman 1999, Caravan et al 1999, Liu and Edwards 2001).Thermodynamic stability of the metalloradiopharmaceutical is a very important aspect, as the dissociation of the radiometal from the chelate in blood circulation may result in the accumulation of radioactivity in nontarget organs, while kinetic inertness also plays a significant role for the *in vivo* stability of a metal chelate (Volkert and Hoffman 1999, Liu and Edwards 2001). However, for the present study, ethylenediaminetetramethylene phosphonic acid (EDTMP) was chosen as the carrier molecule, owing to the excellent success of ^{153}Sm-EDTMP (Quadramet®) as an agent for bone pain palliation resulting from skeletal metastasis. This agent shows excellent pharmacokinetics, such as preferential localization in osteoblastic lesion and rapid excretion of the residual activity through the kidneys, both in animals and human patients. (Singh et al. 1989, Lattimer et al. 1990, Volkert and Hoffman 1999, Laznicek et al. 2001, Maini et al. 2004). Systemic application of ethylene diamine-N,N,N',N'- tetrakis(methylene phosphonic acid) (EDTMP) labeled with ^{153}Sm as a bone-seeking agent has been studied and applied in clinical practice in a large number of patients for more than two decades (Sartor 2004, Coronado et al 2006, Sartor et al. 2007). The clinical efficacy of this radiopharmaceutical is well demonstrated (Brenner et al. 2001, Anderson et al. 2002, Wang et al. 2003, Sartor 2004, Sartor et al. 2004, Coronado et al. 2006, Macedo et al. 2006, Sartor et al. 2007) . However, the short half-life of ^{153} Sm ($T_{1/2}$ 47 h) has been the major impediment, making its transportation difficult and thereby limiting its wider use.

Since Lu^{+3} has similar coordination chemistry as that of Sm^{+3}, it is pertinent to envisage the EDTMP complex of ^{177}Lu, expecting the pharmacokinetic properties of the agent to be similar to that of ^{153}Sm-EDTMP. Working in this direction, we have standardized the preparation of

the ^{177}Lu-EDTMP complex and studied its biologic behavior in different animal models, with an aim to develop a suitable ^{177}Lu-based viable alternative of ^{153}Sm-EDTMP.

A variety of cyclic and acyclic polyamino-polyphosphonates were evaluated as potential radiopharmaceuticals (Liepe et al. 2000, Li et al. 2001, Brenner et al. 2001, Oh et al. 2002, Chakraborty et al 2002, Ogawa et al. 2007). In comparative evaluation studies of the ^{177}Lu complexes of different acyclic and cyclic phosphonate ligands, DOTMP and EDTMP were found to give superior results over other phosphonates (Chakraborty et al. 2002, Das et al. 2002, Das et al. 2008). As already sufficient data are available on the biological tolerance ofthe ligand EDTMP as well as the radiopharmaceutical ^{153}Sm-EDTMP, EDTMP was selected as the carrier ligand for the presented studies (Ando et al. 1998, Rutty Solá et al. 2000, Chakraborty et al. 2002). It was felt that replacing the radionuclide ^{153}Sm with ^{177}Lu in the EDTMP complex will pose minimal additional chemical or radiological toxicity issues. Consequently, first a detailed study on the biodistribution and imaging of ^{177}Lu-EDTMP in rats, rabbits and beagle dogs was conducted. In later studies, we aimed at obtaining detailed biodistribution and pharmacokinetic parameters of ^{177}Lu-EDTMP in several species to study the pharmacological effects. Mouse, rats, rabbits and dogs were used for the biodistribution and imaging studies. Data from the biodistribution studies were used to calculate pharmacokinetic parameters based on a noncompartmental model. Skeletal retention of the agent and its potential radiotoxic effects were studied by injecting ^{177}Lu-EDTMP activity at different levels in beagle dogs.

After the main application field of bone metastasis pain palliation in the case of bones, in the case of bone articulations, the highest incidence of a disesase that can be treated using radioisotope therapy is that of rheumatoid arthritis. Radiation synovectomy is a technique whereby a beta-emitting radiopharmaceutical is delivered into the affected synovial compartment in order to treat rheumatoid arthritis. Beta-emitting radiocolloids are widely used for this purpose. The ideal radionuclide would possess beta emission with a sufficient energy for a maximum tissue penetration of 5 to 10 mm, gamma emission suitable for gamma camera imaging, a short half-life, and ready availability. A ^{198}Au colloid was first used for radiocolloid synovectomy and this isotope has been continuously investigated (Ansell et al. 1963, Ahlberg et al. 1969, Atkins et al. 1979). The main drawbacks of a ^{198}Au colloid are the 411 keV gamma emission which creates an unnecessary radiation hazard, the small particle size, which results in excessive loss from the joint space by lymphatic drainage, and high radiation doses to the proximal lymph nodes. The high costs have also impeded its routine application. Other radiopharmaceuticals containing isotopes such as ^{32}P and ^{90}Y, have been used as alternatives to ^{198}Au, and show less leakage from the joint (Gumpel et al. 1973, Jalava 1973, Tully et al. 1974, Howson et al. 1988). The generator-produced ^{188}Re recently became practically available (Knapp et al 1995, Knapp et al 1997). It has also

extensively been investigated coupled to phosphonate analogs in the field of bone pain palliation, too. (Brenner et al. 2001, Liepe et al. 2000, Liu et al. 2001, Ogawa et al. 2007). Among the ^{188}Re-labelled colloids, ^{188}Re-sulfur colloid has been most extensively investigated (Venkatesan et al. 1990, Wang et al. 1995, Grillenberger et al. 1997, Kim et al 1998) and the use of ^{186}Re-sulfur colloid has also been reported (Venkatesan et al 1990). ^{188}Re-hydroxyapatite has been studied for radiation synovectomy as a biodegradable colloid (Grillenberger et al 1997) and a ^{188}Re microsphere has been introduced for radiation synovectomy (Wang et al. 1998). Jeong et al. studied (Jeong et al 2001) the preparation and use of a ^{188}Re-tin colloid and reported that it is more suitable than a ^{186}Re-sulfur colloid in stability, labeling efficiency and residual radioactivity. Our experiments were designed to study the circumstances of preparation of ^{188}Re-tin colloid and to evaluate its suitability for radiosynoviorthesis in conjunction with dosimetric aspects. On the other hand we aimed at presenting the use of an artificially created animal model for the evaluation of this new radiopharmaceutical.

3.2 Somatostatin receptor radionuclide therapy

In human and veterinary clinical practice most frequently overexpression of somatostatin receptor subtypes is targeted on tumor cells. The isotope atom bound to overexpressed receptors on cell surfaces will be internalized, thus it provides local information by staying inside of the cell-or can exert local therapeutic effects within it.

Somatostatin (SS) was identified by Brazeau and his coworkers (Brazeau et al. 1973) as the factor inhibiting secretion of growth hormone. SS itself exists in the body as two polypeptides each made up of 14 or 28 aminoacids. Its main secreting organs are the central nervous system, the gastrointestinal system and its nervous system and the system of endocrine glands. Its effect is mediated through a family of G-protein coupled 7-transmembrane domain receptor family (ssr). Up to now five subtypes of the receptor are known, abbreviated as ssr_{1-5}. In this grouping, alternative splicing of the protein of ssr_2 leads to ssr_{2a} and ssr_{2b} isoforms (Hoyer et al. 1995, Patel 1999). One or more types of somatostatin receptors are expressed over almost all surfaces of all cells of the body (Hoyer et al. 1995). Generally speaking, somatostatin effects mediated by these receptors inhibit all signals and processes of cell division, production of hormones and cytokines or for example starts the process of apoptosis by ssr_3 receptoron in tumor cells (Hoyer et al. 1995, Sharma et al. 1996). These effects of SS were worthy of exploitation for pharmaceutical purposes, thus early after its discovery started the application and experimentation with the pharmaceutical effects of SS (Hoyer et al. 1995, Rohrer et al.1998).

Because in the meantime somatostatin in its native form has an extremely short half-life, structure of artificial somatostatin analogues was based on unnatural D-aminoacid, while

preserving the loop made up of Phe^{7}, Lys^{9}, Thr^{10} aminoacids. Three peptide molecules were synthetized as a result of the research that have finally gained acceptance and gained marketing authorization and wider clinical application in practice (Lamberts et al 1996, Oberg 1998). All three are composed of eight aminoacids, have a longer blood half-life than that of SS and are used for injection therapy: octreotide {Aminoacid composition: (D) Phe-Cys-Phe-(D) Trp-Lys-Thr-Cys-Thr(ol), code name:SMS 201-995, marketed name Sandostatin®}, lanreotide { Aminoacid composition: (D) bNal-Cys-Tyr-(D) Trp-Lys-Val-Cys-Thr-NH2, code name BIM-23014, marketed name Somatuline®} and vapreotide {(D) Phe-Cys-Tyr-(D) Trp-Lys-Val-Cys-Trp-NH2, code name RC-160, marketed name: Octastatin®}. Among these three molecules, in man octreotide is the one that is most widely used (Virgolini et al 2002); it has as well as gained use in dogs (Lamberts et al. 1990, Robben et al. 2006). Octreotide is most frequently used for adjuvant and endocrine therapies and in the case of chronic untreatable, refractory pain (Newsome et al. 2008).

Octreotide's highest affinity is presented towards a ssr_{2a} –receptors. This is the very receptor in the same time that is best suited to distinguish tumor cells from the normal ones. Tumors arising from the neuroendocrine system or showing neuroendocrine traits (gastrinoma, glucagonoma, phaeochromocytoma, insulinoma, VIPoma, small cell lung cancer) and some other types of tumor cells (medullary thyroid cancer, some mammary cancers, lymphomas, haemangiopericytoma, other tumor of mesenchymal origin, the majority of hepatocellular carcinomas (Bakker et al. 1991, Reubi et al. 1996, Oberg et al. 1998, Jan de Beur 2002, Dalm 2003) will overexpress somatostatin 2a receptors on their surface membrane. To these overexpressed receptor much more somatostatin-analog ligand is bound than to healthy tissues.

Therefore in case of binding an isotope atom to one of these SS analog molecules the labelled octreotide (or other ssr_{2a} ligands with similar qualities) are capable of distinguishing tumorous and non-tumorous cells.

It is worth mentioning that some other cell types that have a prominent role in tumor biology, besides tumor cellss can also show $ssr_{2,5}$ –positivity. These cell types are activated lymphatic cells and budding endothelial cells (Serafini 1995, Talme et al. 2001, Woltering 2003). First mention about exploiting overexpression of surface ssr_{2a} receptors in tumor cells by the means of scintigraphic imaging human clinical application was coming from the team at Rotterdam University and Kantonsspital Basel in 1989 (Krenning et al. 1989). This method of (earlier ^{123}I, acutally almost exclusively ^{111}In, ^{99m}Tc ^{68}Ga) labelled octreotide analogue molecules is applicable to prove the presence of ssr_2-expressing tumor cells and since then has developed itself to an important diagnostic tool. Worldwide several tens of thousands of studies have already been completed using it (Krenning et al. 1993, Reubi et al. 2008, Bodei

et al. 2009). General structure of somatostatin receptor ligand molecules used for isotope scintigraphy or therapy are presented in **Figure 1.**

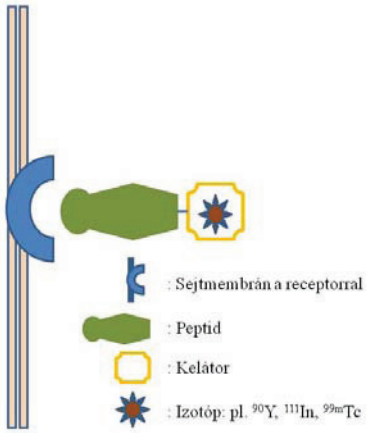

Figure 1. Schematic structure of ligands used for peptide receptor isotope diagnostics and therapy. The peptide is the delivery vector of the isotope bound by the chelator to the cell surface receptor.

In clinical practice mostly the ^{111}In (indium)-labelled diethylene-triamine-pentaacetic acid (DTPA)-Phe-octreotide (pentetreotide, OctreoScan®) is applied for imaging studies.
However, the applied ^{111}In radioisotope is hard to obtain, its imaging features are not optimal, its delivered radiation internal dose is too high, and the carrier pharmaceutical and the isotope itself is very expensive, too. That's why at the beginning of the years 2000 two different peptide molecules were developed (Decristoforo et al. 2000, Hubalewska-Dudejczyk et al. 2005, Hubalewska-Dudejczyk et al. 2007, Goldsmith 2009), that can be labelled by ^{99m}Tc an isotope with much more advantageous imaging propertied and very widely accessible with a solid stability. ^{99m}Tc atom is chelated using a hydrazino-nicotinic acid moiety (HYNIC) and an ethylene diamine diacetic acid (EDDA) coligand molecule. These chelator peptide molecule are HYNIC-T-Octreotide és a HYNIC-Octreotate. The full short name of the labelled radiopharmaceutical is thus ^{99m}Tc-EDDA-HYNIC-TOC and ^{99m}Tc-EDDA-HYNIC-TATE, but mostly HYNIC-TOC and HYNIC-TATE abbreviation is used (Figure 2.).

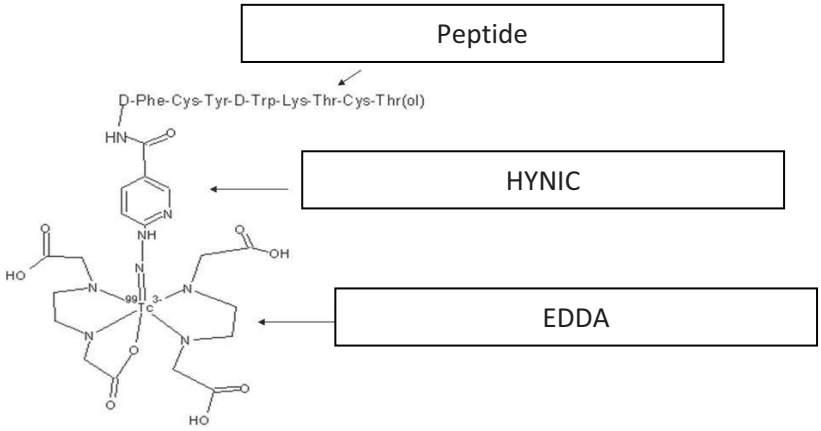

Figure 2. Structure of EDDA-HYNIC-TOC molecule conjugated to ^{99m}Tc. One HYNIC and two EDDA molecules coordinate one ^{99m}Tc.

These latter peptides will surely represent an impprtant role in the future in clinical diagnostics because their affinity to ssr_{2a} is higher, their radiation burden is much less, than that of OctreoScan. The ^{99m}Tc isotope used for labelling is cheap and there is no need to wait for the deliveries of the otherwise expensive ^{111}In-isotope.

Based on the possibilities described above, we have the potential to first identify tumor cells using imaging with a diagnostic isotope, and then we can deliver a therapeutic isotope to those identified tumor cells. This approach is called combined isotope diagnostics and therapy. Basicly using the diagnostic molecule we make a prognostic statement about the success of the therapy performed by a different isotope maybe with a different chelator but the same ligan SS analog.

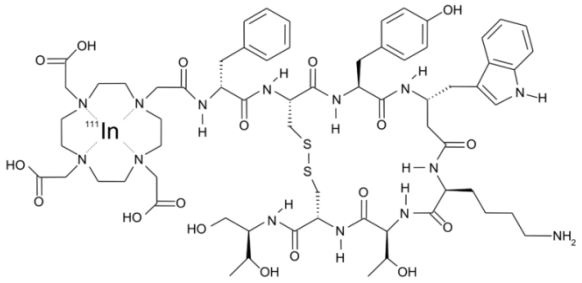

Figure 3: Structure of ^{111}In-DOTA-T-Octreotide. ^{111}In is coordinated by DOTA, the macrocyclic chelator.

Several pairs of isotope-chelator-peptide systems are suitable for the application to combined receptor isotope therapy. The most prominent ones are shown in Table 1 together with their receptor affinities. Isotopes for therapy are presented in Table 2 together with their radiation characteristics.

Peptide molecule	Chelator	Labelling isotope(s)	Somatostatin receptor affinity (K_d, nM)	Clinical uses
(D)Phe^1-Octreotide	DTPA	^{111}In	Ssr 2a: 22 Ssr 3: 182 Ssr 5: 237	Diagnostics (therapy in extremely high doses)
Tyr^3-Octreotide	DOTA	^{111}In, ^{177}Lu, ^{90}Y	Ssr 2a: 11 Ssr 3: 389 Ssr 5: 114	Diagnostics, Therapy: ^{90}Y-DOTA-TOC
Tyr^3-Octreotide	HYNIC	^{99m}Tc	Ssr 2a: 2,65 Ssr 3: n.a5. Ssr 5: n.a.	Diagnostics
Octreotate	DOTA	^{111}In, ^{177}Lu, ^{90}Y	Ssr 2a: 1.6 Ssr 3: 523 Ssr 5: 187	Therapy: ^{177}Lu-DOTA-TATE
Octreotate	HYNIC	^{99m}Tc	Ssr 2a: <2.65 Ssr 3: n.a. Ssr 5:n.a.	Diagnostics

Table 1. Octreotide analogue peptide radiopharmaceuticals used in peptide receptor diagnostics and therapy and their receptor binding. K_d is the dissociation constant, its lower values represent stronger receptor binding. n.a.=no data available

Isotope	Half-life (days)	Energy of main beta particles (MeV)	Mean tissue penetration range (mm)
^{67}Cu	2.58	0.575 gamma:185 keV	1.8
^{90}Y	2.66	2.27	12
^{177}Lu	6.7	0.497 gamma: 171 keV; 210 keV	1.5

Table 2. Main beta-emitting radioisotopes and their characteristics applied in receptor isotope therapy.

(A ^{111}In isotope emits Auger-electrons as well, thus in very high doses it can be applied for therapeutic purposes. This type of radiation dose will be delivered by the isotope atoms around the cell nucleus and will damage the DNA when deposited there.) Definition of receptor status using combined diagnostics is made by PET or SPECT examination with the help of one of the diagnostic peptide radiopharmaceutical.

This does not necessarily mean that the same identical kinetics and receptor binding is present in the case of the diagnostic pharmaceutical as it is its therapeutic counterpart, but in general it is considered a good approximaton of therapeutical biodistribution when only an isotope and a chelator molecule differ.

DOTA-TOC (Smith et al. 2000, Bodei et al. 2009), is a molecule that enable us to perform combined radioreceptor diagnostics and therapy (cf. Table 1): receptor binding is only defined by the differing isotope between diagnostic and therapeutic molecules not even by the chelator. So the consequence from diagnostics and its receptor isotope binding to therapy is much more reliable. Because the electrons (beta-particles) emitteg by the mentioned therapeutic isotopes differ in their mean tissue penetration ranges, higher energy particles deposited by ^{90}Y are more useful for the treatment of bigger, more bulky tumors whereas smaller energy electrons from ^{177}Lu will be more suited to the treatment of smaller, disseminating or metastatic nodules – in the actual human clinical practice this point is also taken into consideration (Brans et al. 2007, Bodei et al. 2009). In the same time the most important side effect of therapy must also be taken into consideration: late onset renal failure caused by the irradiation of kidney-bound radiopeptide molecules (Forrer et al. 2004, Esser et al. 2006, Stoeltzing et al. 2009). That is why it is very important how one will choose the radiopeptide to perform therapies using the options available.

Clinical examination of the radiopeptides available shows that smallest kidney peptide binding and in the same time higher ssr_{2a}-affinity is characteristic to ^{90}Y-DOTA-TOC and ^{177}Lu-DOTA-TATE molecules (Forrer et al. 2004, Esser et al. 2006). Of course these points of view and principles were defined in human clinical practice but we should think about their application in dogs, too.

Earlier scintigraphic studies have been performed in some cases in tumorous dogs using n^{111}In-labelled OctreoScan (Altschul et al. 1997, Robben et al. 1997, Lester et al. 1999, Robben et al. 2005, Garden et al. 2005). So far gastrinoma (Altschul et al. 1997) and insulinoma (Robben et al. 1997, Lester et al. 1999, Robben et al. 2005, Garden et al. 2005) have been diagnosed using the method in dogs. Data available to today witness that like in humans (Robben et al. 2005) dog insulinomas also express and overexpress (Robben et al. 2005, Garden et al. 2005) sst_{2a} in dogs. However radioisotope diagnostic data can be considered quite loose, elég (altogether the mentioned 5 imaging studies have ever been presented (those date between 1997 and 2005) and 3 are case studies).

4. General introduction to the studies

4.1 Bone and joint therapy

4.1.1 Studies on ^{177}Lu-EDTMP for bone therapy

The application of palliative drugs for irretractable metastatic cancer pain has been one of the most prominent fields of success of modern-day Nuclear Medicine. As particles of radiation transfer their energy to cells of tumorous origin and their microenvironment, selective effect is exerted upon the metastasis. Palliation is attributed to a number of intercellular signal communication channels caused by the bystander cell effect (where intact cells neighbouring the cell hit by radiation also start to enter to apoptosis) and partly by apoptosis or radiation-mediated cell kill of tumor cells. We have studied the possibility of obtaining an easy-to-access beta-particle emitting lanthanide radionuclide ^{177}Lu as a nuclear reactor product in the framework of a Hungarian-Indian joint research programme. We examined and established the caracteristics of a production reaction of the linear aminophosphonate EDTMP and its labelling reaction with ^{177}Lu. The application and biodistribution of the labelled radiopharmaceutical was imaged in the rat, rabbit and dog species together with an ex vivo rat biodistribution study. The applicability of ^{177}Lu- EDTMP as a bone targeting agent with no other organ system accumulation is henceforth presented. ^{177}Lu is a widely used and promising radioisotope with short range beta emission and gamma radiation suitable to imaging. Its radiation properties are well suited to palliative therapy of metastases located in the bone compartment as the absorption of beta particles is confined to the immediate cells surrounding the uptake site of the radioisotope. Bone remodeling is characterised by free calcium-hydroxy-apatite surfaces. Phosphonates, such as EDTMP are readily able to distribute from blood to bone compartment and adsorb onto available calcium hydroxyapatite on remodeling bone. The remodeling pace of osteobastic metastases exceeds normal bone remodeling thus the agent is preferentially localized in this type of cancer metastasis to bone. A new pharmaceutic formulation of the organic phosphonate molecule ethylene-diamine tetra-methyl phosphonate has been labelled with ^{177}Lu. As interspecies differences are highlighting the mechanisms behind uptake and distribution into bone, we estimated pharmacokinetic parameters of the compound in mice and rabbits. For biodistribution imaging, rats, rabbits and dogs equally have been injected with non-therapeutic doses of activity. Scintigtigraphic and tomographic imaging was performed (together with CT in the rodent species) to study biodistribution over time. For any radiation dosimetric analysis it is important to establish data on the kinetics of the agent. To this end we have chosen the noncompartmental model and analysed interspecies differences in

pharmacokinetics. Finally in dogs we have conducted a study to achieve data for the definition of Maximal Tolerated Dose (MTD) and to examine toxic side effects of different, gradually increasing doses of intravenously injected activity.

4.1.2 Application of ^{188}Re-tin colloid in a rabbit model of rheumatoid arthritis

Radionuclides of a given decay chain produced by fixing their mother elements on a chromatography column in a shielded container (a „generator") and collected by elution of the here described „generator" are offering an attractive logistics advantage of on-the spot and on-demand availability. One of the actually proposed beta-emitting radionuclides for internal radioisotope therapy, ^{188}Re is available from a generator. Besides its beta emission, just like ^{177}Lu, ^{188}Re also emits We designed a series of experiments to produce a local therapeutic agent, ^{188}Re-tin colloidal particles for intra-articular use. We have chosen the animal model of rabbit antigen-induced arthritis for the proof-of-concept testing of the effects of the radiopharmaceutical, and we characterized the labelling reaction, the size distribution and the consequent radiation dosimetry of the particles while imaging its intra-articular application. We also examined the effects of irradiation delivered by the particles onto the synovial surface using histological specimens of the animal model. The results obtained in our study provided a basis of safe application of ^{188}Re-tin colloid in human knee joint in a clinical trial setting that has since been made reality by prof. Jae Min Jeong and his co-workers in the Republic of Korea (Lee 2003, Shin 2007).

4.2 Somatostatin receptor radionuclide therapy

In the course of development of molecular imaging and molecular therapy using radioisotopes targeted on tumor cells peptides and especially somatostatin receptors have a prominent role. Many tumor types express somatostatin receptors on their surface and in a lot of cases an over-expression has been found. We have been developing the use of spontaneous animal tumors as models to study molecular imaging and therapy based on peptide receptors (dubbed peptide receptor scintigraphy and peptide receptor radionuclide therapy). In this field exploiting expression and over-expression of somatostatin 2A receptors on tumor cells has the most important role as a well circumscribed subset of neuroendocrine tumors over-expresses this surface receptor. To our knowledge the overexpression of somatostatin 2A receptors is also a phenomenon in naturally occurring dog tumors. As in humans, in dogs also tumor cells mainly of neuroendocrine origin express the receptor subtype. Thus the search of such tumors is reduced to a relatively smaller subgroup of dog patients with mostly very infrequent occurrence. We have selected insulinoma of dogs to model human disease and to be the subject of our studies. This decision was taken with

regard to dog insulinoma's relatively less infrequent incidence and former data on proven receptor expression in dogs with this type of tumor. We examined the possibilities of imaging somatostatin 2A receptors with novel targeting peptides previously not utilized in the dog. The peptides are derivatives of somatostatin-analogue octreotide and contain unnatural amino acids to prevent fast enzymatic cleavage and excessively short blood half-life. As the peptides are agonists of the somatostatin receptor, they will be internalized after having bound the cell surface protein. Their „load" coupled to the peptide with a partly covalently attached chelator system will thus remain in the cell.

These peptides are capable of being labelled with different isotopes, using the same peptide vector but a different chelator system for ^{99m}Tc and for trivalent metal ions like ^{90}Y, ^{111}In and ^{177}Lu. We have applied the dual strategy of diagnosing the receptor expression using radiolabelled peptides with a suitable isotope for diagnostics, and thus exploring the possibilities of subsequent radiopeptide therapy. We also applied a radiopeptide first labelled with a diagnostic isotope (^{111}In) in the subsequent therapeutical setting where the same peptide was labelled with a therapeutic beta-emitting isotope (^{90}Y). A dog with advanced insulinoma tumor was treated this manner and we observed an outstanding 19-month survival after treatment. Also modelling human applications, therapy was conducted in two cycles 4 weeks apart applying 185 and 370 MBq of radioactivity intravenously. We have followed the status and side effect profile of the dog treated during the course of 19 months and found no abnormalities and signs of side effects. The effects of therapy included total symptom-free period for 17 months, decreases in plasma insulin levels below the normal limit immediately after therapy and stable decrease of insulin level to half of the originally measured pre-therapeutical level during the course of the disease. We considered the effect of therapy as a partial remission and symptom-free survival. The detected tumor itself became undetectable using the same ultrasound reference as for the diagnostic workup.

This approach has led us to state that dog insulinomas are good models of somatostatin receptor 2A binding radioligand diagnostics and therapeutics and that both diagnosis and therapy are given impressive results with the use of PRRS/PRRT in spontaneous dog tumors expressing somatostatin receptor 2A.

5. Presentation of experimental studies

5. 1 Biological evaluation of beta-emitting radiopharmaceuticals for the therapy of bone and joint system

5.1.1 Healthy animal studies on a novel ^{177}Lu-labelled ethylene-diamine tetrakis methylene diphosphonate preparation

a) Materials and Methods

Production of ^{177}Lu

Natural lutetium oxide (Spectroscopic grade >99.99% pure, 2.6% ^{176}Lu), used as the target for the production of ^{177}Lu, was obtained from American Potash Inc. 1,2-ethylenediamine, orthophosphorus acid and formaldehyde used for the synthesis of EDTMP were procured from Aldrich Chemical Company. All other chemicals used were of AR grade and were supplied by reputed chemical manufacturers. Whatman 3 MM chromatography paper (UK) was used for paper chromatography and paper electrophoresis studies. ^{177}Lu was produced by the irradiation of natural Lu_2O_3 (2.6% ^{176}Lu) target at a thermal neutron flux of ~6 X 1013 n/cm^2.s for a period of 21 days. The radiochemical processing of the irradiated target to obtain $^{177}LuCl_3$ solution used for the preparation of ^{177}Lu-EDTMP complex, as well as the assay of ^{177}Lu activity and its radionuclicidic purity, were carried out following the procedure reported in the literature (Pillai et al. 2001).

FT-IR spectra of synthesized EDTMP were recorded by using a Jasco FT/IR-420 spectrophotometer. ^{1}H- and ^{31}P-NMR spectra were recorded in a Varian VXR 300S spectrometer at 300 MHz for ^{1}H and 121.4 MHz for ^{31}P, using D_2O as the solvent.

The activity assay, as well as the determination of radionuclidic purity of ^{177}Lu that was produced, was carried out by high-resolution gamma ray spectrometry, using an HPGe detector (EGG Ortec/Canberra detector) coupled to a 4-K multichannel analyzer (MCA). 152Eu reference source used for both the energy as well as the efficiency calibration of the detector was obtained from Amersham Inc. All other radioactivity measurements were carried out by using a NaI(Tl) scintillation counter on the adjustment of the baseline at 150 keV and keeping a window of 100 keV for utilizing the 208-keV (11%) y-photopeak of ^{177}Lu for detection.

Synthesis of EDTMP

The direct synthesis of the α-aminomethylphosphonic acid, that is, EDTMP have been achieved by using orthophosphorus acid, 1,2-ethylenediamine, and formaldehyde by following a Mannich-type reaction in strong acidic medium. To a solution of 3.3 g (40.24 mM)

of anhydrous orthophosphorus acid in 5 mL of concentrated HCl, 0.60 mL (9.55 mM) of 1,2-ethylenediamine was added slowly. The mixture was refluxed and 3.6 mL of 36% formaldehyde was added dropwise over a period of 15 minutes to the refluxing mixture. The refluxing was continued for another 2 hours, and subsequently, the mixture was cooled to room temperature. The reaction mixture was concentrated under a vacuum and kept at room temperature, whereby EDTMP was precipitated. The crude product was recrystallized from hot water to obtain 3.83 g (92%) of purified product (melting point, 215°C). The scheme for the synthesis of EDTMP is given in Figure 4.

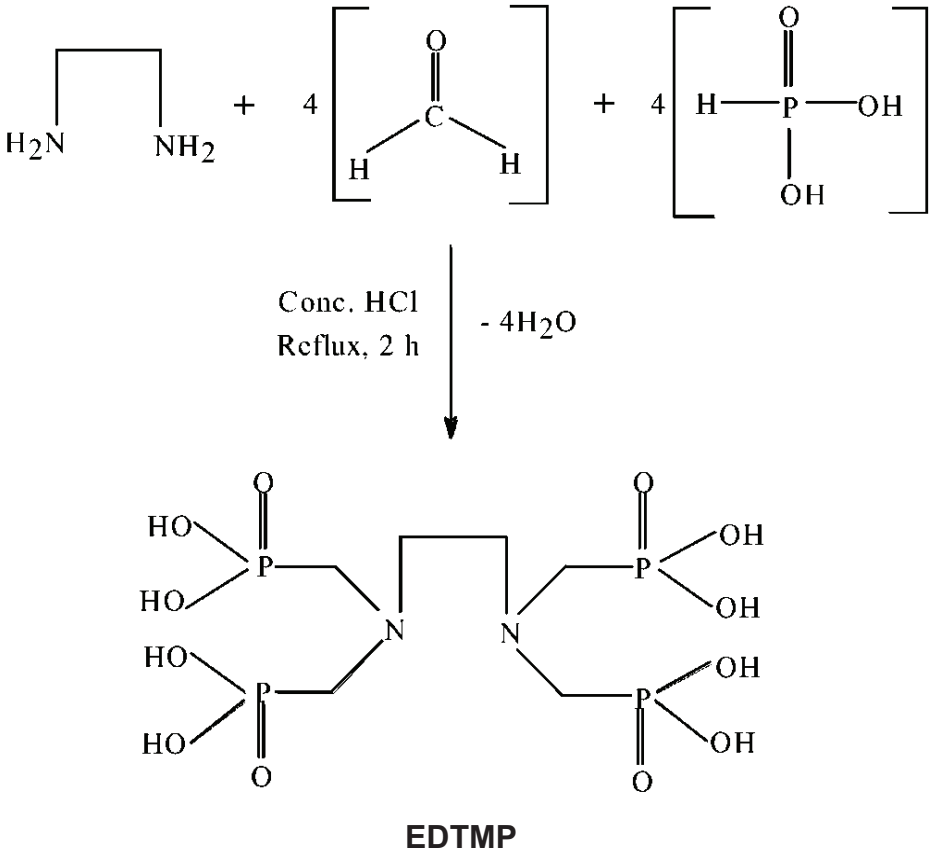

Figure 4. Scheme for the synthesis of ethylenediaminetetramethylene phosphonic acid.

Preparation of ^{177}Lu-EDTMP

For the preparation of ^{177}Lu-EDTMP complex, 35 mg (80.28 *μM)* of EDTMP was dissolved in 0.4 mL of 0.5 M $NaHCO_3$ solution (pH ≈9). To the resulting solution, 0.01-0.2 mL of ^{177}LuCl3 solution [0.09-1.85 GBq (2.5-50 mCi) of ^{177}Lu activity, 0.01-0.2 mg (0.057-1.14 μM*)* of Lu] was added, followed by the addition of the required volume of normal saline, such that the final volume of the reaction mixture was 1 mL. The pH of the reaction mixture was kept within the range of 5-8, and it was incubated at room temperature for 15 minutes to facilitate complexation. The complexation yield and radiochemical purity of ^{177}Lu-EDTMP was determined by employing paper chromatography, using ammonia:ethanol:water (1:10:20 v/v)

as the eluting solvent and paper electrophoresis techniques, as reported earlier (Chakraborty et al. 2002)

The stability of the ^{177}Lu-EDTMP complex was studied by incubating the complex (prepared using 80.28 μM of EDTMP and 1.14 μM of Lu) at room temperature for a period of 30 days (>4 half-lives of ^{177} Lu) after preparation. The radiochemical purity of the complex was determined at regular time intervals by employing standard quality-control techniques.(Chakraborty et al. 2002)

Biodistribution and imaging studies in mice and rats

^{177}Lu-EDTMP was injected in CD-1 mice intravenously via the tail vein using a microsyringe (Hamilton Co., Switzerland), and the mice were sacrificed at different time points starting from 30 min and ending at 8 week pi of the tracer. Five animals were taken for each time point. For the early time points (0.5 to 24 h), 8-10 MBq of ^{177}Lu-EDTMP activity in a volume of 30 |il was injected. For the intermediate time points (2 to 5 days), 26-30 MBq of activity in a final volume of 30-50 μl and, for late time points (1 to 8 weeks), 46-50 MBq in a volume of 60-120 μl were applied. At the appropriate time points, mice were euthanized with intraperitoneal injection of a veterinary euthanasia agent, T-61 ad us. vet. (Bayer, Inc., Leverkusen, Germany). Organs of interest were dissected, washed, dried and weighed. These included femur bone, bone marrow, muscle, heart, lung, liver, kidneys and thyroid glands. For thyroid, the larynx and the first two cartilages of the trachea were included. A total of 0.2-0.5 ml of blood was collected by cardiac puncture to measure the blood activity. Bone marrow samples were obtained by rinsing a random femur head, lumen and condyli with 0.5 ml of physiological saline and collecting the washing fluid together with the resulting mass of bone marrow. Radioactivity was measured in a well-type gamma counter (NZ-310, Gamma, Hungary) previously calibrated for ^{177}Lu. In mice, percent organ contribution to body mass was assumed as bone mass 10%, blood 8%, bone marrow 8% and muscle 27% of body mass.

SPECT-CT studies

Three CD-1 mice were injected with 50 μl (30 MBq) of ^{177}Lu-EDTMP. Three hours postinjection, mice were anaesthetized by intraperitoneal injection of ketamine [4 mg/kg body weight (bw)] (SBH-Ketamin, SBH Ltd.) and xylazine (1 mg/kg bw) (Xylavet, Alfasan, Holland). A dedicated small animal imaging system, NanoSPECT/CT (Mediso) equipped with a multiplexed multi-pinhole (nine pinholes, aperture 1.4 mm) collimator was used to acquire whole-body SPECT/CT images. Energy window was centered at 208 keV with ±10% width

for all imaging studies. Acquisition times were defined to obtain 100 000 counts for each projection with 24 projections. Images and maximum intensity projections (MIPs) were reconstructed using the dedicated software Invivoscope (Bioscan, Inc., Washington, USA) and Mediso InterViewXP (Mediso).

Autoradiography in mice

For whole-body autoradiography, three mice were injected intravenously with 5 MBq of ^{177}Lu-EDTMP. The animals were euthanized at 3 day p.i. and frozen in liquid nitrogen. Fifty-micrometer-thin cryostat sections were pre pared using Leica CM 3600 instrument (Leica Co., Germany). The sections together with activity standards containing 0.18, 1.8 and 9.2 kBq were exposed to phosphor imaging plates (Molecular Dynamics Phosphor Imager, GE Healthcare, USA).

Imaging studies for biodistribution measurements in rats

The biologic behavior of the ^{177}Lu-EDTMP complex was also ascertained by carrying out simultaneous scintigraphic imaging studies in normal Wistar rat, too. Then, 0.1-0.2 mL (15-20 MBq of ^{177}Lu) of the complex solutions were injected through the tail vein of the animals, weighing ≈250-300 g. Sequential scintigraphic images were acquired in the single-head digital SPECT gamma camera at 30 minutes, 1, 3, 24, 48, 96, and 168 hours postinjection, using a LEHR col- limator to determine the *in vivo* localization of the injected radioactivity. Prior to the acquisition of the images, the animals were anesthetized by using a combination of xylazine hydrochloride and ketamine hydrochloride. The gamma camera was previously calibrated for the 208-keV gamma photon of ^{177}Lu with a 20% window. All the images were recorded by acquiring 500 Kcounts, using a 256 X 256 matrix size. Blood samples were also drawn from the animals at the above-mentioned time points and counted to ascertain ^{177}Lu activity, if any, present in the blood.

SPECT Imaging studies in rats

Forty megabecquerel of ^{177}Lu-EDTMP was injected into the tail vein of three rats and imaged after 3 h using the NanoSPECT/CT system. The anaesthesia and imaging parameters used were the same as described above except that a pinhole aperture with 2.0 mm in diameter was applied.

Biodistribution and imaging studies in rabbits

Three New Zealand white rabbits (Biofarm, Ltd., Hungary) were used for each time point varying from 30 min to 8 weeks. ^{177}Lu-EDTMP tracer was injected via the auricular vein. Rabbits used for early time points (30 min to 1 week) received 100 MBq (in 0.3-0.4 ml), while the ones used for later time point studies received 200 MBq (in 0.6- 0.7 ml) of activity. Animals were anaesthetized with intramuscular injection of ketamin (dose 100 mg/kg bw) and xylazine (dose 10 mg/kg bw). One millilitre of blood was drawn from the heart and then the animals were euthanized with intracardial injection of 1 ml T-61 ad us. vet. Bone (tibia was taken as sample), bone marrow, muscle, heart, lung, liver, kidneys and thyroid glands were collected. Organs were cleaned, dried and weighed. Radioactivity in the organ was measured in a well-type gamma counter (NZ-310, Gamma, Hungary). Bone marrow was obtained by physical removal of it from the tibial plateau, epicondyli and tibial lumen. In rabbits, percent organ contribution to body weight was assumed as bone mass 5%, blood 8%, bone marrow 8% and muscle 50% of body mass. Pharmacokinetic parameters were calculated as described above.

The distribution pattern of ^{177}Lu-EDTMP in New Zealand white rabbits was also determined by carrying out serial scintigraphic imaging studies. For this, ≈0.3 mL (111-148 MBq) of ^{177}Lu-EDTMP preparation was injected intravenously (i.v.) into healthy adult New Zealand white rabbits, weigh- ing 3-4 kg, through the ear vein. Sequential whole-body images were acquired in the single- head digital SPECT gamma camera at 1, 3, 6, 24, 48, and 72 hours and at 7, 14, and 28 days postinjection, using a LEHR collimator. The gamma camera was previously calibrated for the 208-keV gamma photon of ^{177}Lu with a 20% window. All the images were recorded by acquiring 500 Kcounts, using a 256 X 256 matrix size. Regions of interest (ROIs) were drawn on the dorsoventral/ventrodorsal (DV/VD) images over different major organs. Counts per minute (cpm) values were quantified by using dedicated software (Xeleris), from which the percentage uptake in different organs were determined. Blood samples were drawn at the same time intervals mentioned above from the ear vein of the animals and counted for ^{177}Lu activity to ascertain the blood clearance pattern.

Biodistribution and imaging studies in dogs

Long-term biologic evaluation of ^{177}Lu-EDTMP was conducted in healthy Beagle dogs These studies in dogs consisted of imaging VD and DV views by using a Nucline XRing/R (Mediso) gamma camera equipped with a high-resolution, general-purpose collimator. Whole-body (512x1024) and spot images (256x256) were acquired at different time points starting at 30 min and up to 4 weeks pi. Prior to imaging, animals were anaesthetized by intravenous injection of ketamin and xylazine at a dose of 100 and 5 mg/kg bw, respectively.

Images were processed with the Pmod 2.7 software package (Pmod Technologies Co., Zurich, Switzerland).

Study of toxicological effects in dogs

Four activity levels (9.25, 18.5, 27.75 and 37 MBq/kg) were studied. Three randomized healthy male beagle dogs weighing between 13.2 and 23.4 kg were used for each activity level. The tracer was injected through the cephalic vein. Venous blood samples (4 ml, cephalic or jugular vein) were drawn from each of the injected animals, to determine the biochemical parameters. Serum levels of alanine aminotransferase, alkaline phosphatase, gamma-glutamyl transferase, urea and creatinine were measured. Urea/ creatinine ratio was calculated to verify possible renal damage. Automated complete blood counts performed included white blood cells (WBC), red blood cells and platelets. All measurements were done by a dedicated veterinary laboratory (VetMedLabor, Ltd., Budapest, Hungary). Toxicity to bone marrow was defined as reduction in platelet concentration below 100 G/L (10^3/µl) or WBC level below 4 G/L.

Cumulative urine up to 72 h was collected in fractions during the time intervals 0-6h,6-24 h, 1 -2 days and 2-3 days via an indwelling Foley catheter. At each time point the urinary bladder was rinsed with saline and the final volume was documented. Activity concentration in the corresponding pooled fractions was determined in 1-ml samples using the NZ-310 gamma counter.

Pharmacokinetic analysis in mice and rabbits

Pharmacokinetic parameters were derived from the mean values of biodistribution data acquired at different time points by applying Topfit v. 2.0 pharmacokinetic software (Fischer Verlag, Jena, Germany) using the noncompartmental model. Time activity curves were drawn using Prism v. 5.0 software (GraphPad, Inc., USA).

b) Results

^{177}Lu-EDTMP Preparation and synthesis

Irradiation of natural Lu_2O_3 target at a thermal neutron flux of ≈6 X 1013 n/cm2.s for 21 days yielded ^{177}Lu with a specific activity of ≈12 GBq/mg (≈324 mCi/mg) at 6 hours post-EOB.

^{177m}Lu was found to be the only radionuclidic impurity present in the processed ^{177}Lu, and the level of radionuclidic impurity burden was determined by the procedure mentioned in the literature (Pillai et al. 2003, Chakraborty et al. 2006). It was observed that 5.5 kBq of ^{177m}Lu

was present per 37 MBq of ^{177}Lu (0.2 μCi of ^{177m}Lu/mCi of ^{177}Lu) at EOB, which corresponds to only 0.02% of the total activity produced, indicating that the radionuclidic purity of ^{177}Lu produced was 98.98%.

The characterization and chemical purity of EDTMP synthesized in-house were carried out with the help of Fourier-transform infrared (FT- IR), ^{1}H-nuclear magnetic resonance (NMR), and ^{31}P-NMR studies. The peak multiplicities and integrations of the ^{1}H-NMR spectrum were consistent with the structure of EDTMP. An eight-proton doublet observed at 3.55 ppm in the ^{1}H-NMR spectrum of EDTMP could be attributed to the coupling of the a-methylene protons with the adjacent phosphorus atom, indicating the formation of the a-methylene phosphonic acid. The ^{31}P-NMR spectrum provides confirmatory evidence of the formation of EDTMP. A triplet observed at —*8* 9.86 ppm (J = ≈12 Hz) indicated the coupling of the phosphorus atom with the a-methylene group. This triplet appeared as a singlet in the proton-decoupled ^{31}P-NMR spectrum, thereby confirming the formation of the $CH_2PO(OH)_2$ group.

^{177}Lu-EDTMP complex prepared was characterized and its radiochemical purity was ascertained by using a combination of paper chromatography and paper electrophoresis techniques.26 The complex was obtained with a radiochemical purity of >99%, using 35 mg (80.28 μM*)* of EDTMP and 0.01-0.2 mg (0.057-1.14 μM*)* of Lu in the form of $LuCl_3$**,** in a 1-mL reaction volume, within a pH range of 5-8. Experiments carried out by keeping the ligand concentration fixed at 35 mg/mL and gradually increasing the concentration of Lu indicated that excellent complexation yields (>98%) were achievable over a wide range of (ligand):(metal) ratios ranging between 1400:1 to 70:1. This indicates that the ^{177}Lu-EDTMP complex can be prepared by using ^{177}Lu having a wide range of specific activity without affecting the extent of complexation. The ^{177}Lu-EDTMP complex exhibited excellent stability at room temperature. The complex was found to retain its radiochemical purity to the extent of > 98% after 30 days at room temperature up to which the study was carried out.

Biodistribution and imaging studies in mice and rats

The results ofthe biodistribution studies in mice at different time points studied are summarized in Table 3. Rat biodistribution is detailed in Table 4. Accumulation of activity in the bone is fast and peaks at 2 h pi. (40.82±3.98 % IA in bone). Activity accumulation was primarily observed in the bones with fast excretion via the urinary system. No organs other than the bone showed retention of activity in significant amount at any time point.

Organs/tissues	Time points											
	30 min				1 h				2 h			
	%IA	S.D.	%IA/g	S.D.	%IA	S.D.	%IA/g	S.D.	%IA	S.D.	%IA/g	S.D.
Blood	0.83	0.00	0.64	0.07	7.16	7.66	4.48	4.98	0.13	0.02	0.11	0.02
Muscle	1.10	0.01	0.21	0.04	0.67	0.27	0.10	0.04	4.25	4.79	0.97	1.12
Bone	38.46	2.62	18.00	2.23	40.82	3.98	19.22	1.81	38.38	3.17	19.55	3.28
Bone marrow	0.00	0.01	3.69	2.32	0.00	0.00	1.66	0.50	0.00	0.00	0.00	0.00
Thyroid	0.19	0.00	0.32	0.02	0.08	0.02	0.17	0.06	0.06	0.03	2.04	0.61
Heart	0.04	0.00	0.65	0.04	0.02	0.01	0.39	0.13	0.01	0.00	0.13	0.03
Lung	0.14	0.02	0.28	0.01	0.10	0.04	0.17	0.04	0.04	0.02	0.17	0.07
Liver	0.33	0.01	1.44	0.22	0.21	0.05	0.85	0.28	0.18	0.02	0.15	0.02
Kidneys	0.41	0.02	0.21	0.04	0.23	0.06	0.10	0.04	0.18	0.01	0.70	0.11

Organs/tissues	Time points											
	3 days				5 days				1 week			
	%IA	S.D.	%IA/g	S.D.	%IA	S.D.	%IA/g	S.D.	%IA	S.D.	%IA/g	S.D.
Blood	0.00	0.00	0.00	0.00	0.00	0.00	0.00	0.00	0.00	0.00	0.00	0.00
Muscle	0.10	0.11	0.02	0.02	0.38	0.40	0.08	0.08	0.02	0.00	0.00	0.00
Bone	30.34	8.01	13.20	3.48	31.22	7.65	14.86	2.79	28.28	6.14	12.30	2.90
Bone marrow	0.00	0.00	0.00	0.00	0.00	0.00	0.00	0.00	0.00	0.00	0.00	0.00
Thyroid	0.02	0.01	0.56	0.54	0.03	0.01	0.75	0.32	0.02	0.02	0.48	0.34
Heart	0.00	0.00	0.02	0.00	0.00	0.00	0.02	0.00	0.00	0.00	0.03	0.01
Lung	0.01	0.00	0.05	0.02	0.01	0.00	0.03	0.01	0.01	0.00	0.04	0.01
Liver	0.10	0.01	0.08	0.00	0.12	0.02	0.12	0.02	0.13	0.02	0.11	0.00
Kidneys	0.04	0.00	0.18	0.02	0.02	0.01	0.11	0.02	0.02	0.00	0.06	0.01

Blood mass was calculated as 8% of body mass, bone mass was calculated as 10% of body mass, bone marrow mass was considered identical to blood mass. % IA: Percent of injected activity.

Time points																
3h				6 h				24 h				48h				
%IA	S.D.	%IA/g	S.D.	%IA	S.D.	%IA/g	S.D.	%IA	S.D.	%IA/g	S.D.	%IA	S.D.	%IA/g	S.D.	
0.11	0.02	0.08	0.01	0.07	0.02	0.05	0.01	0.01	0.01	0.01	0.01	0.01	0.00	0.01	0.00	
0.24	0.09	0.04	0.02	1.57	1.23	0.25	0.19	0.59	0.65	0.12	0.13	0.06	0.05	0.01	0.01	
36.76	3.39	15.52	3.22	35.52	5.77	13.12	3.11	33.54	10.03	15.76	5.49	30.91	9.90	14.68	3.56	
0.00	0.00	0.00	0.00	0.01	0.00	0.01	0.01	0.43	0.52	0.44	0.53	0.00	0.00	0.00	0.00	
0.02	0.01	0.54	0.28	0.02	0.01	0.61	0.30	0.04	0.04	0.84	0.51	0.01	0.01	0.20	0.20	
0.01	0.01	0.11	0.05	0.02	0.02	0.52	0.56	0.02	0.02	0.20	0.20	0.00	0.00	0.03	0.01	
0.02	0.00	0.12	0.03	0.02	0.01	0.11	0.02	0.02	0.01	0.08	0.04	0.01	0.00	0.04	0.01	
0.14	0.02	0.13	0.03	0.23	0.07	0.17	0.06	0.09	0.05	0.11	0.05	0.12	0.03	0.13	0.02	
0.15	0.01	0.60	0.12	0.96	0.98	2.01	1.74	0.14	0.04	0.66	0.22	0.05	0.01	0.24	0.04	

Time points																
2 weeks				4 weeks				6 weeks				8 weeks				
%IA	S.D.	%IA/g	S.D.	%IA	S.D.	%IA/g	S.D.	%IA	S.D.	%IA/g	S.D.	%IA	S.D.	%IA/g	S.D.	
0.00	0.00	0.00	0.00	0.00	0.00	0.00	0.00	0.00	0.00	0.00	0.00	0.00	0.00	0.00	0.00	
0.54	0.42	0.11	0.09	0.20	0.27	0.15	0.18	0.31	0.30	0.09	0.04	0.23	0.23	0.09	0.09	
29.21	3.44	12.44	1.74	28.63	6.28	14.66	2.95	28.20	2.78	11.84	1.72	21.33	2.10	10.13	2.12	
0.00	0.00	0.00	0.00	0.00	0.00	0.00	0.00	0.00	0.00	0.00	0.00	0.00	0.00	0.00	0.00	
0.04	0.01	1.31	0.38	0.05	0.03	1.00	0.56	0.01	0.03	0.23	0.52	0.00	0.00	0.04	0.02	
0.00	0.00	0.03	0.00	0.00	0.00	0.03	0.01	0.00	0.00	0.04	0.01	0.00	0.00	0.05	0.03	
0.01	0.01	0.06	0.03	0.01	0.00	0.03	0.01	0.01	0.00	0.05	0.01	0.01	0.01	0.04	0.01	
0.14	0.03	0.13	0.02	0.14	0.02	0.14	0.03	0.11	0.02	0.09	0.03	0.11	0.11	0.08	0.03	
0.03	0.01	0.10	0.03	0.01	0.00	0.05	0.01	0.00	0.00	0.06	0.01	0.01	0.01	0.02	0.01	

Table 3.
Biodistribution of ^{177}Lu-EDTMP in mice per organ and per gram of organ weight at various time points postinjection

	% injected dose (ID)/g of organ		
Organ	*3 hours*	*24 hours*	*48 hours*
Blood	0.02 (0.00)	0.00 (0.00)	0.00 (0.00)
Liver	0.03 (0.01)	0.03 (0.01)	0.02 (0.01)
Gastrointestinal	0.13 (0.03)	0.07 (0.03)	0.06 (0.03)
Kidneys	0.22 (0.04)	0.19 (0.07)	0.13 (0.05)
Stomach	0.21 (0.05)	0.10 (0.02)	0.02 (0.01)
Heart	0.00 (0.00)	0.00 (0.00)	0.00 (0.00)
Lungs	0.02 (0.01)	0.00 (0.00)	0.01 (0.01)
Femur	1.74 (0.30)	2.05 (0.48)	2.01 (0.07)
Muscles	0.03 (0.02)	0.00 (0.00)	0.00 (0.00)
Spleen	0.02 (0.01)	0.02 (0.01)	0.02 (0.01)
Excretiona	49.34 (7.68)	47.53 (9.17)	48.36 (4.07)

Note. Figures in parenthesis show standard deviations *n* = 5).
aPercentage of activity excreted is determined by subtracting the activity accounted in all the organs from the total injected activity.
EDTMP, ethylenediamine tetramethylene phosphonic acid.

Table 4. Biodistribution Pattern of ^{177}Lu-EDTMP Complex in Wistar Rats

Imaging studies in mouse and rat

Figure 5. shows maximal intensity projection (MIP) SPECT images in a mouse overlaid on CT images. Results of the digital autoradiography study in mouse are presented Figure 6., clearly illustrating the distribution of ^{177}Lu-EDTMP with predominant accumulation in the skeleton. Internal reference activity sources are also shown in the figure (black round spot). Figure 7. describes rat scintigrams of bone, while Figure 8. shows MIP images of overlaid SPECT and CT studies in a rat at two different lateral projections.

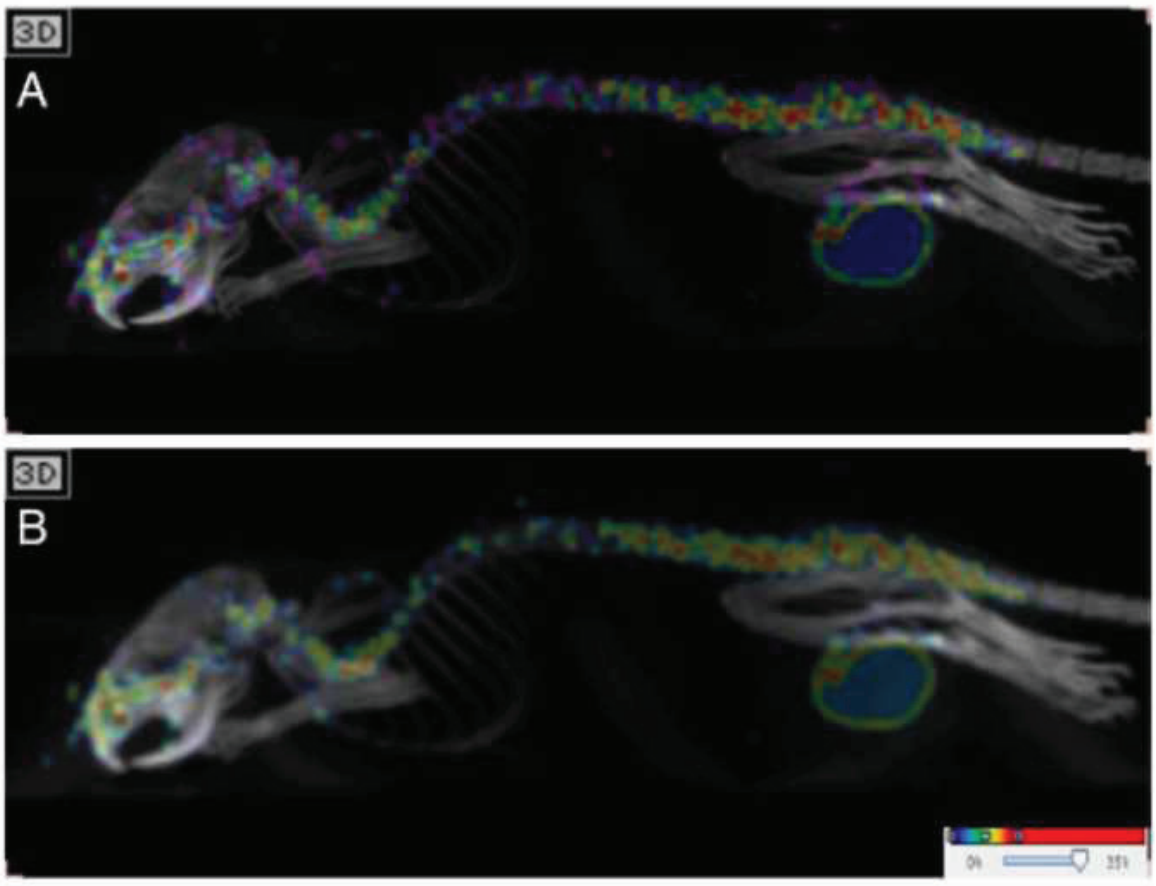

Figure 5. Maximum intensity projections acquired at 3 h pi from mice injected with 30 MBq of ^{177}Lu-EDTMP. SPECT and CT images were reconstructed and are presented as overlaid images. Projection image in (A) shows the vertebral column; projection image in (B) shows the right knee joint. Structures with metabolically active bone clearly show intense traceruptake. Activity accumulation other than in bone is seen only in the bladder.

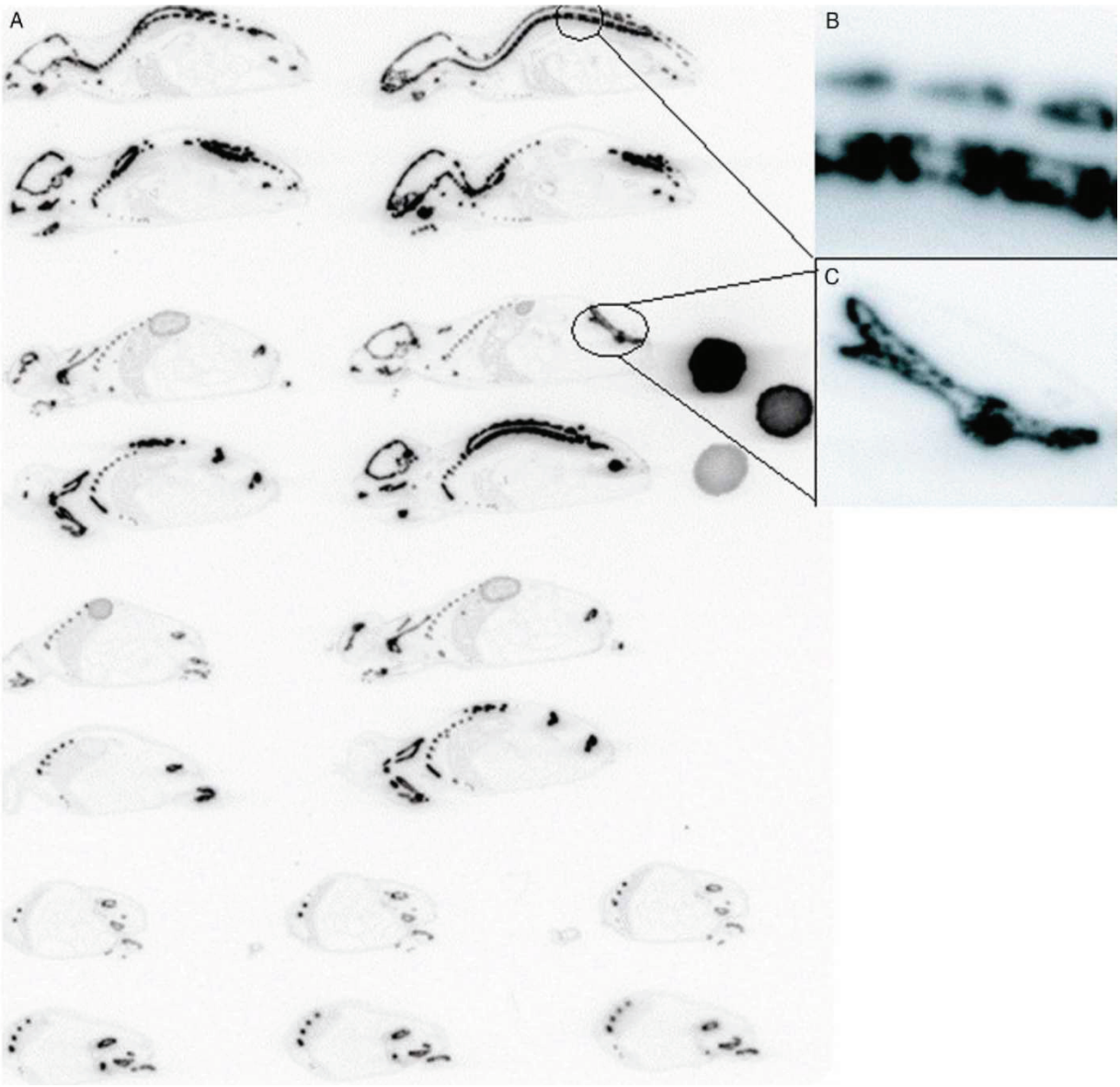

Figure 6. Results of the autoradiography studies. Sagittal sections of a mouse at 3 days p.i. of 5 MBq ^{177}Lu-EDTMP are presented in (A). Circular spots at the right side of the image (third and fourth panel) represent internal reference activities containing 0.18, 1.8 and 9.2 kBq in the order of darkness. Regions of thoracic vertebrae and ischiadic bone with the acetabular joint are magnified in Parts (B) and (C), respectively, to show uptake with high fixation in the bone surfaces and the remodeling region with a relative absence of uptake in the internal spongiosa of the bones.

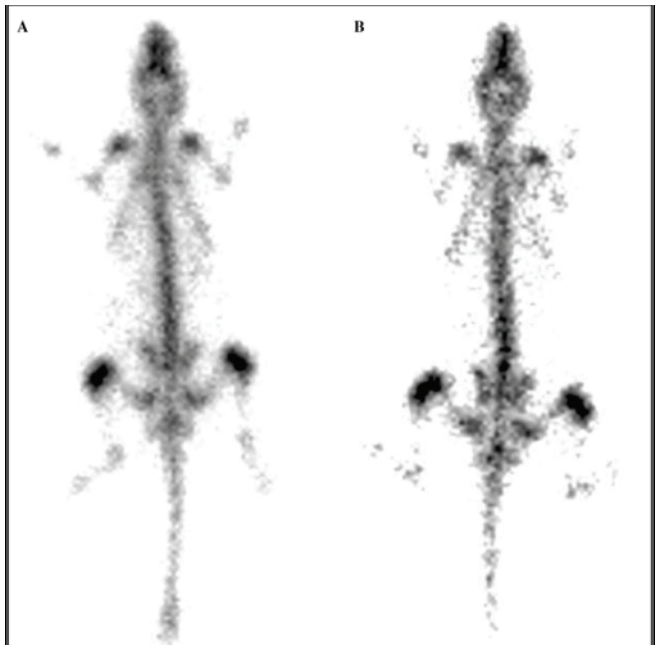

Figure 7. Scintigraphic images of ^{177}Lu-EDTMP in the Wistar rat **(A)** 24 hours postinjection, dorsoventral view. **(B)** 7 days postinjection, dorsoventral view.

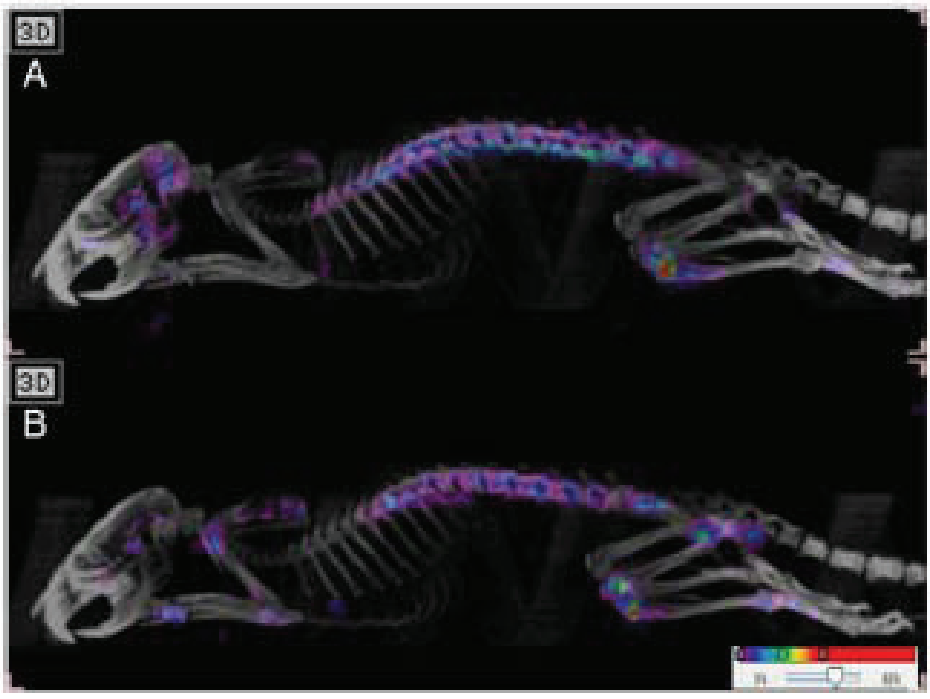

Figure 8. SPECT/CT images of a Wistar rat injected with 40 MBq of ^{177}Lu-EDTMP 3 h pi. The images shown are taken at the level of the midline (A) and the right knee joint (B). Remodeling bone structures predominantly accumulate the radiopharmaceutical.

Biodistribution and imaging studies in rabbits

Organs/tissues	Time points											
	30 min				1 h				2 h			
	%IA	S.D.	%IA/g	S.D.	%IA	S.D.	%IA/g	S.D.	%IA	S.D.	%IA/g	S.D.
Blood	2.95	0.14	0.02	0.00	1.62	0.46	0.01	0.00	0.51	0.3	0.00	0.00
Muscle	0.18	0.12	0.00	0.00	0.71	0.24	0.00	0.00	1.11	0.88	0.00	0.00
Bone	36.57	5.52	0.33	0.04	40.99	4.54	0.29	0.05	38.83	4.71	0.27	0.04
Bone marrow	0.01	0.01	0.00	0.00	0.01	0.02	0.00	0.00	0.03	0.08	0.00	0.00
Thyroid	0.25	0.16	0.42	0.18	0.1	0.05	0.17	0.00	0.06	0.02	0.10	0.11
Heart	0.05	0.12	0.01	0.00	0.03	0.01	0.00	0.00	0.41	0.53	0.00	0.00
Lung	0.12	0.06	0.00	0.00	0.13	0.07	0.00	0.00	0.45	0.38	0.02	0.00
Liver	0.82	0.91	0.00	0.00	0.92	0.26	0.01	0.00	0.54	0.31	0.01	0.01
Kidneys	1.39	0.48	0.03	0.02	1.02	0.16	0.02	0.00	0.98	0.19	0.02	0.00

Organs/tissues	Time points											
	5 days				1 week				2 weeks			
	%IA	S.D.	%IA/g	S.D.	%IA	S.D.	%IA/g	S.D.	%IA	S.D.	%IA/g	S.D.
Blood	0.00	0.00	0.00	0.00	0.00	0.00	0.00	0.00	0.00	0.00	0.00	0.00
Muscle	0.01	0.01	0.00	0.00	0.02	0.00	0.00	0.00	0.32	0.25	0.00	0.00
Bone	23.09	2.62	0.23	0.03	25.92	1.97	0.26	0.02	24.96	2.57	0.25	0.03
Bone marrow	0.01	0.01	0.00	0.00	0.00	0.00	0.00	0.00	0.00	0.00	0.00	0.00
Thyroid	0.00	0.00	0.00	0.00	0.01	0.01	0.00	0.00	0.01	0.01	0.00	0.00
Heart	0.01	0.00	0.00	0.00	0.00	0.00	0.00	0.00	0.00	0.00	0.00	0.00
Lung	0.06	0.02	0.00	0.00	0.01	0.00	0.00	0.00	0.01	0.01	0.00	0.00
Liver	0.03	0.01	0.00	0.00	0.13	0.04	0.00	0.00	0.08	0.06	0.00	0.00
Kidneys	0.02	0.02	0.00	0.00	0.01	0.00	0.00	0.00	0.02	0.02	0.00	0.00

Time points																
3h				6h				24 h				48h				
%IA	S.D.	%IA/g	S.D.	%IA	S.D.	%IA/g	S.D.	%IA	S.D.	%IA/g	S.D.	%IA	S.D.	%IA/g	S.D.	
3.17	0.05	0.02	0.00	0.08	0.01	0.00	0.00	0.03	0.02	0.00	0.00	0.01	0.01	0.00	0.00	
0.65	0.37	0.00	0.00	0.51	0.56	0.00	0.00	0.26	0.29	0.00	0.00	0.04	0.02	0.00	0.00	
36.91	8.92	0.26	0.06	33.42	2.00	0.27	0.04	28.68	3.18	0.24	0.02	25.87	3.91	0.23	0.07	
0.01	0.00	0.00	0.00	0.00	0.00	0.00	0.00	0.00	0.00	0.00	0.00	0.00	0.00	0.00	0.00	
0.03	0.01	0.04	0.00	0.03	0.02	0.04	0.02	0.05	0.03	0.05	0.04	0.05	0.05	0.00	0.00	
0.22	0.30	0.03	0.00	0.07	0.05	0.00	0.00	0.08	0.04	0.00	0.00	0.02	0.02	0.00	0.00	
0.04	0.04	0.00	0.00	0.06	0.05	0.00	0.00	0.06	0.03	0.00	0.00	0.03	0.04	0.00	0.00	
0.35	0.40	0.01	0.00	0.29	0.08	0.00	0.00	0.39	0.24	0.01	0.00	0.10	0.02	0.00	0.00	
0.55	0.30	0.01	0.02	0.72	0.50	0.01	0.00	0.21	0.08	0.01	0.00	0.05	0.03	0.00	0.00	

Time points																
3 weeks				4 weeks				6 weeks				8 weeks				
%IA	S.D.	%IA/g	S.D.	%IA	S.D.	%IA/g	S.D.	%IA	S.D.	%IA/g	S.D.	%IA	S.D.	%IA/g	S.D.	
0.00	0.00	0.00	0.00	0.00	0.00	0.00	0.00	0.00	0.00	0.00	0.00	0.00	0.00	0.00	0.00	
0.06	0.06	0.00	0.00	0.03	0.03	0.00	0.00	0.01	0.00	0.00	0.00	0.01	0.00	0.00	0.00	
25.02	1.22	0.25	0.01	24.05	1.98	0.24	0.02	21.95	1.05	0.22	0.01	20.43	2.53	0.20	0.02	
0.00	0.00	0.00	0.00	0.00	0.00	0.00	0.00	0.00	0.00	0.00	0.00	0.00	0.00	0.00	0.00	
0.10	0.08	0.00	0.00	0.02	0.02	0.00	0.00	0.00	0.00	0.00	0.00	0.00	0.00	0.00	0.00	
0.01	0.01	0.00	0.00	0.01	0.01	0.00	0.00	0.00	0.00	0.00	0.00	0.00	0.00	0.00	0.00	
0.01	0.01	0.00	0.00	0.01	0.00	0.00	0.00	0.00	0.00	0.00	0.00	0.00	0.00	0.00	0.00	
0.09	0.06	0.00	0.00	0.01	0.00	0.00	0.00	0.01	0.00	0.00	0.00	0.01	0.00	0.00	0.00	
0.03	0.03	0.00	0.00	0.01	0.01	0.00	0.00	0.00	0.00	0.00	0.00	0.00	0.00	0.00	0.00	

Table 5. Biodistribution of ^{177}Lu-EDTMP in rabbits per organ and per gram of organ weight at various time points in rabbits.

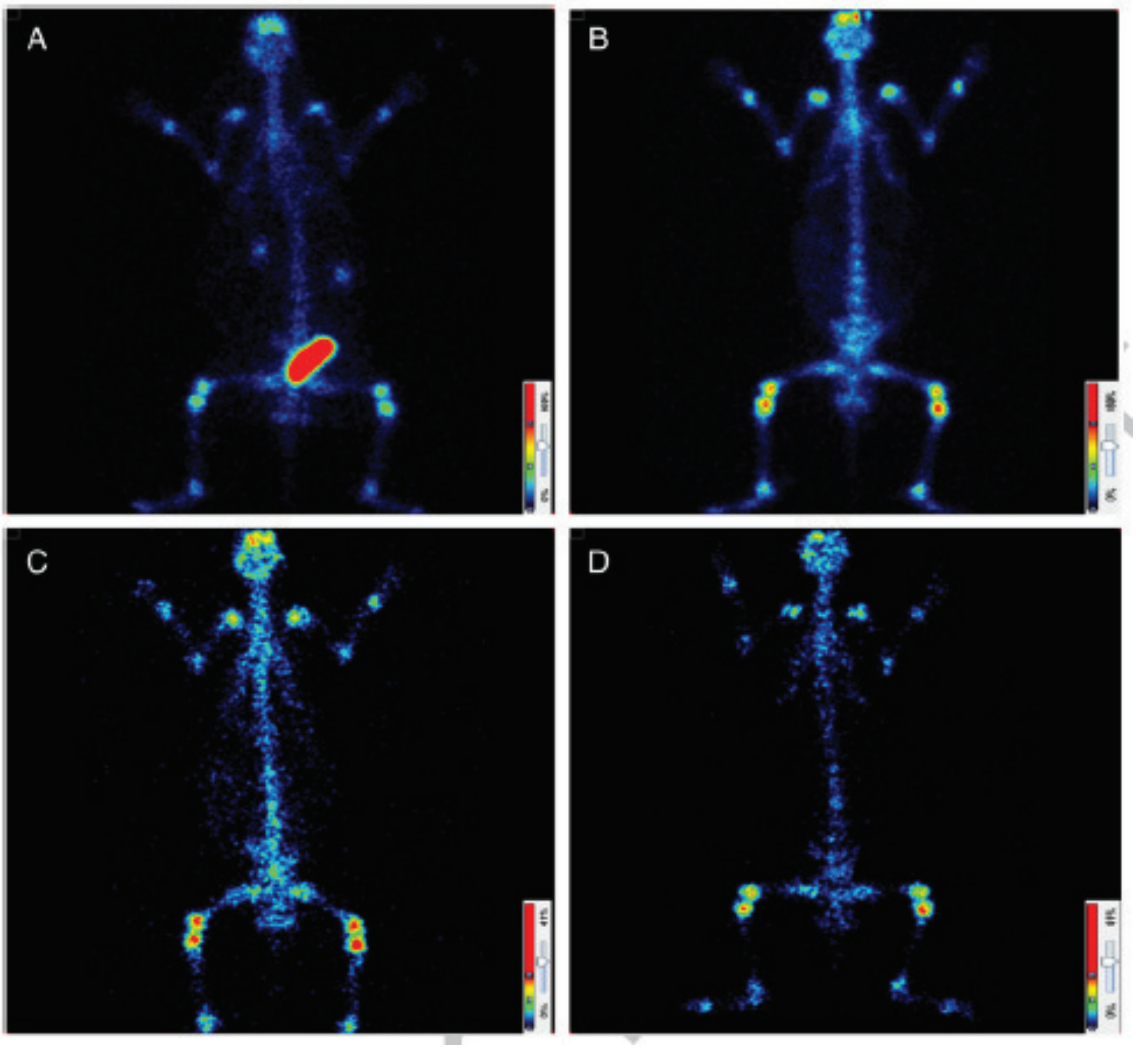

Figure 9. Planar ventrodorsal scintigraphic images of rabbits 1 h (A), 1 day (B), 1 week (C) and 4 weeks (D) postinjection of 40 MBq of ^{177}Lu-EDTMP.

Biodistribution and imaging studies in dogs

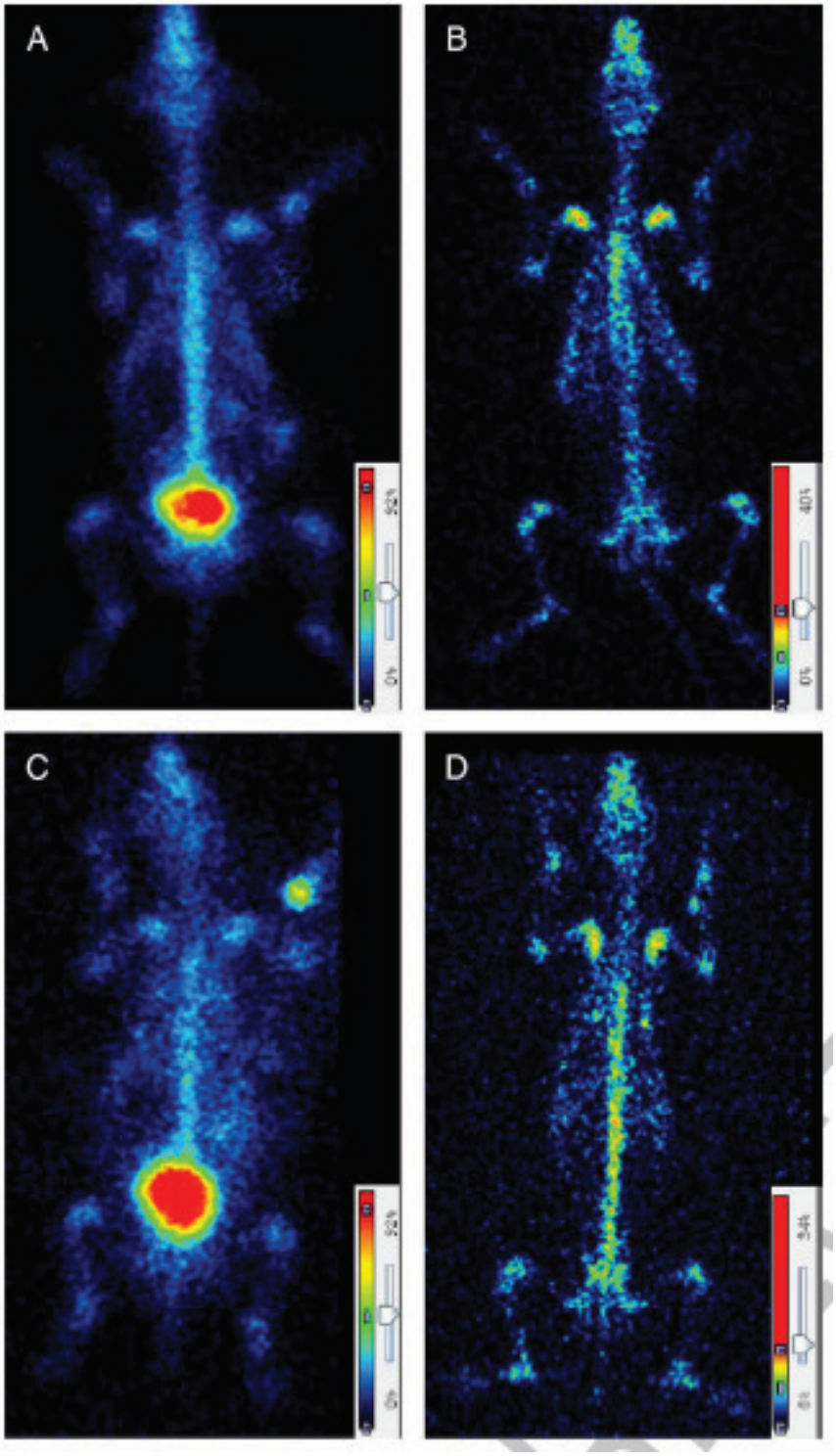

Figure 10. Planar ventrodorsal scintigraphic images of beagle dogs at different activities and different time points. (A) and (B) represent the images of a dog injected with 9.25 MBq/kg bw

of ^{177}Lu-EDTMP at 1 h and 1 week, respectively. (C) and (D) represent the images of a dog injected with 37 MBq/ kg bw at 1 h and 1 week pi, respectively.

Study of toxicological effects in dogs

The studies are summarized below in Tables 6, 7 and in Figure 11.

Dog dosing group	Radioactivity cumulated in urine in % of IA in the indicated period postinjection				
	0-6h	6-24 h	24-48 h	48-72 h	Total 0-72 h
37 MBq/kg bw.	34.8 (9.1)	3.0 (0.6)	1.5 (0.5)	0.4 (0.2)	39.0 (8.4)
19.8 MBq/kg bw	41.9 (7.9)	2.2 (1.3)	1.1 (0.3)	0.2 (0.1)	46.4 (7.7)
18.6 MBq/kg bw	36.2 (9.5)	5.0 (1.3)	2.1 (1.3)	0.3 (0.1)	42.5 (7.3)
9.3 MBq/kg bw	38.1 (7.8)	4.2 (2.1)	1.1 (0.3)	0.3 (0.1)	44.2 (6.0)

Values are shown as mean (S.D.) Percent of urinary excretion over time period in groups of three dogs treated with different activities of ^{177}Lu-EDTP.

Table 6.
Results of urine collection in the dog dose groups

Parameters	Normal range	Pretreatment	2 days	1 week	2 weeks	3 weeks	4 weeks	5 weeks
ALT	10–60 IU/L	52.6 (25.7)	38.5 (38.5)	46.6 (36.7)	106 (13.3)	48.6 (43.6)	45.3 (12.4)	56.0 (5.5)
ALKP	40–300 IU/L	87 (41.9)	96 (49.5)	64 (13.4)	256 (40.4)	78 (11.1)	217 (33.4)	87 (26.3)
GGT	0–10 IU/L	0.0 (0.0)	0.5 (0.4)	0.9 (0.4)	2.1 (1.2)	1.3 (0.4)	3.7 (0.5)	0.0 (0.0)
Urea	4.5–9.0 mmol/L	4.5 (0.4)	4.5 (0.4)	5.8 (0.5)	3.6 (0.4)	4.5 (0.5)	5.6 (1.1)	4.8 (1.0)
Serum creatinine	40–140 µmol/L	75 (12.4)	56.2 (12.3)	70.6 (22.2)	58.5 (15.4)	59.5 (17.8)	68.6 (19.3)	62.9 (13.2)
Serum urea/creatinine ratio	Below 0.10	0.06 (0.01)	0.08 (0.03)	0.09 (0.04)	0.06 (0.01)	0.08 (0.03)	0.08 (0.01)	0.08 (0.03)

Values are shown as mean (S.D.).
ALT — Alanine transaminase; ALKP — alkaline phosphatase; GGT — gamma-glutamyl transferase.

Table 7.
Biochemical parameters of the dogs treated with 37 MBq/kg bw of ^{177}Lu-EDTMP

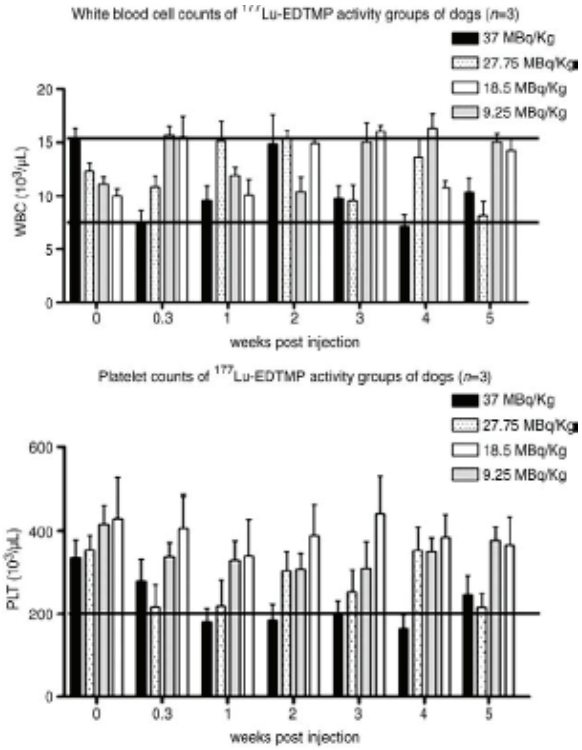

Figure 11. White blood cells (top) and platelet counts (bottom) at different time points of rabbits injected with four different levels (9.25–37 MBq/kg bw) of ^{177}Lu-EDTMP activity. Bars represent standard deviation (n=3). The lines parallel to the x-axis represent the normal range (top) and lower cut off limit (bottom).

Pharmacokinetics

These data have been evaluated with the results of biodistribution in mice and rabbits and are visualized in Figure 12. and Table 8.

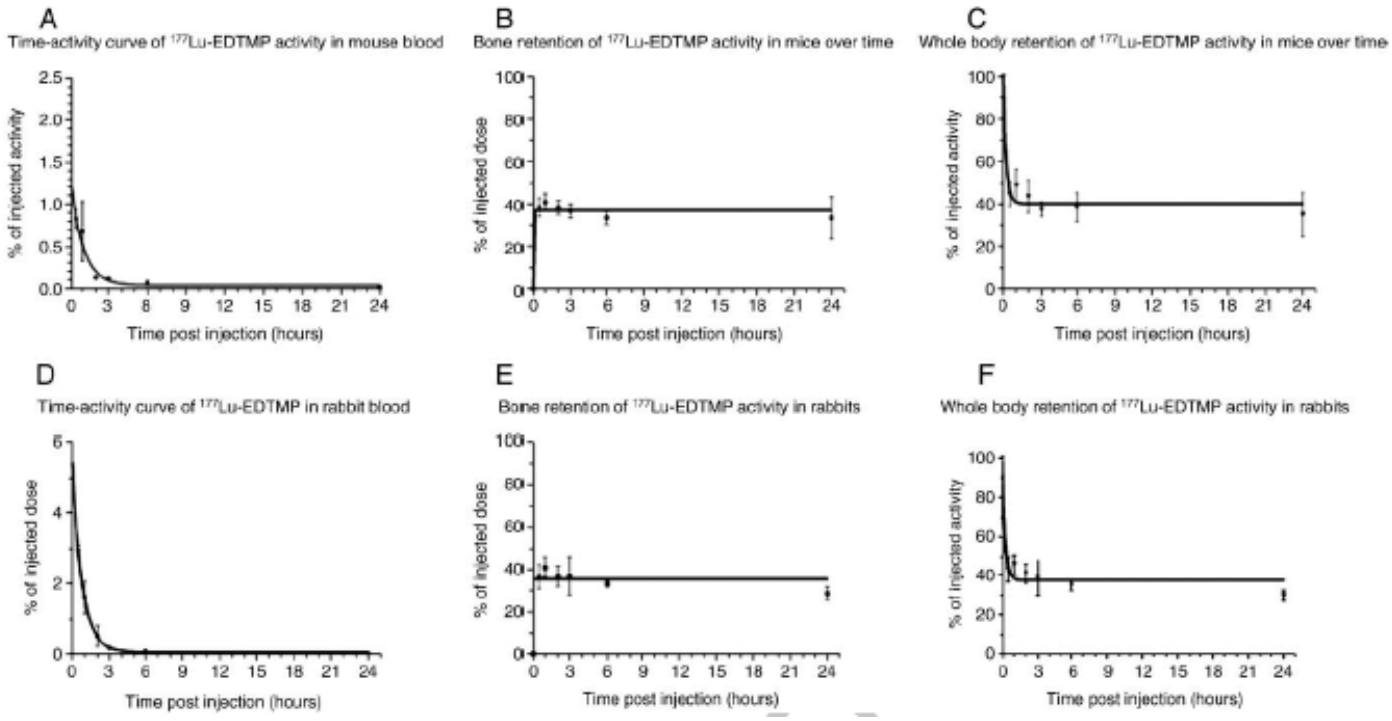

Figure 12. Time–activity curves of blood, bone and whole body in mice and rabbits. The sum of activity measured in all the organs and carcass was considered as whole-body radioactivity. Time–activity levels in mice blood (A), bone (B) and whole body (C); and rabbits' blood (D), bone (E) and whole body (F) during the first 24 h are presented in the figure. Bars represent standard deviation.

MICE

Organs/tissues	$t_{1/2}$ (h)	AUD (%h)	AUC_{∞} (%h/g)	MRT (h)	MRT_{∞} (h)	V_z (ml)	V_{SS} (ml)	TC (ml/min)
Blood	7.20	7.35	7.35	3.74	3.74	141	50.9	0.23
Muscle	1170	406.24	794.65	618	1800	141	226	2.10×10−3
Bone	2130	37666	103293	641	3040	2.98	2.95	1.61×10−3
Thyroid	923	36.11	36.11	517	517	3690	1430	4.62×10−3
Heart	209	9.31	9.31	263	263	3240	2820	1.79×10−1
Lungs	753	13.93	24.78	263	1430	4380	577	6.72×10−2
Liver	2260	169.13	528.39	649	3340	618	632	3.15×10−3
Kidneys	304	38.97	43.36	375	517	1010	1190	3.84×10−2

RABBITS

Organs/tissue	t1/2 (h)	AUD (%h)	AUC∞ (%h/g)	MRT (h)	MRT∞ (h)	Vz (ml)	V_{SS} (ml)	TC (ml/min)
Blood	8.91	30.97	30.97	2.83	2.83	41.5	9.12	5. 38×10−2
Muscle	250	115.99	119.60	348	389	302	326	13.9×10−2
Bone	1870	31806.8	87063.5	639	2800	3.11	3.22	1.91×10−5
Thyroid	297	14.53	14.53	397	397	2950	2740	1.15×10−2
Heart	215	7.15	7.15	325	325	4350	4550	2.33×10−1
Lungs	181	11.10	11.10	310	310	2350	2790	1.50×10−1
Liver	219	65.54	68.69	276	340	460	495	2.43×10−2
Kidneys	102	29.19	29.19	160	160	505	546	5.71×10−2

$t_{1/2}$ — terminal elimination half-life; AUC_{∞} — area under the curve extrapolated to $t=\infty$; AUD — area under the data;
MRT — mean residence time at **t** time; MRT_{∞} — mean residence time extrapolated to $t=\infty$; V_z — volume of distribution; V_{SS} — volume of distribution steady state; TC — total clearance.

Table 8.

Standard pharmacokinetic parameters of ^{177}Lu-EDTMP calculated in mouse and rabbit on the basis ofbiodistribution results and the noncompartmental model

The pharmacokinetic parameters calculated from the biodistribution data are presented in Table 8 for both species.Time-activity curves of ^{177}Lu-EDTMP in blood, bone and whole body are given in Figure 12 A-C.

c) Discussion

^{177}Lu-EDTMP complex was prepared in high yield and excellent radiochemical purity (>99%), using ^{177}Lu produced by the thermal neutron irradiation of natural Lu_2O_3 target and EDTMP synthesized in-house. The complex exhibited excellent *in vitro* stability (>98% radiochemical purity) at room temperature up to 30 days postpreparation. Studies showed that the complex could be prepared in high yield and stability with a wide range of specific activity of ^{177}Lu.

The composition of the freeze-dried EDTMP kits used in our studies was matched to the registered product of ^{153}Sm-EDTMP. Detailed quality control of the kits including sterility, apyrogenicity and long-term stability was established. The radiochemical purity as well as the stability ofthe complex over a period of time was studied. The ^{177}Lu-EDTMP complexation yield was greater than 99% to start with and there was no significant reduction in the radiochemical purity over several days of storage. Injection of the labeled product in this study did not result in systemic reaction in any of the species studied.

Biodistribution studies were done both in mice and in rabbits, and the percent injected activity (%IA) associated with each organ was calculated based on the activity measured on the whole organ or part of the tissues. There is significant difference in the body composition between different species such as mice and rabbits. Body composition of CD-1 mouse (n=10) and New Zealand white rabbit (n=6) strains was measured preceding the present studies. Based on our previous experience and the present studies, we took 10% for bone and 27% for muscle in the case of mice and 5% for bone and 50% for muscle in case of rabbits.

The results of the biodistribution studies in mice and rabbits summarized in Tables 3 and 5 show that ^{177}Lu- EDTMP concentrates in the bone; very high uptake is seen in early time points and persists till the last time point studied. Activity not bound to bone is excreted via the kidneys and bladder. The activity from blood is cleared very fast. Pharmacokinetic parameters in mice and rabbits summarized in Table 8, give important information about the biokinetics of ^{177}Lu-EDTMP. We chose the noncompartmental model for calculation of the pharmacokinetic parameters as one of the reported studies found seven compartments for ^{99m}Tc-methylydene diphosphonate which were not realistically handled in the calculations (Sagar et al. 1979). Data obtained in our study were relevant to the noncompartmental model which has minimal number of presumptions and restrictions. Results of the pharmacokinetic modeling studies support stable and long-lasting binding of ^{177}Lu-EDTMP to bone. The terminal half-life in bone was 2130 and 1870 h, whereas in blood was 7.3 and 8.9 h in mice and rabbits, respectively. All organs other than bone having long terminal elimination half-

lives contained minuscule fraction of radioactivity as reflected by very small values of area under the curve (AUC∞). The bone-to-muscle ratio of AUC∞, was 130, while the bone-to-blood ratio of AUC∞, was 14 053 in mice. In rabbits, the bone-to-muscle ratio of AUC∞, was 732 and the bone-to-blood ratio of AUC∞ was 2811. A higher bone mass index and faster bone metabolism with higher mineralization rate might explain the faster tracer uptake and slightly higher whole-body uptake in mice (Toegel et al. 2006, Kumar et al. 2007). The difference in the body composition of rabbits and mice will lead to varied accumulated radioactivity in the skeleton of those two species. In turn, this could result in different radiation doses. Both the species studied have an important role in extrapolating the results to humans. Mice provide a basis for extrapolation to the adult human, while rabbits offer a model for physiologic processes and biodistribution in the growing bone (nutrition of epiphyseal plates is the same in the rabbit as in man) (Essmann et al. 2003, Essmann et al. 2005).

Autoradiography studies show uptake of the activity by both long and spongeous bones in the remodeling regions and bone surfaces (Figure 6). Joints and surfaces of the vertebrae and the ischiadic bone accumulate more radioactivity than the internal spongiosa of the same bones (Figures 6, blown-up Sections B and C).

Imaging studies in rabbits and dogs showed protracted bone localization (Figures 10 and 11). Rapid bone uptake together with fast blood clearance of the tracer results in good quality images at all time points. By using imaging studies and the activity measured in urine of dogs, it is reasonable to state that the pharmacokinetic behavior of ^{177}Lu-EDTMP in dogs is similar to mice and rabbits.

There was no difference among the four different activity groups (9.25, 18.5, 27.75 and 37 MBq/kg bw) in terms of the activity excreted or excretion rate in urine (Table 6). As the specific activity of the tracer used was identical and only the activity injected varied, it can be inferred that there is no mass effect of the tracer on body localization. The nonbone accumulated activity is excreted preferentially through the renal route. By pooling the results of the animals of all groups, it can be seen that 96.6% of the urinary excretion occurs in the first 24 h. The results provide strong support to the inference that there will not be any significant radiationrelated adverse effects to any organs other than the bone due to activity accumulation. Activity uptake in bone marrow is also insignificant. The energy deposition of ^{177}Lu beta particles is almost totally achieved within the volume of a small-diameter (maximally 5 mm) sphere (Bernhardt et al. 2001, Syme et al. 2004). From the radioactivity accumulated in the bones, the radiation damage could only reach the bone marrow.

Biochemical parameters to assess the liver and kidney function determined in the four activity groups each consisting of three dogs did not reveal any abnormalities for the length

of the follow-up period of 5 weeks. Biochemical parameters of the highest activity group (37 MBq/kg bw) alone are presented in Table 7. The reason for an above normal alanine transaminase value in the second week is not understood as it is not part of any definite trend and hence no inference is drawn. The tracer being excreted mainly through the renal pathway, the kidney and bladder are the critical organs (Eary et al 1993, Brenner et al. 2003) in this regard. Measured biochemical parameters and serum urea-to-creatinine ratio do not indicate any damage to the renal system, even at the highest level of activity injected (Table 7).

A drop below normal values for platelet and WBC counts was seen in the highest activity group (Fig. 9). As opposed to platelets, the trend in the WBC counts was not unidirectional. This could probably be due to a reactive leukocytosis to iatrogenic urethritis caused by catheterization. This change in WBC counts indicates that the proliferative capability of the bone marrow in dogs is not hindered even at the highest level of injected activity. Neither WBC nor platelet counts reached the toxicity levels. The results clearly suggest that there are no adverse effects or toxicity up to 37 MBq/kg bw of injected activity.

We examined the biodistribution, pharmacokinetic, biochemical and hematologic parameters of ^{177}Lu-EDTMP in different species in order to collect data to support a human clinical trial. The biodistribution, autoradiography and imaging studies of ^{177}Lu-EDTMP clearly demonstrate that the tracer is taken up almost exclusively by the skeletal system, with minimal activity accumulation in any other organ. Multidose studies up to 37 MBq/kg bw in dogs did not result in any adverse effects as seen from the biochemical parameters and hematological measurements. Based on the results of the present studies, we consider ^{177}Lu-EDTMP a suitable radiopharmaceutical for human clinical trials as a metastatic bone pain palliation agent. The animal models and studies described herein were indispensable in the road to open this radiopharmaceutical for human clinical trials, and imply a lot of important dose-related toxicity questions that should be investigated more mainly in the field of growing bone to prepare for eventual pediatric applications.

5.1. 2 Application of a diseased animal model in the evaluation of a new ^{188}Re-tin colloid preparation for radiosynovectomy

a) Materials and Methods

Preparation of the radiocolloid

Aliquots of 0.5 ml of nitrogen-purged 0.1 N HCl containing 5 mg $SnCl_2$ $2H_2O$ (Merck) were dispensed into vials under a nitrogen atmosphere. The vials were capped under nitrogen with a rubber septum and an aluminum seal, and stored in a refrigerator until use. Radiolabeling was performed by adding to each vial a 0.5 ml aliquot of ^{188}Re-perrhenate (~80 MBq) freshly eluted with saline from an alumina-based ^{188}W/^{188}Re generator (Oak Ridge National Laboratory, USA). Incubation was performed for 120 minutes, either at room temperature or at 100°C.

The labeling efficiency was checked by thin-layer chromatography (TLC-SG/acetone, Kieselgel, Merck, Germany). The radioactivity was monitored by cutting the gels into 20 parts, each 1 cm in length, numbering the parts from the starting point and measuring their activities in a well-type gamma counter with an automatic sample changer (NK-350, Gamma, Hungary). Free sodium perrhenate and the examined preparation were dropped in parallel onto TLC plates and after 1 h the plates were processed. Activity vs. distance curves were plotted and the labeling efficiency was calculated. The radiolabeled ^{188}Re-tin colloid was neutralized by the addition of 0.2 M sodium phosphate buffer (pH = 8) solution.

Determination of particle size

The particle diameter spectrum of each colloid preparation was obtained by using a dynamic laser light-scattering device (Dynapro, Protein Solutions, VA, USA). A laser Doppler effect was used to determine the third-degree Brownian motion of the particles, and dedicated software (Dynamics v. 6.0, ProteinSolutions, VA, USA), based on the Stokes-Einstein equation, was applied to determine the average diameter of the particles and the distribution histogram. A spherical molecule standard model was used for the assessment. A 50-ml aliquot of each labeled colloid solution was transferred to the cell of the micro sampler and measured ten times at RT with a laser light of 830 nm wavelength.

Imaging studies

Three, 24, 48 and 72 h after the application of the radiopharmaceutical, images were acquired with a gamma camera (Nucline X-Ring, Mediso, Hungary), with a low-energy high-

resolution collimator at a 512 x 512 x 16 matrix size. Region of interest (ROI) data in counts per minute (cpm) were collected by an image processing software (Interview©, Mediso, Hungary). Knee to knee uptake ratios were calculated for all rabbits receiving any radioactive substance in the knee joint.

Evaluation of the radiocolloid in an animal model of rheumatoid arthritis

Following the antigen induced arthritis model descriptions by (Dumonde et al. 1962, Steinberg et al. 1971), 9 male New Zealand White rabbits (3-4 kg) were injected intradermally over 5 sites on the back with 10 mg of ovalbumin solution (Sigma, Germany) emulsified in 1 ml of Freund's complete adjuvant (Sigma, Germany) as first sensitization. The animals were resensitized 3 weeks later. A dose of 0.1 mL of the above solution was administered aseptically intra-articularly into each right knee joint 2 weeks after the second immunization. The intra-articular injection was performed by entering the joint at the middle of the patellar tendon with a 16 G sterile needle, drawing back approximately 0.1 mL of synovial fluid and injecting the challenger solution. The knees were kept immobile for 1 minute and then moved three times. For each procedure, anesthesia was attained with 10 mg/kg of ketamine (SBH-Ketamin, SBH, Hungary) and 5 mg/kg of xylazine (Primazin, Alfasan, The Netherlands), given intramuscularly. Three weeks after the intra-articular challenge, 5 rabbits were injected intra-articularly under the same conditions as during the challenge with a net activity of 49 MBq in 0.25 mL of freshly prepared ^{188}Re-tin colloid solution produced at RT. Four weeks later, the rabbits were euthanased with pentobarbital (Nem- butal, Phylaxia-Sanofi, Hungary) and the knees were removed, and subjected to histopathology. Four arthritic rabbits kept as untreated controls, were sacrificed at the same time and also subjected to histopathology. Additionally, 2 healthy non-treated rabbits were subjected to the same intra-articular injection procedure, receiving around 50 MBq of freshly eluted ^{188}Re perrhenate in 0.1 mL of physiological saline. They were treated in the same manner as the treated rabbits during the experiments, with the exception of the blood sampling.

An 18G-cannula (Medicor, Hungary) was implanted into the jugular vein of the treated rabbits, and 2-mL blood samples were taken at 1, 3, 24 and 48 h after the application of the radiopharmaceutical.

The knee joints were dissected, placed into 10% m/v buffered formalin solution for 3 days, and joints were embedded in paraffin. Series of 20-/vm thick longitudinal sections were made and stained with hematoxylin-eosin, and synovial membranes, synovial spaces, cartilage, and bones were evaluated for the presence and quality of inflammation and/or fibrous tissue proliferation.

b) Results

Radiocolloid characteristics

The labeling efficiency was determined on the basis of chromatograms. Mean values of three measurements are shown for the RT chromatogram in Figure 1. The labeling efficiency was 97.3% for the preparation at 100°C and 68.7% for that at RT. The solution was clear and transparent after labeling at 100°C and opaque, milky, very slowly sedimenting (during two hours, practically no sedimentation was seen), non-turbid for the reaction carried out at RT; the situation remained similar throughout all procedures.

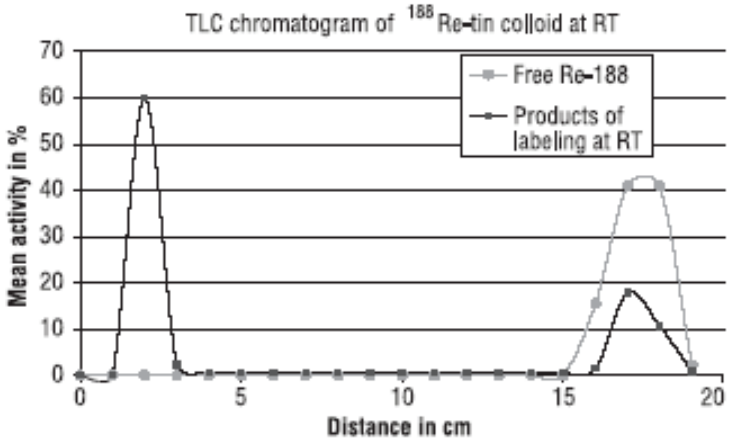

Figure 13. TLC chromatogram of 188Re-tin colloid produced by reaction at room temperature.

The particle size distribution was first assessed by the evaluation of ITLC (paper) chromatograms, where the different peaks represent different particle sizes formed in the reaction. For the reaction performed at 100°C, the distribution led to a non-uniform spectrum with a larger number of smaller particle peaks. The chromatogram of the RT product is shown in Figure 13. The size distribution was also measured with the laser scattering method. These measurements confirmed that the size distribution was more uniform for the preparation produced at RT than for that produced at 100°C. In the product of the 100°C reaction, 15% of the particles measured < 1 μm and 85% of the particles measured > 3 /μm. A more uniform size pattern, with the 1% of the particles measuring < 1 /μm versus 99% measuring > 3 μm, was seen after the RT reaction. The dedicated software of the device gave an assessed mean value of 4.535 /μm for the colloid produced at RT.

Imaging studies

Retention of ^{188}Re-tin colloid in the synovial space of the AIA rabbits was observed up to 72 h. No leakage to the inguinal lymph node (the predilection site of the accumulated outflow of radioactivity) or other lymph nodes could be observed (Fig. 14). Figure 14 presents static

scintigraphic images of the knee regions of a rabbit at 3, 24, 48, and 72 h after the injection into the knee. The knee to knee radiopharmaceutical uptake ratios were stable in time; the averages and standard deviations are listed in Table 9. In wholebody scans, no other activity accumulation was seen anywhere in the body (e.g. in the predilection sites such as the thyroid gland and the gastric mucosa). The scans of healthy rabbits receiving only intra-articular ^{188} Re perrhenate solution revealed uptake in the predilection sites — stomach mucosa and thyroid gland were visualized in the images, most prominently 3 h after injection (Fig. 15). Later healthy rabbit scans demonstrated a very fast excretion of perrhenate via the kidneys and bladder: 48 and 72 hours post injection, only background activity could be observed in healthy rabbits receiving perrhenate eluate.

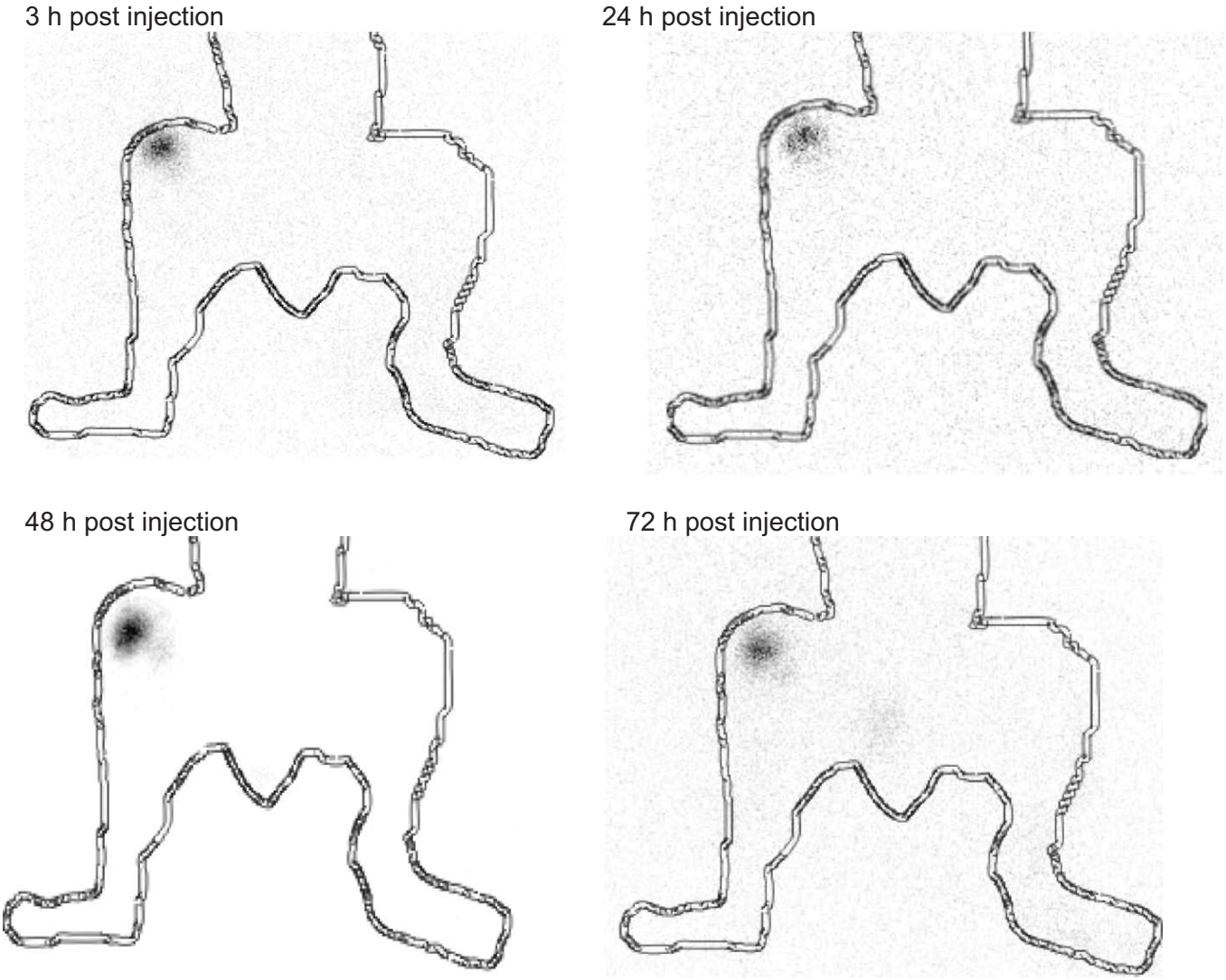

Figure 14. Static images of the knee of a rabbit taken at 3, 24, 48 and 72 h after injection. Differences in background are due to the automatic cutoff level setting of the camera software. Rabbit contours were generated from the acquisition data by using the Interview© software**.**

Table 9. Average treated/control values (cpm/cpm) in knee joints of treated rabbits

Animal	Treated/Control	SD
Rabbit A	12.10	2.47
Rabbit B	10.07	1.25
Rabbit C	9.96	1.02
Rabbit D	9.25	1.06
Mean	10.34	0.87

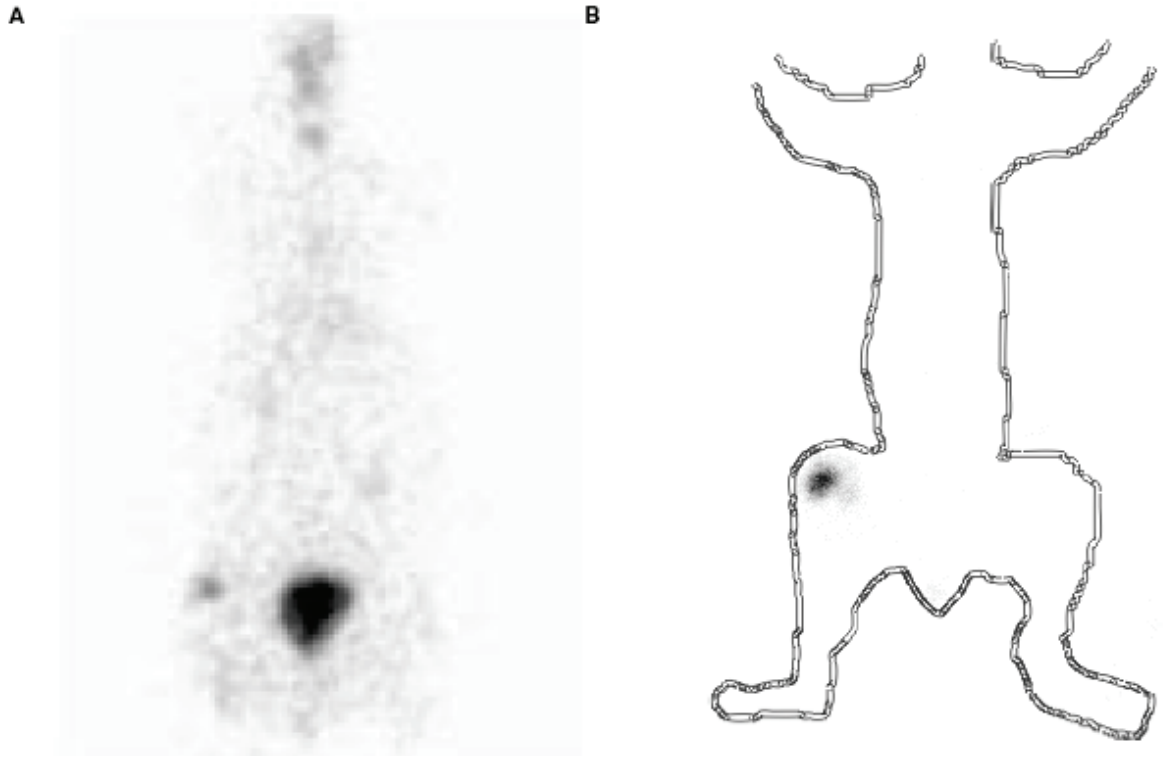

Figure 15. Comparison of biodistributions of the same amount and activity of intra-articular perrhenate eluate (A) and 188Re-tin colloid solution (B) in rabbit, 3 h post injection.

Animal model evaluation of the radiocolloid

We detected a severe inflammation of the synovial membrane and knee cartilage surfaces, characterized by the infiltration of heterophilic leukocytes, macrophages and a smaller number of lymphocytes, together with thickening of the synovial membrane in the control animals. In intact rabbits receiving intra-articular ^{188}Re perrhenate solution, a mild heterophilic granulocytosis was present. Histopathological examination 4 weeks post injection clearly showed the development of fibrous connective tissue in all of the AIA knees. This was not seen in any animal in the other groups. No adverse effect was observed on the bone surface at the delivered doses.

c) Discussion

For radiation synovectomy, the radiocolloid particle size should be between 2 and 30 μm (Shortkroff et al. 1995). If the particle size is < 1 μm, leakage from the synovial space can occur and the material would not be phagocytosed by the synovial tissue. Our measurements, with the method of laser scattering to determine particle size, revealed that 99% of the^{188}Re-tin colloid particles produced by the reaction at RT have adequate size to prevent their outflow from the joint. Analysis of the TLC results showed, that although the calculated labeling efficiency was 93% when the reaction mixture was heated at 100°C,

smaller particles were present which made the preparation unsuitable for intra-articular administration. As the reaction product at 100°C yielded a less uniform pattern with more particles smaller than the desired size, we decided to use the RT product in the animal experiments even though its labeling efficiency determined by ITLC was only 68%. In contrast, the scintigraphic images indicated that the ^{188}Re-tin colloid was well retained in the synovial space for up to 72 h in arthritic rabbits with AIA, and no leakage was visualized. No sign of distribution similarity could be detected by scintigraphy in rabbits receiving intraarticular $^{188}ReO_4^-$eluate and rabbits treated with intra-articular ^{188}Retin colloid solution. We presumed that that during the reaction of ^{188}Re tin colloid production, the unbound part of ^{188}Re would diffuse out of the joint. Retention of the radiopharmaceutical in the treated knee joint was confirmed by a time-independent, nearly constant activity ratio for the treated and control knees. As leakage could not be observed, our hypothesis is that different forms of ^{188}Re, probably $^{188}Re_2O_3$ and $^{188}Re_2O_5$ were also produced by the reaction and bound to the synovial membrane or taken up by synovial cells. Experiments to prove the presence of the above reduced rhenium oxides are continued in our laboratory. However, it is fundamental that a constantly higher ratio of labelled colloid be resent in the reaction product as only this assures stable pharmacokinetics and thus dosimetric planning in patients. The histologic effects observed in our study are consistent with the observations of Wang (Wang et al. 2001). The formation of fibrous connective tissue and thinner synovial membranes was observed only in the treated arthritic knees, presumably as a consequence of the beta irradiation emitted by the intra-articularly injected ^{188}Re-tin colloid.

5.2 Somatostatin receptor radionuclide therapy

5.2.1 General Materials and Methods

Radiochemical labelling

a) DOTA-TOC labelling with ^{111}In és ^{90}Y isotopes:
Adding 300 µL 0.4 M Na-acetate/gentisic acid buffer to the aqueous solution of DOTA-TOC molekula (from the inventory of Istituto Europeo di Oncologia, Milan, Italy) (60 µg/30 µL) wer set the pH to 5.0. To this solution a 185 MBq activity of carrier-free $^{111}InCl_3$ solution was added, and the reaction mixture was incubated at 90 ˚C for 30 minutes. Thereafter quality control was performed with C-18 filled (SepPak, Waters, USA) mini chromatography column separation method. The percentual proportion between peptide-bound and free ^{111}In was determined in the reaction product. Radioactivites were determined with a well-type gamma counter (NK-310, Gamma, Hungary).
Labelling of DOTA-TOC molecule with ^{90}Y was performed using the same strategy, with the difference that 10 µg peptides were calculated for 50 µL acetate/gentisic acid buffer and 370 MBq activity of carrier-free $^{90}YCl_3$ solution in the reaction mixture.
b) HYNIC-TOC molecule labelling with ^{99m}Tc isotope:
The peptide is available in the form of a lyophilised kit (from the inventory of Kantonsspital, Basle, Switzerland). This kit was mixed with the pertechnetate eluate of a ^{99m}Tc-generator (Izotóp Intézet Kft., Hungary) with approx. 1000-3000 MBq of activity in 1 mL volume, then the reaction mixture was incubate for 25 minutes at 100˚C-as the producer specified it. Quality control was performed with the same C18 mini column chromatography as in case a)

Imaging Studies

Scintigraphy was performed using a Mediso Nucline XRing/R (Mediso, Hungary) type Single Photon Emission Computed Tomography (SPECT) camera, dynamic studies in a matrix of 128, planar 2D images in a 256x256-byte. (SPECT imaging gives us a 3D image of the distribution in space of the gamma-photon sources within the animal.) Gamma-photons arriving to the detector were filtered in an energy window of ^{111}In : 250 keV with 20% width, in the case of ^{99m}Tc: 140 keV energy window was used with 20% width. For the imaging of ^{90}Y studies, because this isotope has no emitted gamma photons, we used characteristic X-ray spectrum of the radiation (Bremsstrahlung) as a result of the deposition of beta-particle energy in tissues of the animal. Bremsstrahlung was detected in a window centered at 140 keV with a window width of 100%.
SPECT imaging was acquired in a 256x256x16 bit matrix, up to a total count value of 3 000 000 per animal. Images were reconstructed and evaluated using InterView (Mediso,

Hungary) software. SPECT projection were reconstructed in space by the use of an Ordered Subsets Expectation Maximization (OSEM) algorithm. Sedation was given to the animals right before scintigraphy with an iv. ketamin-xylazin mixture (SBH-Ketamin, SelBruHa, Hungary, Xylavet, Alfasan, Holland) administered in a dose of 20 mg/bwkg and 2,5 mg/bwkg. Blood glucose levels were controlled during the examinations.

Immunohistochemistry methods

In all cases of the owner's consent on pathology we took biopsies from the organs. Biopsies were stored for a maximum of 2 days in 4% neutralized formaldehyde solution befor processing to immunohistochemistry. Section of 5 µm and unstained were immersed in a pH=6.0 0,1 M Na-citrate buffer and microwaved in an oven for an initial 2 minutes at 800 W and 30 minutes of 300 W. After this treatment immunohistochemistry was performed with an anti-ssr_{2a} antibody (1:750-dilution, SS-800 type Ab, Biotrend, Germany). A biotinylated secondary antibody (DAKO K6075, DakoCytomation, Denmark) was used for amplification, and processing and visualization was done with the DAKO EnVision kit (DakoCytomation, Denmark), labeling receptor-positive cells red. After this, tissue specimens were subjected to a normal hemalaune-eosine staining.
In all cases experimental imaging and therapy was expected by the owner of the animals under given informed consent.

5.2.2 Diagnostics using 111In-DOTA-TOC in healthy Beagle and dog with insulinoma

a) Study materials and methods

Clinical anamnesis

Our Institute was referred by the Internal Medicine Department of Faculty of Veterinary Science, Szent István University utaltak to examine an 8 years old mixed colour foxterrier bitch (13 kg) (Animal 1). Anamnesis included eight months of recurring more and more frequent periodic hypoglycemic seizures, that were observed 4-5 times daily at the time of examination. The dog earlier had been subjected to a detailed workup for epilepsy and received antiepileptic treatment (without results) (daily 2x1 Sevenaletta tabl.). At the Dept. Internal Medicine, the first blood glucose level measured was 2,4 mM in a conscious state, that fell into 1,2 mM during the seizures. Abdominal ultrasound performed at the Dept.has revealed a 4 cm x 1.5 cm and a 3 mm x 3 mm tumorous focus in the right lobe of the

pancreas. In addition heterogenous ultrasonic appearance of the liver suspected of disseminated liver metastases. The owner turned to our Institute after this finding.

Imaging

^{111}In-DOTA-TOC was applied in an intravenous injection in an activity of 169 MBq / 1 mL for the conscious animal through an indwelling cannula. Imaging was done 2, 4 and 24 hours post injection, for 40 minutes of acquisition. This included whole-body imagin (10 minutes) abdominal imaging (5 minutes) from ventrodorsal view and a SPECT of the abdominal region. The animal was remaining in our institute for the duration of radioactive studies in a separate box. After death we took samples for immunohistochemistry.
The same scintigraphy was applied for comparison to a 5 years old healthy Beagle male is with 100 MBq ^{111}In-DOTA-TOC.

b) Results

Planar scintigraphy has shown some foci in the liver and pancreas of the animal. This foci are well identifiable in SPECT planes as seen in a Figure 16, in the state imaged 4 hours post injection. For comparison the figure presents biodistribution in the healthy dog, too. In the animal with insulinoma the body as well as both lobes of the pancreas contain foci with high uptake, thus with overexpressed receptor, suspected of being the tumor and metastases.
24 hours post injection, just after the second imaging scan, the animal fell into a hypoglycemic coma and died. SPECT studies (Figure 17 A-C) and gross pathology have shown more, visible tumorous foci in the pancreas and in the liver. (Figure 17 D), amongst there, int he pancreas a primary tumor of 3 x 2 cm size and several miliary sites were also there in the organ. Immunohistochemistry has shown that most of the cells overxpress ssr_{2a}. Immunohistochemistry result from the biggest focus is also shown in Figure.

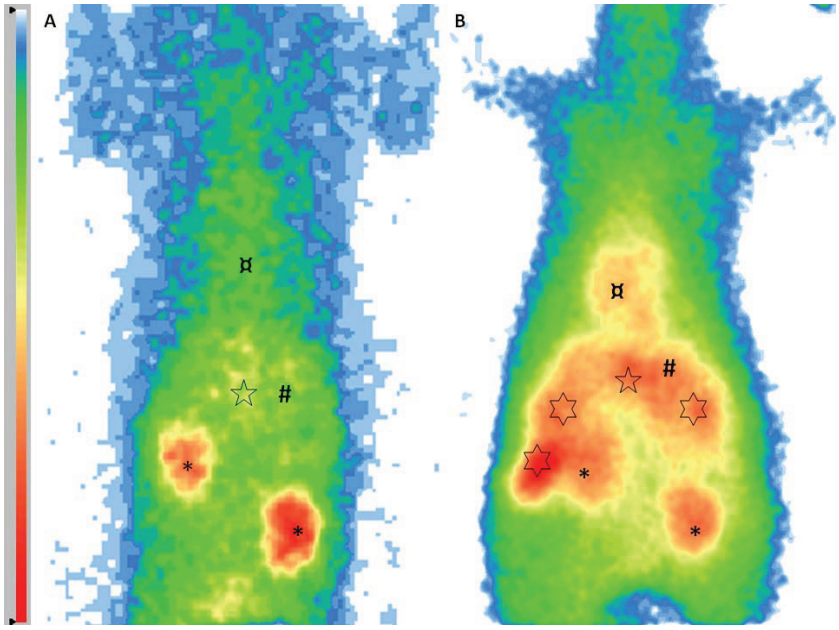

Figure 16. ^{111}In-DOTATOC planar ventrodorsal view scintigraphic images 4 h post injection of the abdominal region of a healthy Beagle dog (A) and a dog with insulinoma (B). Signs are identified on the images as follows:

* = kidneys,

¤ = heart,

= liver

☆ = pancreas

✡ = radiopharmaceutical uptake within tumorous foci

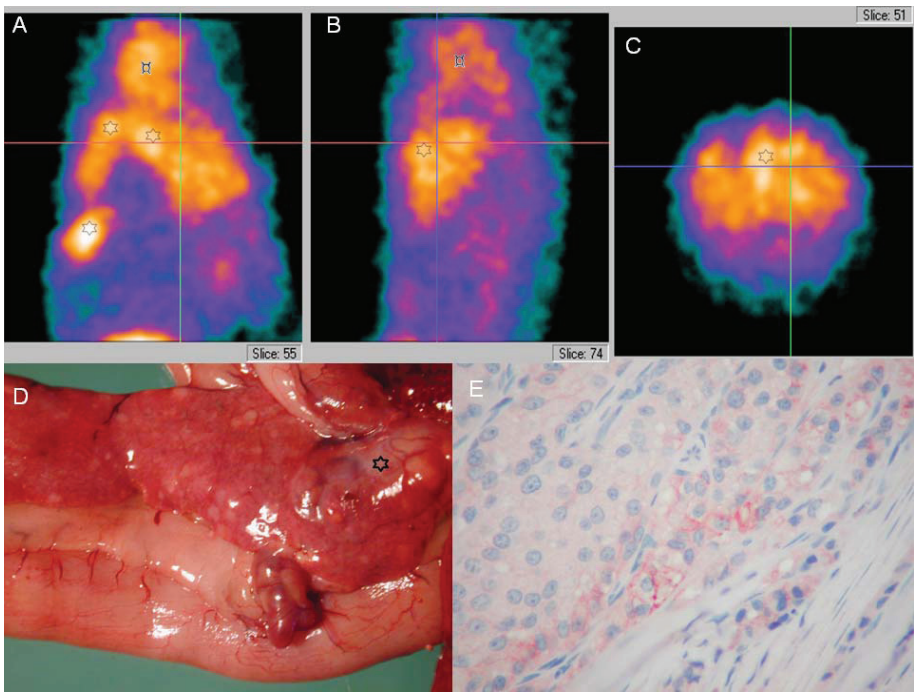

Figure 17. Clinico-pathological identification of insulinoma using receptor scintigraphy, pathology and immunohistochemistry.

A-C panel: SPECT image planes 4 h post injection of ^{111}In-DOTATOC in a dog with insulinoma. The section planes presented are A: horizontal, B: saggital, C: frontal planes of the trunk in the level of the liver. Identification of signs in the images:

¤ = heart,

✡ = radiopharmaceutical uptake within tumorous foci

5.2.3 Therapeutic studies using ^{90}Y-DOTA-TOC in a dog with insulinoma

a) Study materials and methods

Clinical anamnesis

The owner of this animal was also referred to our institute from the Dept. Internal Medicine. The dog (Animal 2), a 12 years-old, 16 kg black mixed breed male had presented a hindlimb weakness while walking, occurring more and more frequently and then the owners turned to the Dept. Internal Medicine, because the animal started to present periodic seizures. Ultrasonography revealed an echo-rich focus of 1,5x1,5 cm size in the pancreas. Blood glucose levels (2,1 mM) and ultrasonography resulted in the referral of the animal to our group one week before the imaging with a suspicion for insulinoma. In the same time blood samples were also taken from the animal for further plasma insulin level determinations.

As at that time we did not have the diagnostic ^{99m}Tc-HYNIC-TOC molecule, our decision was to inject ^{90}Y-isotope labelled DOTA-TOC peptide because its status deteriorated constantly, with daily 6-8 seizures despite of the constant honey feeding.

Radiotherapy

Based on human clinical experience (where a mean activity of 2,4 GBq is given in one cycle, usually using 4-7 cycles) we injected185 MBq for the first time, and a month later 370 MBq of ^{90}Y-DOTA-TOC radiopharmaceutical was injected intravenously, and in the first time 1, 4 and 24 hours post injection imaging was performed. Animal was kept separately in both cases for 2 weeks after radiotherapy with the urine and stools collected as a radioactive waste. Blood was sampled 2 days post the first RIT cycle then 2 and 4 weeks later, then again 2 days after the second RIT cycle, and 2, 4, 6, 8 and 12 weeks later, to determine insuline levels. A full blood cell count panel and AST, ALT, ALKP, LDH, creatinine, urea levels were also determined. 2, 4, 6 and 8 weeks after therapy ultrasonography was performed as a control in

the Dept. Internal Medicine. Later after the death of the animal immunohistochemistry was also performed.

b) Results

Figure 18. summarizes images obtained in the course of therapy with the animal. Insulin levels are given in Figure 19. and Table 10. Ultrasonic measurements are presented in Table 11. It is visible that after therapy insuline levels decrease and then return to an albeit high, but lower than the original value. We could find no abnormalities in neither blood panels nor other physicals. However a dramatic improvement of the animal was observed within 24 hours after injection. Seizures 6-8 times a day were stopped, comportment and general status of the animal was visibly much better. 22 days after the therapy we decided to perform a second RIT. From then on, general status of the animal was stabilized as good for 18 months, without any sign of clinical insulinoma, then in one month the seizures became more and more frequent so the owner decided to ask for euthanasia of the animal in month 19 after the first therapy.

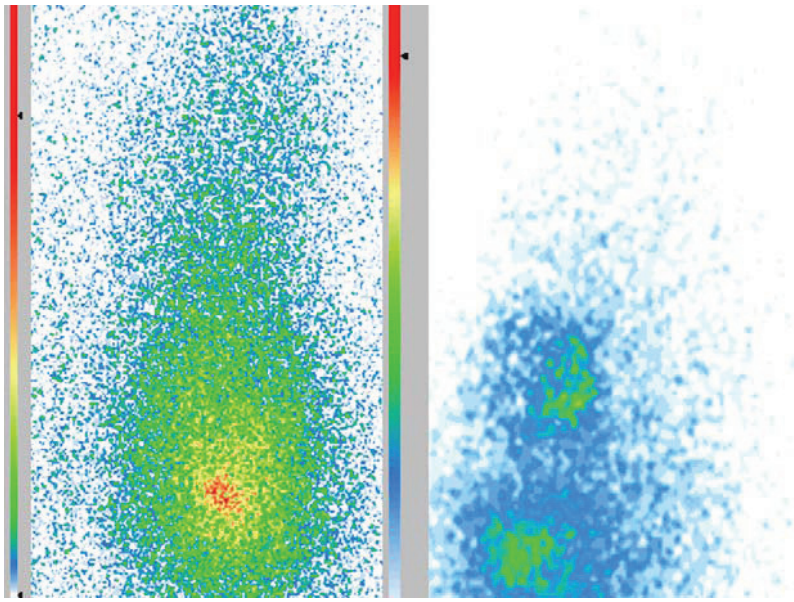

Figure 18. Images taken post 2 hours (lef panel) and 4 hours (right panel) of ^{90}Y-DOTATOC injection in a dog with insulinoma. Planar Bremsstrahlung (characteristic X-ray) scintigraphy images. Urinary bladder (in both panels at the bottom part) and the tumor (middle of right panel) are visible as sites of radiopharmaceutical accumulation.

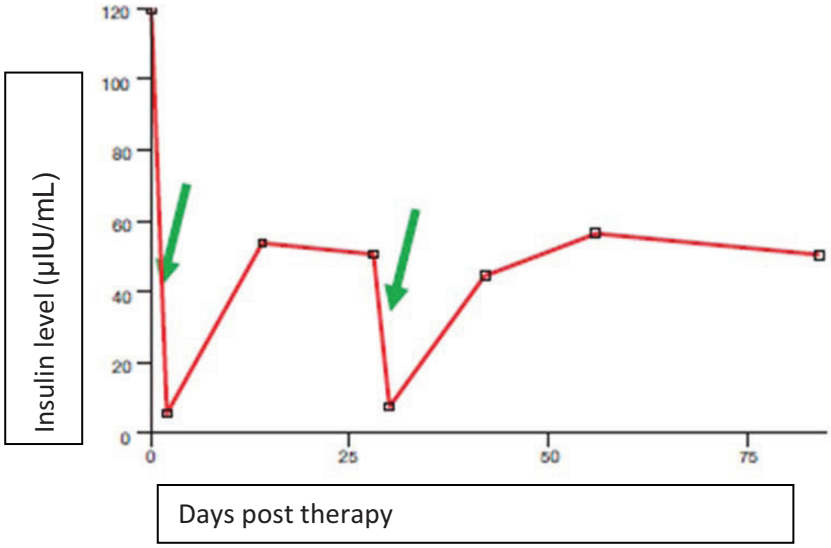

Figure 19. Insulin levels (µIU/mL) in the plasma of a dog with insulinoma versus time relative to therapies (days) with ^{90}Y-DOTATOC. Two green arrows indicate the radiopharmaceutical injection days.

Time post therapy (days)	Plasma insulin level (maximal normal value: 20 µIU/mL)
0 (preceding)	120.00
2	5.70
14	53.70
28	50.53
30 (2 days post Cycle 2)	7.50
42	44.43
56	56.46
84	50.45

Table 10. Ultrasound monitoring of the insulinoma size in Animal 1.

5.2.4 Diagnostic ^{99m}Tc-scintigraphy in healthy Beagles and in dogs with insulinoma

a) Study materials and methods

Clinical anamnesis and imaging

HYNIC-TOC diagnostic peptide molecule to be labelled with ^{99m}Tc was obtained by our institution in the course of an international trial just after the first RIT cycle described above. Then, for comparison, ^{99m}Tc-HYNIC-TOC biodistribution was imaged in both the aforementioned Animal 2 with insulinoma, and a healthy male and a female Beagle. Out of these studies anouther dog with insulinoma kutyán (Animal 3) was also subjected to ssr_{2a} scintigraphy. This animal was also examined at the Dept. Internal Medicine with hindlimb lameness; after a measured low blood glucose value an abdominal ultrasonography was done. The animal, a 10 years 20 kg boxer-mixed breed bitch did not present such severe symptoms as in Animals 1 or 2, but the ultrasound images have shown a diffuse echodensity in the head of the pancreas. The animal lost conscience for cca. 1 hours following the ultrasound examination, and two days after an ssr_{2a} isotope diagnostic study was performed. We applied 310 MBq of activity. All animals were examined with the very same protocol: 1 and 4 hours postinjection, whole-body scintigraphy, ventro-dorsal abdominal scintigraphy and a trunk SPECT study was done in each imaging session.

b) Results

Images of a healthy Beagle are seen on Figure 20. Four hours post injection in a ventro-dorsal view. Figure 21. shows Animal 2 with insulinoma in scintigraphy and three planes of the SPECT study together with the visible focus of high uptake. Figure 22. shows the same in the case of Animal 3, again with insulinoma. In all images due to high presence of somatostatin receptors in the dog stomach. The same uptake can be seen in the heart as well. Functional presence of dog antral and pyloral ssr_{2a} –is well documented in the literature, and we describe the phenomenon in accordance. There was no constant visibility of the spleen. Besides the mentioned organ, as expected, kidneys have shown high uptake. Gallbladder is also visible. In SPECT planes you can identify the tumor as shown by the hair cross in Animals 2 and 3.

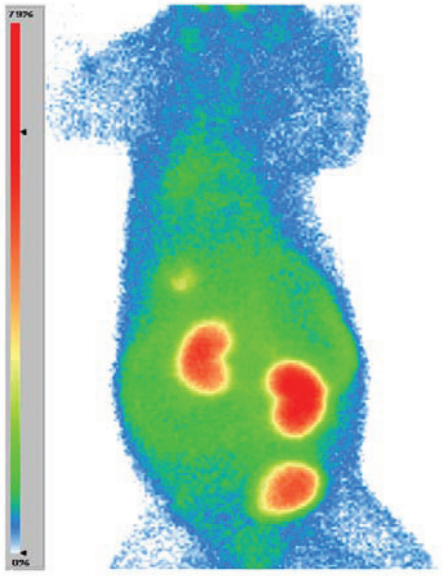

Figure 20. Biodistribution of ^{99m}Tc-HYNIC-TOC in healthy Beagle dog 2 hours post injection with a ventrodorsal scintigraphic view. Kidneys, bladder, gallbladder, stomach, heart and larger vessels are visible.

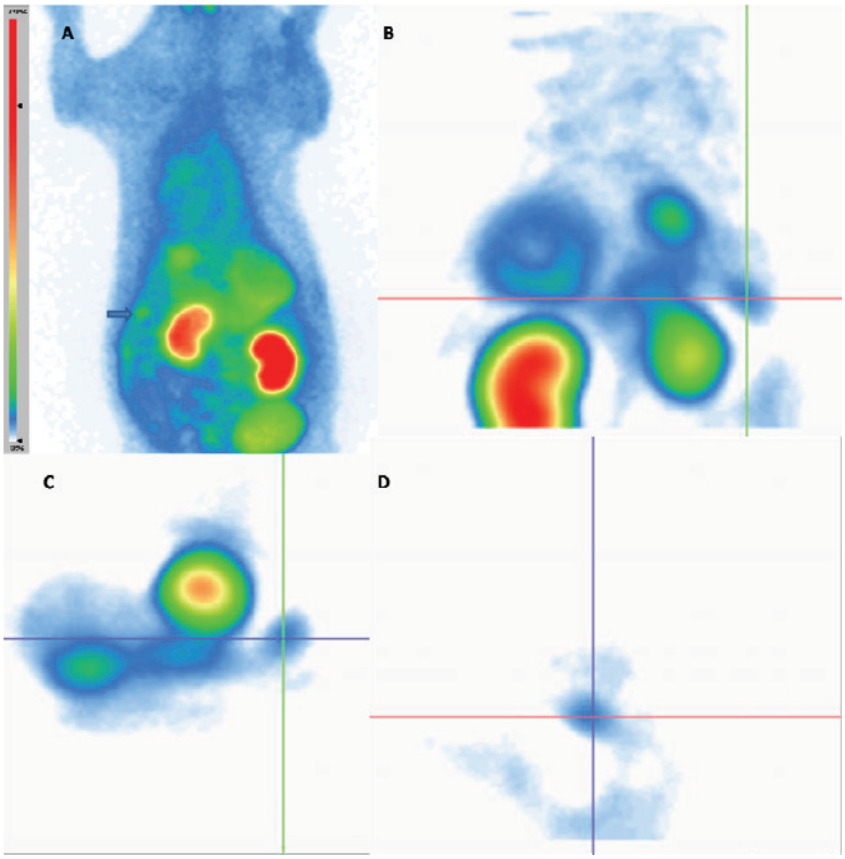

Figure 21. Dog with insulinoma, scintigraphic and SPECT imaging using ^{99m}Tc-HYNICTOC with a ventro-dorsal planar view 4 h post injection (A) and SPECT section planes 4 h post injection in the planes of a tumorous focus with radiopharmaceutical uptake in the horizontal

(B), frontal (C) and saggital (D) planes. Kidneys, urinary bladder, stomach, gallbladder, and heart are also visualized.

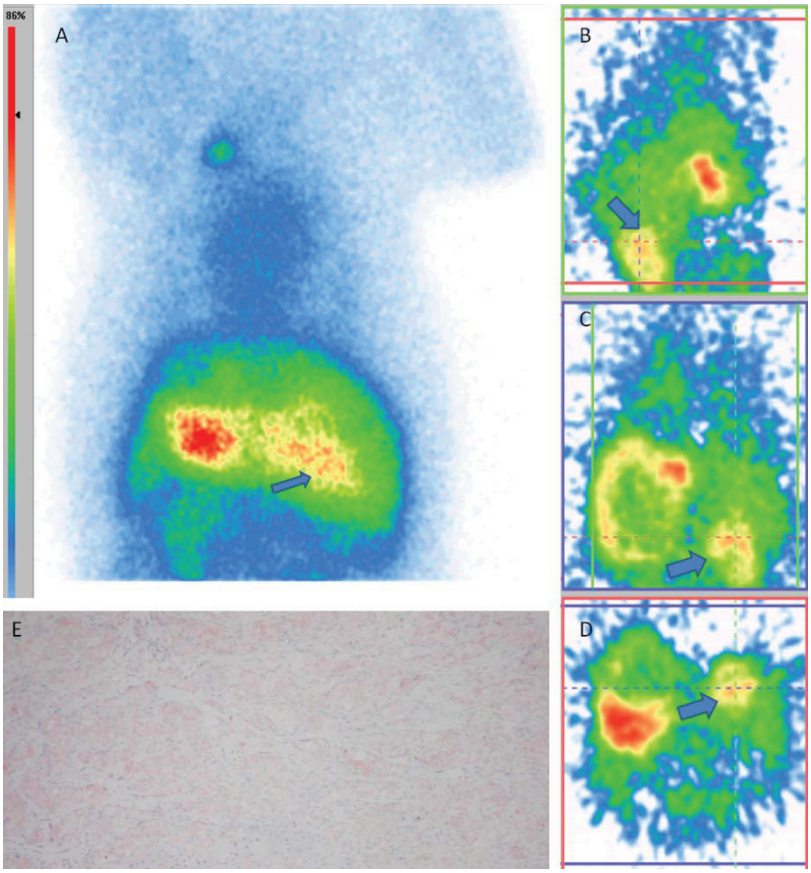

Figure 22. Dog with insulinoma ('dog 3'), scintigraphic and SPECT imaging using ^{99m}Tc-HYNICTOC with a ventro-dorsal planar view 4 h post injection (A) and SPECT section planes 4 h post injection in the planes of a tumorous focus with radiopharmaceutical uptake in the horizontal (B), frontal (C) and saggital (D) planes. Liver (its diffuse echondensity was also seen on ultrasound), heart, right kidney and an axillary lymph node are visualized, the latter most probably being caused by paravenous injection of the agent. Panel E shows immunohistochemistry examination of the insulinoma focus identified (magnification 40x).

5.2.5 General Discussion

We used novel, previously undescribed somatostatin analogues for somatostatin receptor detection in dogs with insulinoma tumors to study possibilities of both animal model use of natural cancers in dogs and have an insight into veterinary therapy. According to earlier studies in the field and according to our own observations, the method of somatostatin receptor diagnostic scintigraphy can be applied in tumorous dogs with insulinoma with good prospective results. (Of course a special care should be made to maintain blood glucose levels during anaesthesia). According to Robben, the sensitivity of scintigraphic imaging

seems higher that that of CT or Ultrasound (Robben et al 2005). Our cases also support this hypothesis as we could identify one or more tumors in each animal subjected to scintigraphy and SPECT. To our knowledge we were the first to use ^{99m}Tc-labelled octreotide analogue in the dog and we could observe an appropriate and useful imaging process. This radiopharmaceutical gives a quality image one hour after injection from the abdomen whereas in the case of OctreoScan 4-24 hours of waiting are necessary, it is cheaper and much more simple both in preparation and in logistics than ^{111}In labelled ssr_{2a} ligands (Hubalewska-Dudejczyk et al. 2007, Goldsmith 2009). As to the again previously unused DOTA-TOC molecule int he dog, labelled with ^{111}In we were succesful in diagnosing an animal with insulinoma. In comparison to human biodistribution, heart uptake of ssr_{2a} is a considerable difference. In accordance with the earlier studies by Joris Robben (Robben et al. 1997) and other studies describing ssr_{2a} activity (Funk and Greenberg 1997), ^{99m}Tc-labelled octreotide having a higher affinity for ssr_{2a} receptor than ^{111}In-DOTA-TOC has shown uptake in all the animals in the stomach. However it is surprising that there is no uptake in dog spleen contrarily to the human images.

We elaborated a novel immunohistochemistry method for the detection of dog tissues with regard to ssr_{2a} receptor expression using a mouse antibody, and in the tumors imaged with scintigraphy we could see receptor positivity in vitro, too.

We realized combined diagnostics and therapy using TOC as a peptide molecule, labelled with ^{90}Y for DOTA as the chelator and ^{99m}Tc for HYNIC as the chelator.

To our knowledge we have been the first to perform a ^{90}Y-DOTA-TOC therapy (twice) in a dog. This resulted in both the amelioration of clinical status and it resembled human results also in time course and tumor reduction resulting in normal quality of life for an extended period. It is of notice that both in dog and man in the case of insulinoma we often see central and peripheral nervous symptoms due to paraneoplastic syndrome (Fukazawa et al. 2009) that could even be first signs of the original tumor. These symptoms are cleared away by excising the tumor or by means of RIT, even independently of blood glucose levels.

The latere diagnostic scintigraphy could however image the tumor again, but due to the older age of the dog the owners did not ask for a third therapy attempt.

Dog insulinoma is not a very frequent cancer, however a good diagnosis will have tremendous impact on further management. Many studies state that a veterinary patient with a tumor over 1 cm will have around 50% probability of micrometastases in mesenterial lymph nodes and the body of pancreas. (Caywood et al. 1988, Tobin et al.1999). In the case of a small solitary nodule (below 1 cm) surgical resection is proposed (Caywood et al. 1988). In the case of multifocal or large-size tumor after histopathological decision it could be beneficial to turn to medical treatment (Tobin et al. 1999, Polton et al. 2007) including RIT presurgically. The same process gave a good result in human patients for Stöltzing et al,

who report on successful decrease of size of liver metastases of insulinoma with ^{90}Y-DOTA-TOC and then the successful use of surgery and chemotherapy (Stöltzing et al. 2009).

We consider that evaluation and comparison of these results obtained in naturally occurring animal models of disease will be of help for both human and veterinary care improvement. The most important element where these animal models will be of future use is RIT dosimetry: we have to deliver the highest dose possible to the highest number of tumor cells with the least collateral damage to healthy cells. This is very effectively helped by the use of natural tumors in companion animals: polyclonal tumor cell population mind az is only characteristic of human and animal natural cancers not other models. So human consequences can be drawn from the results of therapeutic methods obtained in naturally occurring polyclonal dog tumors. For this, a knowledge of the differences is also important, and our studies gave an impetus on this field, too, revealing stomach, heart and to a certain extent kidney uptak differences. Heart uptake can be seen in both DOTATOC and HYNIC-peptide scans. We presume that dog hearts contain Growth Hormone Secretagogue, (GHS) receptors (eg. CD36 glycoprotein) that can react as intermediate affininty SS analogue receptors and are present in rat and to a lesser extent, human myocardium (Deghenghi et al. 2001, Bodart et al 2002), but this hypothesis is still to be proven.

Our results indicate that the most important excretory route in the dog is the kidney like in humans, but unlike in humans bile also contains excreted radioactivity as contrary to human cases. This has to be taken into account when designing, performing and evaluating both dog imaging and dog model or even dosimetry studies.

In summary we consider that these studies open the way for further, wider application of veterinary somatostatin imaging scintigraphy, (receptor-positive lymphomas and sarcomas could also be subjects of these types of studies) and to the application of the therapy for other dog natural diseases, such as arthitis (Dalm et al. 2003). At the end human pharmaceutical development and care for the tumorous patients can both benefit from a wider application of natural dog studies-and that's where lies ultimately the benefit and uniqueness of natural dog disease models.

6. Overview of results (new scientific findings)

In the course of the studies presented, new beta-emitting radiopharmaceuticals for the therapy of the bone and joint system and somatostatin-expressing tumors have been evaluated through the use of healthy, artificially diseased and spontaneously diseased animals. This concept haa yielded new results in both the radiopharmaceutical sciences as the emphasis was on evaluating and developing new radiopharmaceuticals, as well as gave new results in application of animal models and finally, gave results in veterinary science. These new results that have not been described elsewhere are presented here in anabbreviated list form.

1. We have synthetized ^{177}Lu-EDTMP using carrier-free ^{177}Lu and formulated it pharmaceutically according to a previously not applied formulation with ^{177}Lu labels that is easy to tolerate *in vivo*, too.
2. We have shown the bone-seeking behaviour of ^{177}Lu-EDTMP in the mouse, rat, rabbit and dog species using nuclear imaging equipment. The application of a novel, world-unique SPECT system using multiplexed multi-pinhole collimation has played a significant role in the determination and identification of ^{177}Lu-EDTMP depositing in remodeling rodent bone areas and not in „inactive" bone.
3. We were the first to provide direct imaging proof that ^{177}Lu-EDTMP is preferentially binding to the cortical areas and not the spongiosa of the remodelling bones. Thus, the radiation dose of the isotope is confined to these areas rather than into bone marrow.
4. We have determined the differences between mouse and dog imaging of ^{177}Lu-EDTMP in the same time points post injection where dog uptake of radioactivity is present in a later maximum than in the mouse.
5. We have explored and defined the pharmacokinetics of ^{177}Lu-EDTMP in mouse and rabbit and we have determined that an important difference exists between mouse and rabbit bone Area Under the Data values representing differences in calcium bone turnover. Rabbit ^{177}Lu-EDTMP bone fixation has been proven to be less active than turnover in the mouse. This has very important implications for human therapeutic dose planning.
6. We have presented that in dogs, ^{177}Lu-EDTMP is not exerting toxic effects to bone marrow after application in a therapeutic dose and we set the minimal values of injected activity in this species.
7. We have developed a new method of preparation of a radiosynoviorthesis agent, ^{188}Re-tin particles at room temperature reaction.
8. We have shown that the agent ^{188}Re-tin particle is not leaking out of rabbit arthritic knee joint at any time after application thus it is suitable for human intra-articular therapy as well.

9. We have shown using histology that beta particles arising from ^{188}Re are anti-inflammatoric and have a beneficial effect against synovial thickening in the antigen induced arthritic rabbit knee model.

10. We have prepared the radiopharmaceutical ^{99m}Tc-HYNIC-TOC that shows binding to somatostatin 2A receptors in the dog, too.

11. We have shown that in the dog species the expression pattern of somatostatin receptors in the organs is different from that of man. We have shown that of ^{111}In and ^{99m}Tc-labelled somatostatin analogue peptides are differently binding to heart, stomach and spleen in the dog and in man. Dogs present receptors in the stomach and heart and we could not detect those receptors in spleen whereas in humans the situation is vica versa.

12. We have proven that dog spontaneous insulinomas express somatostatin 2A receptors with a direct immunohistochemistry method previously not presented in the literature.

13. We have also proven that dog somatostatin receptor peptide radionuclide SPECT is feasible with both ^{111}In and ^{99m}Tc using DOTA-TOC as targeting peptide.

14. We have shown that dog insulinoma can be used as a spontaneous model of PRRT and have achieved an outstanding case survival result with repeated ^{90}Y-PRRT. This survival is the first proof of targeted peptide radiation therapy in the dog.

7. References

Adams RL, Adams IP, et al. (2005) Somatostatin receptors 2 and 5 are preferentially expressed in proliferating endothelium. Br J Cancer. 92:1493-1498.

Altschul M, Simpson KW, et al.(1997) Evaluation of somatostatin analogues for the detection and treatment of gastrinoma in a dog. J Small Anim Pract. 38:286-291.

Anderson MP, Wiseman AG, Dispenzieri A, et al. (2002) High-dose samarium-153 ethylene diamine tetramethylene phosphonate: low toxicity of systemic irradiation in patients with osteosarcoma and skeletal metastases. J Clin Onc 20:189-196.

Ando A, Ando I, Tonami N, et al. 177Lu-EDTMP (1998) A potential therapeutic bone agent. Nucl Med Commun19:587-594.

Awasthi V, Meinken G, Springer K, et al. (2004) Biodistribution of radioiodinated adenovirus fiber protein knob domain after intravenous injection in mice. J Virol 78:6431-6439.

Bakker WH, Albert R, et al (1991) [111In-DTPA-D-Phe1]-octreotide, a potential radiopharmaceutical for imaging of somatostatin receptor-positive tumors: synthesis, radiolabeling and in vitro validation. Life Sci. 49:1583-1591.

Bakker WH, Krenning EP, et al. (1991) In vivo use of a radioiodinated somatostatin analogue: dynamics, metabolism, and binding to somatostatin receptor-positive tumors in man. J Nucl Med 32:1184-1189.

Banerjee S, Samuel G, Kothari K, et al. (2001) 99mTc and 186Re complexes of tetraphosphonate ligands and their pharmacological behaviour in animal models. Nucl Med Biol 28:205-211.

Bares R, Galonska P, et al. (1993) Somatostatin receptor scintigraphy in malignant lymphoma: first results and comparison with glucose metabolism measured by positron-emission tomography. Horm Metab Res Suppl. 27:56-58.

Bauman G, Charette M, Reid R, Sathya J.(2005) Radiopharmaceuticals for the palliation of painful bone metastasis—a systemic review. Radiother Oncol 75:258-270.

Berenson JR, Rajdev L, Broder M. (2006) Managing bone complications of solid tumors. Cancer Biol Ther 9:1086-1095.

Bernhardt P, Benjegard SA, Kolby L, et al. (2001) Dosimetric comparison of radionuclides for therapy of somatostatin receptor-expressing tumors. Int J Rad Onc Biol Phys 51:514-524.

Bertherat J, Tenenbaum F et al. (2002) Somatostatin Receptors 2 and 5 Are the Major Somatostatin Receptors in Insulinomas: An in Vivo and in Vitro Study J Clin Endocrin Metabol 88: 53-60.

Bhandari S, Watson N, et al. (2008) Expression of somatostatin and somatostatin receptor subtypes 1-5 in human normal and diseased kidney. J Histochem Cytochem. 56:733-743.

Bishayee A, Rao DV, Srivastava SC, et al. (2000) Marrow- sparing effects of 117mSn(4 +) diethylenetriaminepen- taacetic acid for radionuclidic therapy of bone cancer. J Nucl Med 45: 2043-2052.

Blum J, Handmaker H, et al. (2000) A multicenter trial with a somatostatin analog (99m)Tc depreotide in the evaluation of solitary pulmonary nodules. Chest. 117:1232-1239

Bodart V, Febbraio M, et al. (2002) CD36 mediates the cardiovascular action of growth hormone-releasing peptides in the heart. Circulation Research 90:844–849.

Bodei L, Ferone D, Grana CM, Cremonesi M, Signore A, Dierckx RA, Paganelli G (2009): Peptide receptor therapies in neuroendocrine tumors. J Endocrinol Invest. 32:360-9.

Brans B, Bodei L et al.(2007) Clinical radionuclide therapy dosimetry: the quest for the „Holy Gray". Eur J Nucl Med Mol Imaging 34: 772-786

Brazeau P, Vale W, et al. (1973) Hypothalamic polypeptide that inhibits the secretion of immunoreactive pituitary growth hormone. Science 179:177-179.

Brenner W, Kampen WU, Brummer C, von Forstner C, Zuhayra M, Czech N, Muhle C, Henze E. (2003). Bone uptake studies in rabbits before and after high-dose treatment with 153Sm-EDTMP or 186Re-HEDP. J Nucl Med 44:247-251.

Brenner W, Kampen WU, Kampen AM, Henze E. (2001) Skeletal uptake and soft-tissue retention of 186Re-HEDP and 153Sm-EDTMP in patients with metastatic bone disease. J Nucl Med 42:230-236.

Caravan P, Ellison JJ, McMurrym TJ, et al. (1999) Gadolinium(III) chelates as MRI constrast agents: Structure, dynamics, and applications. Chem Rev 99:2293-2297.

Caywood DD, Klausner JS, et al. (1988) Pancreatic insulin-secreting neoplasms: Clinical, diagnostic, and prognostic features in 73 dogs. J Amer Anim Hosp Assoc. 24:577–584

Chakraborty S, Das T, Banerjee S, Balogh L, Chaudhari PR, Sarma HD, et al. (2008) 177Lu-EDTMP: a viable bone pain palliative in skeletal metastasis. Cancer Biother Radiopharm 23:202-213.

Chakraborty S, Das T, Banerjee S, et al. (2006) Preparation and preliminary biological evaluation of 177Lu-labeled hydroxyapatite as a promising agent for radiation synovectomy of small joints. Nucl Med Commun 27:661-667.

Chakraborty S, Das T, Unni PR, et al. (2002) 177Lu-labeled polyaminophosphonates as potential agents for bone pain palliation. Nucl Med Commun 23:67-75.

Cheung A, Driedger AA. (1980) Evaluation of radioactive phosphorus in the palliation of metastatic bone lesions from carcinoma of breast and prostate. Radiology134:209-214.

Cicek M, Oursler MJ. (2006) Breast cancer bone metastasis and current small therapeutics. Cancer Metastasis Rev 25:635-644.

Coronado M, Redondo A, Coya J, et al. (2006) Clinical role of Sm-153- EDTMP in the treatment of painful bone metastatic disease. Clin Nucl Med 31:605-610.

Dalm V.A.S.H., P.M. Van Hagen, et al. (2003) Role of octreotide scintigraphy in rheumatoid arthritis and sarcoidosis Q J Nucl Med 47:270-278

Das T, Chakraborty S, Banerjee S, et al. (2006) 177Lu-labeled metronidazole for possible use in targeting tumor hypoxia. Radiochim Acta 94:375-382.

Das T, Chakraborty S, Banerjee S, et al. (2004) Preparation and preliminary biological evaluation of a 177Lu-labeled sanazole derivative for possible use in targeting tumor hypoxia. Bioorg Med Chem 12:6077-6087.

Das T, Chakraborty S, Sarma HD, Banerjee S. (2008) 177Lu-DOTMP: a viable agent for palliative radiotherapy of painful bone metastasis. Radiochim Acta 96:55-61.

Das T, Chakraborty S, Unni PR, Sarma HD, Samuel G, Banerjee S, Venkatesh M, Ramamoorthy N, Pillai MRA. (2002) 177Lu labeled cyclic polyaminophosphonates as potential agents for bone pain palliation. Appl. Radiat. Isot 57:177-184.

D'Asseler Y. (2009): Advances in SPECT imaging with respect to radionuclide therapy. Q J Nucl Med Mol Imaging. 53,343-347.

Daut RL, Cleeland CS. (1982) The prevalence of severity of pain in cancer. Cancer 50:1913-1917.

de Klerk JMH, van het Schip AD, Zonnenberg BA, et al. (1996) Phase I study of rhenium-186-HEDP in patients with bone metastases originating from breast cancer. J Nucl Med 37:244-256.

Decristoforo C, Melendez-Alafort L, et al. (2000) 99mTc-HYNIC-[Tyr3]-octreotide for imaging somatostatin-receptor-positive tumors: preclinical evaluation and comparison with 111In-octreotide J Nucl Med. 41:1114–1119

Deghenghi R, Papotti M. (2001) Somatostatin octapeptides (lanreotide, octreotide, vapreotide, and their analogs) share the growth hormone-releasing peptide receptor in the human pituitary gland. Endocrine 14:29–33.

Deligny CL, Gelsema WJ, Tji TG, et al. (1990) Bone-seeking radiopharmaceuticals. Nucl Med Biol 17:164.

DiMasi J. (2002): The value of improving the productivity of the drug development process. Pharmacoeconomics. 20 Suppl 32:1-10.

Eary JF, Collins C, Stabin M, et al. (1993) Samarium-153-EDTMP biodistribution and dosimetry estimation. J Nucl Med 34:1031-1036.

Esser JP, Krenning EP, et al. (2006) Comparison of [(177)Lu-DOTA(0),Tyr(3)]octreotate and [(177)Lu-DOTA(0),Tyr(3)]octreotide: which peptide is preferable for PRRT? Eur J Nucl Med Mol Imaging. 33:1346-1351.

Essman SC, Lattimer J, Cook JL, Turnquist S, Kuroki K. (2003) Effects of 153Sm-ethylenediaminetetramethylene phosphonate on physeal and articular cartilage in juvenile rabbits. J Nucl Med 44:1510-1515.

Essman SC, Lewis MR, Miller WH. (2005) Intraorgan biodistribution and dosimetry of 153Sm-ethylenediaminetetramethylene phosphonate in juvenile rabbit tibia: implications for targeted radiotherapy of osteosarcoma. J Nucl Med 46:2076-2082.

Feeney DA, Anderson KL. (2007) Nuclear imaging and radiation therapy in canine and feline thyroid disease. Vet Clin North Am Small Anim Pract. 37:799-821, viii.

Finlay IG, Mason MD, Shelley M. (2005) Radioisotopes for the palliation of metastatic bone cancer: a systematic review. Lancet Oncol 6:392-400.

Forrer F, Uusijarvi H, et al. (2004) A comparison of (111)In-DOTATOC and (111)In-DOTATATE: biodistribution and dosimetry in the same patients with metastatic neuroendocrine tumours. Eur J Nucl Med Mol Imaging. 31:1257-1262

Fukazawa K, Kayanuma H, et al.(2009) Insulinoma with basal ganglion involvement detected by magnetic resonance imaging in a dog. J Vet et Med Sci. 71:689-692

Funk LC, Greenberg RG (1997). Characterization of somatostation receptor subtypes mediating inhibition of nutrient-stimulated gastric acid and gastrin in dogs Regulatory Peptides 68:197-203

Garden OA, Reubi JC, et al. (2005) Somatostatin receptor imaging in vivo by planar scintigraphy facilitates the diagnosis of canine insulinomas. J Vet Intern Med.19:168-176

Goeckeler WF, Edwards B, Volkert WA, et al. (1987) Skeletal localization of samarium-153 chelates: Potential therapeutic bone agents. J Nucl Med 28:495-512.

Goldsmith SJ. (2009) Update on nuclear medicine imaging of neuroendocrine tumors. Future Oncol. 5:75-84.

Gordon I., Paoloni M., Mazcko C., Khanna C. (2009): The comparative oncology trials consortium: using spontaneously occurring cancers in dogs to inform the cancer drug development pathway. PLoS Med. 6, e1000161.

Grewal RK, Dadparvar S et al. (2002) Efficacy of Tc-99m depreotide scintigraphy in the evaluation of solitary pulmonary nodules. Cancer J. 8:400-404.

Haberkorn U., Altmann A., Eisenhut M. (2002): Functional genomics and proteomics—the role of nuclear medicine. Eur J Nucl Med Mol Imaging. 29, 115-32.

Hamilton, J. G., Soley, M. H. (1940) Studies in iodine metabolism of the thyroid gland in situ by the use of radioiodine in normal subjects and in patients with various types of goitre. Amer J Physiol. 131:131-135

Hicks R.J. (2005): Small Animal PET: New Drug, New Models, New Tracers. Peter MacCallum Cancer Centre. Biomed Imaging Intervent J. 1, e7- 49.

Hosain F, Spencer RP. (1992) Radiopharmaceuticals for palliation of metastatic osseous lesions: Biologic and physical background. Semin Nucl Med 22:11-16.

Hoskin PJ. (2003) Bisphosphonates and radiation therapy for palliation of metastatic bone disease. Cancer Treat Rev 29:321-325.

Hoskin PJ. Radiotherapy of bone pain. (1995) Pain63:137-145.

Hoyer D, Bell GI, et al. (1995) Classification and nomenclature of somatostatin receptors. Trends Pharmacol. Sci. 16:86– 88.

Hubalewska-Dydejczyk A, Fröss-Baron K, et al. (2007) 99mTc-EDDA/HYNIC-octreotate in detection of atypical bronchial carcinoid. Exp Clin Endocrinol Diabetes.115:47-49.

Hubalewska-Dydejczyk A, Szybinski P, et al. (2005) (99m)Tc-EDDA/HYNIC-octreotate - a new radiotracer for detection and staging of NET: a case of metastatic duodenal carcinoid. Rev Nucl Med Cent East Eur.8:155-156.

Jan De Beur SM, Streeten E, et al (2002). Localisation of mesenchymal tumours by somatostatin receptor imaging Lancet 359:761-763

Johnson JC, Langhorst SM, Loyalka SK, et al. (1992) Calculation of radiation dose at a bone-to-marrow interface using Monte Carlo modeling techniques (ESG4). J Nucl Med 33:623-627.

Joseph K, Stapp J, et al. (1993) Receptor scintigraphy with 111In-pentetreotide for endocrine gastroenteropancreatic tumors. Horm Metab Res Suppl 27:28-35.

Kato H., Nakajima M., Sohda M, Tanaka N., Inose T., Miyazaki T., Fukuchi M., Oriuchi N.,

Endo K., Kuwano H. (2009): The clinical application of (18)F-fluorodeoxyglucose positron emission tomography to predict survival in patients with operable esophageal cancer. Cancer 115:3196-3203.

Ketring AR. (1987) 153Sm-EDTMP and 186Re-HEDP as bone therapeutic radiopharmaceuticals. Nucl Med Biol 14:223-229.

Knapp FF, Mirzadeh S, Beets AL, et al. (1998) Reactor produced radioisotopes from ORNL for bone pain palliation. Appl Radiat Isot 49:309-315.

Krenning EP, Breeman WAP, et al. (1989) Localisation of endocrine-related tumours with radioiodinated analogue of somatostatin, Lancet 1:242–244.

Krenning EP, Kwekkeboom DJ, et al. (1993) Somatostatin receptor scintigraphy with [111In-DTPA-D-Phe'1- and 123I-Tyr31-octreotide: The Rotterdam experience with more than 1000 patients. Eur J Nucl Med 20:716-731

Kumar V, Kumar D, Howman-Giles RB, Little DG. (2007) Is 99mTc-labelled pamidronate a better agent than 99mTc-medronate for bone imaging? Nucl Med Commun 28:101-107.

Kwekkeboom DJ, Bakker WH, Kam BL, et al. (2003) Treatment of patients with gastro-entero-pancreatic (GEP) tumors with the novel radiolabelled somatostatin analogue [177Lu-DOTA0,Tyr3]octreotate. Eur J Nucl Med Mol Img 30:417-421.

Lamberts SW, Bakker WH, et al.(1990) Treatment with Sandostatin and in vivo localization of tumors with radiolabeled somatostatin analogs. Metabolism 39 (9 Suppl 2):152-155.
Lamberts SW, Krenning EP, et al. (1991) The role of somatostatin and its analogs in the diagnosis and treatment of tumors. Endocr Rev 2:450-482.

Lamberts SW, van der Lely, AJ, et al. Octreotide. (1996) New Engl J Med 334:246–254.

Lattimer JC, Corwin LA, Srapleton J, et al. (1990) Clinical and clinicopathologic effects of samarium-153-EDTMP ad- ministered intravenously to normal beagle dogs. J Nucl Med 131:586-595.

Lawrence JH. (1940) Nuclear physics and therapy: Preliminary report on a new method for the treatment of leukemia and polycythemia. Radiology 35:51-60.

Laznicek M, Lazincova A, Budsky F, et al. (1994) Comparison of biological characteristics of EDTMP complexes with 99mTc, 111In, and 153Sm in rats. Appl Radiat Isot 45:949-954.

Lee E.B., Shin K.C. et al. (2003) 188Re-tin-colloid as a new therapeutic agent for rheumatoid arthritis. Nucl Med Commun. 24:689-696.

Leitha T. (2009) Nuclear medicine: proof of principle for targeted drugs in diagnosis and therapy. Curr Pharm Des. 15:173-187.

Lester NV, Newell SM, et al. (1999) Scintigraphic diagnosis of insulinoma in a dog. Vet Radiol Ultrasound 40:174-178.

Lewington VJ. (1996).Cancer therapy using bone-seeking iso- topes. Phys Med Biol 41:2027-2032.

Li S, Liu J, Zhang H, Tian M, Wang J, Zheng X. (2001) Rhenium-188 HEDP to treat painful bone metastases. Clin Nucl Med 26:919-922.

Liepe K, Franke WG, Kropp J, Koch R, Runge R, Hliscs R. (2000) Comparison of rhenium-188, rhenium-186-HEDP and strontium-89 in palliation of painful bone metastases. Nuklearmedizin 39:146-151.

Liepe K, Runge R, Kotzerke J. (2005) The benefit of bone-seeking radiopharmaceuticals in the treatment of metastatic bone pain. J Cancer Res Clin Oncol 131:60-66.

Liu S, Edwards DS. (2001) Bifunctional chelators for therapeutic lanthanide radiopharmaceuticals. Bioconj Chem 12:7-11.

Macedo A, Araujo A, Carvalho Melo F, et al. (2006) Cost-effectiveness of samarium-153-EDTMP for the treatment of pain due to multiple bone metastases in hormone-refractory prostate cancer versus conventional pain therapy, in Portugal. Acta Med Port 19:421-426.

Maggi A., Ciana P. (2005): Reporter mice and drug discovery and development. Nat Rev Drug Discov. 4:249-55.

Maini CL, Bergomi S, Romano L, et al. (2004) 153Sm-EDTMP for bone pain palliation in skeletal metastsses. Eur J Nucl Med Mol Img 31 (Suppl. 1):S171.

McEwan AJ. Pain from metastatic bone tumors. (1999) In: Aktolun C, Tauxe WN, eds. Nuclear Oncology. Berlin- Hiedelberg: Springer.

Mercadante S, Fulfaro F. Management of painful bone metastases. Curr Opin Oncol 2007;19:308-14.

Mertens WC, Porter AT, Reid RH, et al. Stroncium-89 and low-dose infusion cisplatin for patients with hor- mone refractory prostate carcinoma metastatic to bone—a preliminary report. J Nucl Med 1992;33:1437.

Minutoli F, Herberg A, Spadaro P, et al. (2006) [186Re]HEDP in the palliation of painful bone metastases from cancers other than prostate and breast. Q J Nucl Med Mol Imaging 50:355-62.

Mishani E., Hagooly A. (2009): Strategies for molecular imaging of epidermal growth factor receptor tyrosine kinase in cancer. J Nucl Med. 50:1199-1202

Mulligan T, Carrasquillo JA, Chung Y, et al. (1995) Phase I study of intravenous 177Lu-labeled CC49 murine mono- clonal antibody in patients with advanced adenocarcinoma. Clin Cancer Res 1:1447-1448.

Newsome S, Frawley BK, Argoff CE. (2008) Intrathecal analgesia for refractory cancer pain. Curr Pain Headache Rep. 12:249-256.

Oberg K (1998). Advances in chemotherapy and biotherapy of endocrineors. Curr. Opin. Oncol. 10: 58–65.

Ogawa K, Mukai T, Asano D, et al. (2007) Therapeutic effects of a 186Recomplex-

conjugated bisphosphonate for the palliation of metastatic bone pain in an animal model. J Nucl Med 48:122-7.

Oh SJ, Won KS, Moon DH,et al. (2002) Preparation and biologicalevaluation of 188Re-ethylenediamine-N,N,N',N' tetrakis(methylene phosphonic acid) as a potential agent for bone pain palliation. Nucl Med Commun 23:75-83.

O'Mara RE. New P-32 compounds in therapy of bone lesions. In: Spencer RP, ed. (1978) Therapy in Nuclear Medicine. New York: Grune and Stratton.

Panagi Z, Beletsi A, Evangelatos G, et al. (2001) Effect of dose on the biodistribution and pharmacokinetics of PLGA and PLGA-mPEG nanoparticles. Int J Pharm 221:143-146.

Pandit-Taskar N, Batraki M, Divgi CR. Radiopharmaceutical therapy for palliation of bone pain from osseous metastases. J Nucl Med 2004;45:1358-65.

Paoloni MC, Tandle A, Mazcko C, Hanna E, Kachala S, Leblanc A, et al. (2009): Launching a novel preclinical infrastructure: comparative oncology trials consortium directed therapeutic targeting of TNFalpha to cancer vasculature. PLoS One 4,:e4972.

Patel Y. (1999) Somatostatin and its receptor family. Front. Neuroendocrinol. 20:157–198

Pillai MRA, Chakraborty S, Das T, Venkatesh M, Ramamoorthy N. (2003) Production logistics of 177Lu for radionuclide therapy. Appl Radiat Isot 59:109-18.

Polton GA, White RN, et al. (2007) Improved survival in a retrospective cohort of 28 dogs with insulinoma. J Small Anim Pract. 48:151-156.
Firestone R. Re istotopes In: Shirley VS, ed. Table of Isotopes, (1996) 8th ed. New York: John Wiely and Sons.

Reubi JC, Maecke HR. Peptide-based probes for cancer imaging. J Nucl Med. (2008) 49:1735-1738.

Reubi JC, Waser B, et al. (1992) In vitro and in vivo detection of somatostatin receptors in human malignant lymphomas. Int J Cancer. 50:895-900.

Reubi JC, Waser B. et al. (1996) Somatostatin and vasoactive intestinal peptide receptors in human mesenchymal tumors: in vitro identification. Cancer Res.56:1922–1931.

Reubi JC. (2004) Somatostatin and other Peptide receptors as tools for tumor diagnosis and treatment. Neuroendocrinology 80 Suppl 1:519-627

Robben JH, Pollak YW, et al. (2005). Comparison of ultrasonography, computed tomography, and single-photon emission computed tomography for the detection and localization of canine insulinoma. J Vet Intern Med. 19:15-22.

Robben JH, van den Brom WE et al. (2006) Effect of octreotide on plasma concentrations of glucose, insulin, glucagon, growth hormone, and cortisol in healthy dogs and dogs with insulinoma. Res Vet Sci. 80:25-32.

Robben JH, Visser-Wisselaar HA, et al. (1997) In vitro and in vivo detection of functional somatostatin receptors in canine insulinomas. J Nucl Med. 38:1036-1042.

Robinson RG, Spicer JA, Preston DF, et al. (1987) Treatment of metastatic bone pain with strontium-89. Nucl Med Biol 14:219-222.

Rohrer SP, Birzin ET, et al. (1998) Rapid identification of subtype-selective agoniststhe somatostatin receptor through combinatorial chemistry. Science 282:737– 740.

Rutty Sola AG, Arguelles MG, Botazzini D, et al. (2000) Lutetium-177 EDTMP for bone pain palliation. Preparation, biodistribution and preclinical studies. Radiochim Acta 88:157-161.

Sagar VV, Piccone JM, Charkes ND. (1979) Studies of skeletal tracer kinetics: III. Tc-99m(Sn)methylenediphosphonate uptake in the canine tibia as a function of blood flow. J Nucl Med 20:1257-1261.

Sartor O, Reid RH, Bushnell DL, Quick DP, Ell PJ. (2007) Safety and efficacy of repeat administration of samarium Sm-153 lexidronam to patients with metastatic bone pain. Cancer 109:637-43.

Sartor O, Reid RH, Hoskin PJ, et al. (2004) Samarium-153-lexidronam complex for treatment of painful bone metastases in hormonerefractory prostate cancer. Urology 63:940-945.

Sartor O. (2004) Overview of samarium Sm-153 lexidronam in the treatment of painful metastatic bone disease. Rev Urol 6 (Suppl 10): S3-S12.

Serafini AN. (1995) Somatostatin receptor scintigraphy of malignant lymphoma – current status Yale J Biol Med 70:555-559

Serafini AN. (2001) Systematic metabolic radiotherapy with samarium-153 EDTMP for the treatment of painful bone metastases. Q J Nucl Med 45:91-97.

Sharma, K, Patel, YC, et al. (1996) Subtype-selective induction of wild-type p53 and apoptosis, but not cell cycle arrest, by human somatostatin receptor 3. Mol. Endocrinol. 10: 1688-1696

Shin K, Lee JC et al. (2007): Radiation synovectomy using 188Re-tin colloid improves knee synovitis as shown by MRI in refractory rheumatoid arthritis. Nucl Med Commun. 28:239-44.

Shini J, Amir D, Soskolne WA, et al. (1990). Correlations between uptake of technetium, calcium, phosphate, and mineralization in rat tibial bone repair. J Nucl Med 31:2001-2005

Silberstein EB. (1996) Dosage and response in the radiopharmaceutical therapy of painful osseous metastases. J Nucl Med 37:249-252.

Simpson KW, Stepien RL et al. (1995) Evaluation of the long-acting somatostatin analogue octreotide in the management of insulinoma in three dogs. J Small Anim Pract. 36:1-5

Singh A, Holmes RA, Farhangi M, et al. (1989) Human pharmacokinetics of samarium-153-EDTMP in metastatic cancer. J Nucl Med 30:1814-1818.
Smith MC, et al. (2000) OctreoTher: ongoing early clinical development of a somatostatin-receptor-targeted radionuclide antineoplastic therapy. Digestion. 62 Suppl 1:69-72

Srivastava S, Dadachova E. (2001) Recent advances in radionuclide therapy. Semin Nucl Med 31:330-336.

Stoeltzing O, Loss M, et al. (2009) Staged surgery with neoadjuvant (90)Y-DOTATOC therapy for down-sizing synchronous bilobular hepatic metastases from a neuroendocrine pancreatic tumor. Nierenbecks Arch Surg. 2009 Jun 9. Epub ahead of print

Syme AM, Kirkby C, Riauka TA, Fallone BG, McQuarrie SA. (2004) Monte Carlo investigation of single cell beta dosimetry for intraperitoneal radionuclide therapy. Phys Med Biol 49:1959-72.

Talme T, Ivanoff J et al. (2001) Somatostatin receptor expression and function in normal and leukaemic T-cells. Evidence for selective effects on adhesion to extracellular matrix components via SSTR-2 and/or 3. Clin Exp Immunol 125:71-79.

Tobin RL, Nelson RW, Lucroy D et al. (1999) Outcome of surgical versus medical treatment of dogs with beta cell neoplasia: 39 cases (1990-1997). J Am Vet Med Assoc. 215:226-30

Toegel S, Hoffmann O, Wadsak W, et al. (2006) Uptake of bone-seekers is solely associated with mineralisation! A study with 99mTc-MDP, 153Sm-EDTMP and 18F-fluoride on osteoblasts. Eur J Nucl Med Mol Imaging 33:491-494.

Trejtnar F, Novy Z, et al. (2008) In vitro comparison of renal handling and uptake of two somatostatin receptor-specific peptides labeled with indium-111. Ann Nucl Med. 22:60-70

Twycross RG (1982), Fairfield S. Pain in far advanced cancer. Pain 14:303-310

Virgolini I, Traub T, et al. (2002) Experience with In-111 and Yttrium-90 labelled somatostatin analogs Curr. Pharm. Design 8:1781-1807.

Volkert WA, Hoffman TJ. (1999) Therapeutic radiopharmaceuticals. Chem Rev 99:2269-2275.

Wang RF, Zhang CL, Zhu SL, Zhu M. (2003) A comparative study of samarium-153-ethylenediaminetetramethylene phosphonic acid with pamidronate disodium in the treatment of patients with painful metastatic bone cancer. Med Princ Pract 12:97-101.

Weissleder R., Pittet J.M. (2008): Imaging in the era of molecular oncology. Nature. 452:580–589.

Wester H-J. (2007): Nuclear Imaging Probes: from Bench to Bedside. Clin Cancer Res 13:3470-3473

Woltering EA. (203) Development of targeted somatostatin-based antiangiogenic therapy: a review and future perspectives. Cancer Biother Radiopharm.18:601-609.

Zoller F, Eisenhut M, et al. (2009) Endoradiotherapy in cancer treatment - Basic concepts and future trends. Eur J Pharmacol. 2009 Oct 15. [Epub ahead of print]

8. The candidate's publications related to the present dissertation

8.1 Full-text papers published in peer-reviewed journals in English

8.1.1 **D. Máthé**, L. Balogh, A. Polyák, R. Király, T. Márián, D. Pawlak, J. Zaknun, M.R.A. Pillai, Gy.A. Jánoki (2009)
Multi-species animal investigation on biodistribution, pharmacokinetics and toxicity of ^{177}Lu-EDTMP, a potential bone pain palliation agent *Nucl Med Biol, in press, available online 12 Nov 2009* (IF:2.419)

8.1.2 P Hauser, Z Hanzély, **D Máthé**, E Szabó, G Barna, A Sebestyén, A Jeney, D Schuler, Gy Fekete, M Garami (2009)
Effect of somatostatin analogue Octreotide in medulloblastoma in xenograft and cell culture study
J Paediatric Haematol Oncol 26:363-74.(IF:0.897)

8.1.3 Chakraborty S, Das T, Banerjee S, Balogh L, Chaudhari PR, Sarma HD, Polyák A, **Máthé D**, Venkatesh M, Janoki G, Pillai MR. (2008)
177Lu-EDTMP: a viable bone pain palliative in skeletal metastasis. *Cancer Biother Radiopharm.23:202-213.*(IF: 1.318)

8.1.4 **Mathe D**, Chaudhari PR, Balogh L, Polyak A, Kiraly R, Andocs G, Perge E, Glavits R, Janoki GA. (2002)
Preliminary studies with 188rhenium-tin colloid for radiation synovectomy: preparation, size determination, in-vivo distribution, effect and dosimetry studies. *Nucl Med Rev Cent East Eur. 5:99-104.*

8.2 Full-text paper published in peer-reviewed journal in Hungarian

8.2.1 **Máthé D.,** Polyák A, Király R, Perge E, Mészáros Á, Haller K., Jakab Cs., Balogh L, Jánoki Gy. (2009)
Receptor izotóp-diagnosztikai és –terápiás vizsgálatok szomatoszatin analóg peptidekkel kutyákban
Magy Allatorvosok, accepted for publication (IF:0.104)

8.3 Abstracts of oral and poster presentations in peer-reviewed international journals in English related to the subject of the dissertation

8.3.1 **Mathe D.,** Balogh L., Polyak A., Kiraly, R., Korosi, L., Janoki, GA (2007): Biodistribution of 177Lu-EDTMP in different healthy animal species and dogs with osteosarcoma. *Eur J Nucl Med Mol Imaging* 34 Suppl2 S189

8.3.2 Hauser P., Timar F., Hanzely Z., **Mathe D.,** Szabo E., Jeney A., Schuler D. (2007): Effect of somatostatin analogue octreotide to medulloblastoma in cell culture and xenograft. *Ped Blood Cancer* 49, 451

8.3.3 **Mathe D.,** Balogh, L., Chaudhari PR., Polyak A., Kiraly R., Janoki G. (2006): Quantitative evaluation of inflammation by different scintigraphic methods in the antigen induced arthritis model. *Eur J Nucl Med Mol Imaging* 33 Suppl2 S145

8.3.4 **Mathe D.,** Tripunoski T., Andocs G., Balogh L., Polyak A., Chaudhari PR., Janoki GA., Vaskova O. (2006): Use of spontaneous dog osteosarcoma model in the evaluation of tumor uptake and biological effects of (ReHEDP)-Re-188. *Eur J Nucl Med Mol Imaging* 33 Suppl2 S182

8.3.4 Andocs G., Balogh L., Bodo K., Polyak A., **Mathe D.,** Janoki G
(2001): Pharmacokinetic evaluation of Re-188-HEDP in healtly Beagle dogs and dogs having spontaneous osteosarcoma. *Eur J Nucl Med* 28 Suppl1 S668

9. Further publications not related to the present thesis

Full text publications in peer-reviewed international journals in English

Balogh L., Polyak A., **Mathe D.**, Kiraly R., Janoki Gy., Schauss A. G., Turpin A. A., Beer C., Bucci L. R. (2008): Absorption, Uptake and Tissue Affinity of High-Molecular Weight Hyaluronan after Oral Administration in Rats and Dogs. *J Agric Food Chem.* 56:10582-10593. (IF: 2.562)

Bozoky Z., Balogh L., **Mathe D.**, Fulop L., Janoki G.A. (2006): Evaluation of rat and rabbit sera lipoproteins in experimentally induced hyperlipidemia by analytical ultracentrifugation. *Eur Biophys J.* 35:205-213. (IF:1.825)

Chaudhari P.R., **Mathe D.**, Balogh L., Andocs G., Janoki G.A. (2005): Usefulness of (99m)Tc(V)-dimercaptosuccinic acid scintigraphy in the assessment of response to external radiation therapy in soft tissue sarcoma in Giant Snauzer dog. *Nucl Med Rev Cent East Eur.* 8:150-152.

Balogh L., **Mathe D.,** Andocs G., Polyak A., Kiraly R., Thuroczy J., Szilagyi J., Chaudhari P., Janoki G.A. (2005): Veterinary Nuclear Medicine again--commentary and remarks on: Krzeminski M et al. Veterinary nuclear medicine--a review. *Nucl Med Rev Cent East Eur.* 8:50-52.

Bozoky Z., Balogh L., **Mathe D.**, Fulop L., Bertok L., Janoki G.A. (2004): Preparation and investigation of 99m technetium-labeled low-density lipoproteins in rabbits with experimentally induced hypercholesterolemia. *Eur Biophys J.* 33:140-145. (IF: 1.931)

Balogh L., Thuroczy J., Andocs G.**, Mathe D.**, Chaudhari P., Perge E., Biksi I., Polyak A., Kiraly R., Janoki G.A. (2002): Sentinel lymph node detection in canine oncological patients. *Nucl Med Rev Cent East Eur.* 5:139-144.

Full-text publications in peer-reviewed national journals in English

Chaudhari P.R., **Máthé**, **D**., Balogh L., Andocs G., Thuroczy J., Perge E., Széll Z., Jánoki Gy.A. (2007): Microfilariae of Dirofilaria Repens in aspirates of osteosarcoma in dog. *J Vet Parasitol* 21:67-69

Tripuoski T., **Máthé D.,** Andócs G, Balogh L., Polyák A., Ugrinska A., Chaudhari P.R., Gorgoski I., Vaskova O. (2006): Prediction of ^{188}Re-HEDP tumor uptake based on ^{99m}Tc-MDP skeletal scintigraphy using spontaneous osteosarcoma bearing dog as a pathological animal model. *Acta Morphol* 3:38-42

Abstracts of oral and poster presentations in peer-reviewed international journals in English

Mathe D., Balogh L., Polyak A., Kiraly, R., Korosi, L., Janoki, GA (2007): Biodistribution of 177Lu-EDTMP in different healthy animal species and dogs with osteosarcoma. *Eur J Nucl Med Mol Imaging* 34 Suppl2 S189

Mathe D., Foldes I. (2007): Visualization and quantification of mouse thyroid gland 99mTc and 131I-uptake by a small animal SPECT/CT system. *Eur J Nucl Med Mol Imaging* 34 Suppl2 S398

Hauser P., Timar F., Hanzely Z., **Mathe D.,** Szabo E., Jeney A., Schuler D. (2007): Effect of somatostatin analogue octreotide to medulloblastoma in cell culture and xenograft. *Ped Blood Cancer* 49:451

Mathe D., Balogh, L., Chaudhari PR., Polyak A., Kiraly R., Janoki G. (2006): Quantitative evaluation of inflammation by different scintigraphic methods in the antigen induced arthritis model. *Eur J Nucl Med Mol Imaging* 33 Suppl2 S145

Mathe D., Tripunoski T., Andocs G., Balogh L., Polyak A., Chaudhari PR., Janoki GA., Vaskova O. (2006): Use of spontaneous dog osteosarcoma model in the evaluation of tumor uptake and biological effects of (ReHEDP)-Re-188. *Eur J Nucl Med Mol Imaging* 33 Suppl2 S182

Balogh L., Szecsenyi D., Vajdovich P., Perge E., Thuroczy J., **Mathe D.,** Polyak A., Kiraly R., Andocs G., Janoki GA. (2006): In vivo MDR examination by (99m)tc MIBI wash-out scintigraphy in veterinary oncological patients - can we prognostate the clinical response of chemotherapy? *Eur J Nucl Med Mol Imaging* 33 Suppl2 S226

Bozoky Z., Balogh L., **Mathe D.,** Polyak A., Janoki G (2006): Preparation and testing of receptor specific lipoproteins and liposomes labelled by 99m Tc-(technetium) isotopes for the scintigraphic detection of atherosclerotic cells. *Eur J Nucl Med Mol Imaging* 33 Suppl2 S240

Schauss A.G., Balogh L., Polyak A., **Mathe D.,** Kiraly R., Janoki G. (2004): Absorption, distribution and excretion of 99mtechnetium labeled hyaluronan after single oral doses in rats and beagle dogs. *FASEB J* 18, Suppl A150-151

Balogh L., Andocs G., **Mathe D.,** Thuroczy J., Perge E., Erdelyi I., Bodo K., Polyak A., Janoki G. (2001): Detection and identification of sentinel lymphnode in canine oncological patients. Eur J Nucl Med 28 Suppl1 S258

Andocs G., Balogh L., Bodo K., Polyak A., **Mathe D.,** Janoki G (2001): Pharmacokinetic evaluation of Re-188-HEDP in healtly Beagle dogs and dogs having spontaneous osteosarcoma. Eur J Nucl Med 28 Suppl1 S668

Acknowledgements

First of all I would like to acknowledge the Creator and Saviour of all beings for letting us admire the wonders of His world. I am grateful for my wife Krisztina and my family and for the love received from them during work.

Without the care and scientific and human guidance of my supervisor, Dr. Győző A. Jánoki this work could not have been realized. I wish to sincerely thank him for his patience. I have found a remarkable colleague and leader in Dr. Lajos Balogh in the National Institute of Radiobiology from whom I learnt basics of the real veterinary science and received a great amount of help and support.

The interest in a completely different field from founders of Mediso Ltd, László Nagy and István Bagaméry has been a very pleasant help in common applications of the multiplexed multi-pinhole SPECT imaging system that could not be made reality without Dr. Gábor Németh, Illés Müller and the Bioscan Inc. team.

I am grateful to professors Dr. Lóránt Bertók (from my Institute), Dr. Balázs Gulyás (of the Karolinska Institute) and Dr. Pradip Ramdas Chaudhari (of Indo-Hungarian heart) for all the discussions on life and science. The late professor Dr. Péter Rudas is deeply and gratefully acknowledged for all his encouragement in my scientific pursuits. The encouragement of my other consultant, Dr. Katalin Halasy and that of professor Dr. László Fodor from the same Faculty of Veterinary Sciences was also invigorating me. Doctors Viktor Molnár, Péter Csébi, and Csaba Jakab have been and hopefully will continue to be excellent colleagues both in common scientific work and in person. The European Institute of Oncology, Milan team: professor Marco Chinol, Giovanni Tesoriere and Stefano Papi have provided me with valuable insights into the sciences of therapeutic radiopharmacy and football that I will always remember.

I have received a lot of help to work in the international scientific community from professors Alexei Bogdanov, Bertrand Tavitian, Roger Schibli, Helmut Maecke, and Adriana Maggi. I am honoured to having been able to work together with as brilliant scientists as Jenő Láng, Cristina Müller and Luisa Ottobrini. Anyway, without the impact and patience of the first scientist I could work together with in my life, professor Dr. András Csillag from the Dept. Anatomy at Semmelweis University Budapest, I still would not have the courage to do any research. The reviewers of these theses, Dr. Péter Vajdovich and Dr. Iván Földes have done a thorough and time-consuming job and provided me with really kind and useful help.

Last but not least, all my co-workers and co-investigators are acknowledged with many thanks and in the hope of a good continuation.